Author:
Quick, M. C

Title:
A study of the free spiral vortex

A STUDY OF
THE FREE SPIRAL VORTEX.

by

M. C. QUICK.

A Dissertation submitted for the Degree of Doctor of Philosophy in Engineering in the University of Bristol.

March 1961.

SUMMARY

The occurrence of free spiral vortices at pump intakes and reservoir bellmouth spillways can cause considerable loss of efficiency by reducing the quantity of flow and by entraining air. To understand the mechanism and formation of these vortices an investigation has been made under steady and controlled conditions, measurements of surface profile, velocity distribution and discharge being made and compared with the results calculated from non-viscous theory. Vortices in two sizes of geometrically similar apparatus have also been studied to determine the velocity scale relationship for similarity.

The formation of steady vortices has been investigated for outlets drawing water both upwards and downwards from a vessel and the conditions for air entrainment to occur has been shown to be different for these two directions of outlet. The transient formation of vortices at these outlets is also discussed and it is seen that direction of outlet is, then, not important but the outlet velocity compared with submergence is a principal factor. From this work three independent conditions for the prevention of such vortices are found.

The behaviour of a vortex core after it has entered an outlet was also studied. With a downwards outlet the

air-core could persist, but conditions were found when a sudden transition to pipe-full flow could occur and this transition has been called the annular hydraulic jump. An analysis of this transition was made by making certain simplifying assumptions which were shown to be justified by the agreement found between experiment and analysis.

MEMORANDUM

I declare that this dissertation is based on my own independent work in the Department of Civil Engineering.

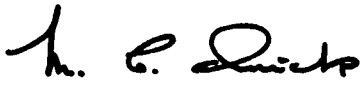

ACKNOWLEDGEMENTS

I should like to thank Dr.Gibbs for his help and encouragement and especially for his patient comments during the preparation of this Thesis. I am also indebted to Professor Sir Alfred Pugsley for allowing this work to be carried out and for the interest he has taken in it.

I wish to record my gratitude to Mr.E.Smith for his excellent assistance in the construction of the apparatus and for the many and searching questions he has asked me during the course of the work.

My thanks are also due to many of the Technical Staff and the Office Staff who have given much willing help.

CONTENTS

Page

FIGURES

Fig.No. Page

Fig. No. Page

Fig.No. Page

FIG 1.

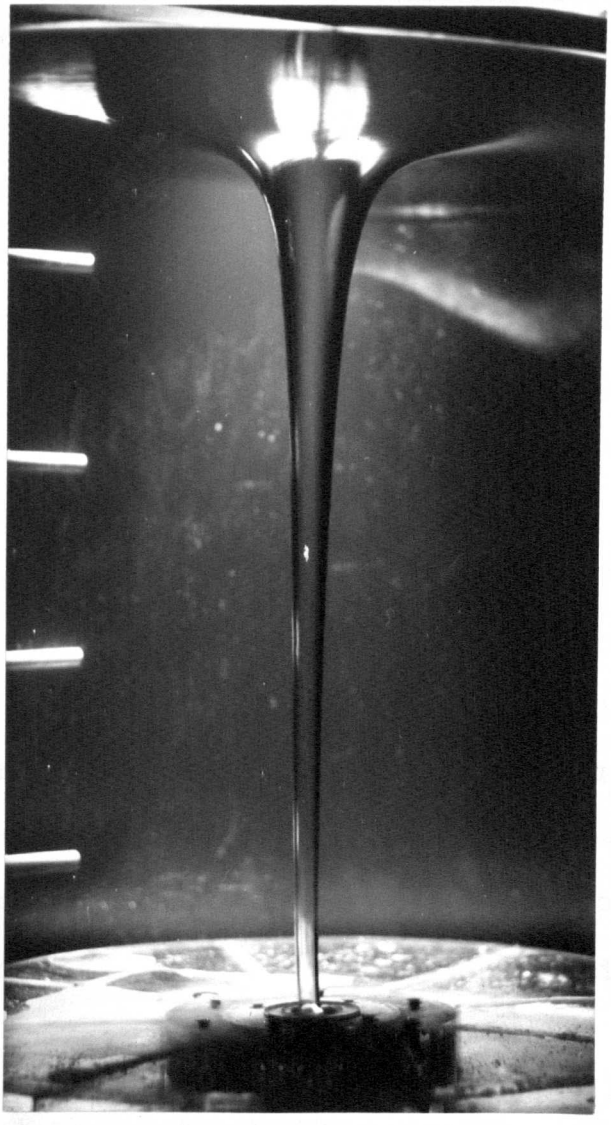

The air-core of a strong free spiral vortex.

CHAPTER I

THE FREE SPIRAL VORTEX

1. Introduction

The typical surface profile produced by a swirling flow at an outlet from a vessel has long been a well known feature of free surface flow. Yet, only in recent years has a detailed study and analysis of this phenomenon been attempted. Non-viscous, hydrodynamic analysis gives the velocity distribution for the potential or free cylindrical vortex and shows that, ideally, the free spiral vortex should have a similar velocity distribution. For many years this was all that was known of the free spiral vortex and it is only in the last twenty years that detailed experimental study, together with further theoretical analysis, has been made. These recent studies have become necessary because of the unexpected occurrence of the free spiral vortex in some hydraulic problems and the associated harmful effects sometimes produced by such vortices.

One problem that has produced considerable interest in the free spiral vortex is the formation of such vortices at pump intakes and bellmouth spillways. When water passes into an intake free spiral vortices will sometimes form, entraining air and reducing the quantity of water flowing.

At a pump intake the entrainment of air can cause vibration of the pump impeller and partial loss of suction, while the variation in quantity can produce changes in pump speed. At a bellmouth spillway the decrease in quantity which occurs when such a vortex forms might, in an extreme example, lead to the overtopping of the dam, but here the air entrainment should not be serious. Several recent papers have been concerned with investigations made on the prevention of such vortices and a study of these papers has shown that some aspects of the problem are not understood. A survey has therefore been made of all recent investigations of the free spiral vortex so that the present state of knowledge can be determined and a profitable line of study found.

The first investigations studied were concerned with the formation of vortices at bellmouthed spillways and the consequent reduction of their coefficients of discharge. The next series of investigations were concerned with the prevention of vortices in pump sumps. Following this work some investigators have studied the free spiral vortex when produced under steady and controlled conditions. More recently there has been work on the use of the free spiral vortex to control flow in drop chambers particularly for application in sewage systems. Before proceeding with a description of the the present work and the conclusions

derived from it a summary will be given of some of this previous work drawing attention to features which were not understood and which seemed to require further investigation.

2. Bellmouth Overflow Spillways

The first recorded work of any consequency in this field is that of G. M. Binnie[1] of Binnie, Deacon and Gourley who carried out some tests on model bellmouths and siphon-bellmouth spillways for the Jubilee reservoir Hong Kong. The models used were quite large, being built to a scale of $\frac{1}{24}$ giving a bellmouth of over 3 feet in diameter. The report mentions the formation of a vortex and its considerable effect on the coefficient of discharge, but then proceeds to make an erroneous distinction between the types of vortex which form, classifying them as "forced single spiral vortex" produced by swirling in the approaching flow and a "free single spiral vortex" caused by "a suction due to a vacuum created inside the bellmouth immediately below the surface". It will be shown in the present investigation that a vortex can only form if there is swirl in the approaching flow when the vortex formed will be of the free spiral type. G. M. Binnie considered a number of ways of preventing a vortex from forming and found that a single baffle placed across the bellmouth was the most satisfactory cure, although not necessarily complete, because a vortex could still form on one side of the baffle.

1. G. M. Binnie: Jour. Inst. Civil Engs.V.10 p,65, 1938.

Following the work by G. M. Binnie some further laboratory experiments on bellmouth spillways were made by A. M. Binnie and R. K. Wright[2]. Their apparatus, essentially a 4 foot diameter tank, had a radial supply similar to that used in the present experiments and a central outlet in the form of a bellmouth standing vertically upwards from the floor of the tank. The flow approaching the bellmouth was entirely radial. It was shown that, for low values of the head above the sill of the bellmouth, the bellmouth acted as a circular weir and the flow was axially symmetrical leaving a central core of air in the outlet tube. When the flow was increased this air-core became unstable and opened and closed alternately, trapping quantities of air which were carried through in the form of bubbles. Under these conditions the flow quantity varied considerably and the opening and closing of the air-core produced much noise. With further increase of the quantity and with no swirl in the approaching flow, a critical depth of water was reached above which the weir drowned and no further air entrainment occurred. In the later experiments swirl was deliberately induced in the approaching flow by using baffles to deflect some of the flow into a tangential direction and it was found that a free spiral vortex with an air-core was formed. Air-entrainment now occurred even at depths much greater than the depth at which air-entrainment

2. A. M. Binnie and R. K. Wright: Jour.Inst.Civil Engs. V.15 p.197 1941.

had previously ceased when no swirl was present. Binnie and Wright concluded that considerable care should be taken to prevent swirl in the approaching flow because the free spiral vortex not only entrained air but also caused a considerable decrease in the coefficient of discharge. Swirl diminished the coefficient of discharge both when the bellmouth acted as a weir and when it was drowned.

3. Air entrainment in pump sumps

A number of papers published have been concerned with the formation of air-entraining vortices in pump sumps and methods for their prevention. The most comprehensive of these papers describes work done at the British Hydromechanics Research Laboratories by D. F. Denny and G. A. J. Young[3] and is representative of most of the work done on this subject up to 1957. A study was made of various shapes of model sumps and it was concluded that the vortices formed because of rotation in the approaching flow.

The influence of a number of variables was studied, including submergence of the intake, suction velocity and, for upward flow into a vertical pipe, clearance between the bottom of the pipe and the bottom of the sump and, finally, distance of the intake from a side wall. Using these

3. Denny and Young. British Hydromechanics Research Association. Publ.SP583, 1957

observations they were able to draw diagrams of submergence against intake velocity and divide the diagrams into vortex forming and vortex free regions. No measurements of vortex strength or swirl in the approaching flow was attempted. The effect of various baffles and rafts were tried and these were sometimes effective in preventing air-entrainment, but it was doubtful if they reduced the swirl in the intake.

The main purpose of their investigation was to attempt to determine a velocity scale relationship between a prototype and its geometrically similar model. Their results indicated that the Froude Number relationship did not give similar results and the model velocities had to be increased before similar behaviour to that of the prototype was obtained. They concluded that models should be run at exit tube velocities equal to those of the prototype, but realised that this could not be universally true because it implied that vortices might form in depths of water of 100 feet or more, which is contrary to experience. It should be noted that this suggested velocity scale exaggeration was only checked once for a $\frac{1}{16}$ size model and its prototype.

It is interesting to quote from their remarks on air-entrainment that "the air carried into the intake in this manner may easily reach 5% of the water flow, and can thus have disastrous effects on the efficiency of the hydraulic machinery, apart from the danger of vibration or corrosion

damage to pipes and tunnels. For instance 1% of air is known to be capable of reducing the efficiency of a centrifugal pump by as much as 15%". They point out that swirl alone, with no air-entrainment, may be troublesome, particularly with axial flow machines. They also state that whether the intake is directed upwards, downwards or sideways is unimportant, but this will later be shown to be not true.

4. Studies of Free Spiral Vortex

The first experimenters to study the free spiral vortex in any detail were A. M. Binnie and G. A. Hookings[4] at Cambridge. In their introduction describing previous work on this subject, they say "what scanty information is available deals mainly with the coefficient of discharge of trumpets for bell-mouth spillways. G. M. Binnie's experiments using very large models do not correlate the swirl in the approaching fluid with the discharge". In Binnie and Hooking's experiments, they used a five foot diameter tank which had both tangential and radial supplies. The centrally placed water outlet could be either of trumpet shape or a uniform pipe and was similar to the apparatus used in the present investigation except that outlet pipe protruded above the floor of the tank. Measurements were made of the quantity of water passing for varying proportions of radial and tangential supply and also of the amount of air carried through.

4. Binnie and Hookings: Proc.Roy.Soc.A 194 p.398 1948

Attempts were made to measure velocities in the tank but, to quote from their paper, "The velocities were too low for a Pitot tube except near the core where its presence upset the flow ... drops of coloured liquid were also unsatisfactory for they were quickly drawn out into long spiral filaments". An approximate value of the swirl was obtained by using a matchstick loaded with lead so that it just floated on end. Its radius of rotation could be controlled by adjusting its weight and a value of the swirl could then be obtained by timing the matchstick for several revolutions. According to these measurements the ratio of the observed swirl at $18\frac{1}{4}$" radius to that calculated for a particular discharge and water depth was 0.18 over a range of discharge for the 2" supply and 0.065 for the $\frac{1}{2}$" supply; this is poor agreement which will be discussed later.

Binnie and Hookings derived an expression for calculating the core size and discharge for a given swirl and depth. This work is quoted in full later in this thesis and is compared with experimental results obtained. The analysis assumes that there is negligible radial velocity at the critical outlet section, which implies that the core surface is vertical at this point. They therefore consider that their analysis is only applicable to a trumpet shaped outlet in which the radial velocity is suppressed. They could not

measure the swirl with any certainty so they made a wall tapping in the throat of the trumpet and measured the pressure (h) at this point in excess of atmospheric pressure. They then assumed the swirl velocity at outlet to be distributed as for a free vortex, so that,

$$h = \frac{c^2}{2g}\left(\frac{1}{b^2} - \frac{1}{a^2}\right)$$

Knowing h, the core radius, b, and the outlet tube radius, a, at this section, they could calculate c, the swirl. Air-entrainment was negligible when a continuous, steady air-core existed but, when this air-core became unsteady, bubbles of air were trapped by the closure of the core and were then carried through. The maximum ratio of air-flow to water flow observed was 0.28 for a bellmouth.

A.M. Binnie and J. F. Davidson[5] continued the study of the free spiral vortex by applying a relaxation analysis to the problem of a circular tank with a central sharp edged orifice as outlet. They determined the shape of the conical hollow jet which is formed and compared their results with certain practical values. There was no direct measurement of velocities with which to compare the results and the value of the swirl was chosen to fit the surface profile. During their experiments they found that for a small swirl the jet at outlet does not diverge because of surface tension

5. Binnie and Davidson: Proc.Roy.Soc. A 199, p.443 1949.

forces, oscillations being set up in which the jet alternately expands and contracts, and this is analysed.

5. The Purposes of the Present Investigation

After studying the papers summarised in the preceding sections and after personal discussion with Mr. A. M. Binnie at Cambridge and Dr. D. F. Denny at the British Hydromechanics Research Association it became clear that the following points were among those requiring solution before definite conclusions can be drawn concerning the formation of air entraining vortices.

Firstly, no measurements of velocity have been made within a so-called free spiral vortex. The non-viscous flow theory assumes that tangential velocity varies inversely with the distance from the centre line of the vortex core, but such a distribution of velocity implies that there will be shearing stresses set up when a viscous fluid is used and at small radii these stresses may become considerable. It has yet to be determined whether these shear stresses distort the ideal velocity distribution only slightly or perhaps very considerably. The theoretical solution obtained by Binnie and Hookings for the free spiral vortex uses the ideal velocity distribution and would be made invalid by any considerable difference between this and the true distribution.

Secondly, there is the problem of dynamic similarity between geometrically similar systems. Suppose that a vortex

is produced in one size of apparatus in which the depth of flow, the quantity and the swirl are measured and suppose that a geometrically similar vortex in a geometrically similar but larger apparatus is produced. What would be the scale factor relating the velocities in the two systems? Denny has suggested equal exit velocities for similarity of vortex formation but this condition has not been substantiated except in one instance.

A third problem which needs to be solved is the way in which the swirl arises in a structure such as a sump. Numerous theories have been put forward, including ones involving spin produced by the pump impeller, or a type of secondary flow when the flow turns a sharp corner into the outlet, also, general swirl in the sump or vortices shed from the sump boundaries. Denny states that the swirl must originate in the flow approaching the outlet but does not specify how this happens.

A fourth problem which appears to have received very little attention is the behaviour of the flow after passing into the outlet pipe. Suppose that a vortex core is formed and the tail of this core enters the outlet pipe. Does this air-core persist in the outlet pipe or is it broken up into air bubbles? When an air-core is formed the flow into the outlet has a high proportion of swirl and it is presumed that

this swirl will be diminished by the action of viscous retardation; it would be useful to know how quickly the swirl would be destroyed. There is also the question of whether the direction of the outlet has any influence on the conditions within itself. It may well be that whether, for instance, the outlet leads vertically downwards or vertically upwards may have a fundamental influence on the behaviour of a vortex core within it.

It is known that much of the vortex formation at pump intakes and reservoir outlets is intermittent, each vortex only lasting for a short period of time and producing surging of the flow. Such an unsteady state is difficult to study, especially when velocity measurements as well as quantity and depth measurements are required. Therefore, to study some of these problems it was decided to design apparatus inwhich a swirl could be generated and controlled. The steady free spiral vortices produced at the outlet to this apparatus could then be observed and detailed measurements made. It was also decided to build a similar but larger apparatus to study the scale relationships. Adaptations of these sets of apparatus could be made to study different outlet conditions and the behaviour of the flow in the outlet tube.

CHAPTER II

ANALYSIS OF THE FREE SPIRAL VORTEX

1. Dimensional Analysis.

When water discharges freely from a tank through an orifice the predominant force acting is that due to gravity. The dimensional parameter which then describes this flow condition is the Froude number, $V/\sqrt{gL}$. It might be argued that in the special case when a free spiral vortex is formed the Froude number is no longer a sufficient parameter, for near the centre of a free spiral vortex the velocity gradient is large and the viscous shearing is considerable, so that viscous forces may no longer be negligible. If this is so, then Reynolds number must also be included to describe the flow.

Consider the scale relationships between a model, Suffix 1, and its prototype, Suffix 2, if both Froude number and Reynolds number are involved.

Froude number gives

$$\frac{V_1^2}{gL_1} = \frac{V_2^2}{gL_2} \qquad ..(1)$$

Reynolds number gives

$$\frac{V_1 L_1}{\nu_1} = \frac{V_2 L_2}{\nu_2} \qquad ..(2)$$

If $L_2 = nL_1$, from Eqn.(1),

$$V_2 = \sqrt{n}\, V_1 \qquad ..(3)$$

Similarly from Eqn.(2),

$$V_2 = \frac{\nu_2}{\nu_1} \frac{1}{n} V_1 \qquad ..(4)$$

Therefore dividing (3) and (4),

$$\nu_1 = \frac{\nu_2}{n\sqrt{n}} \qquad ..(5)$$

This implies that to satisfy both Reynolds number and Froude number simultaneously, then the fluid in the model must have a viscosity of $n\sqrt{n}$ times less than that of the prototype. If the prototype fluid is water, which has a relatively low viscosity, then even with a half size model it is extremely difficult, if not impossible, to find a fluid of a suitable viscosity. With any greater scale factor it is impossible to use a fluid which will satisfy this condition.

It is therefore not possible to have complete similarity between model and prototype unless either viscous effects or gravitational effects are negligible. Under these circumstances, when both effects are significant, two methods have been used for some problems, firstly, a geometrical distortion and, secondly, a velocity scale distortion while using the same fluid in both model and prototype. For the present problem no geometrical distortion has been used but Denny and Young have suggested a velocity distortion.

Consider first geometrically similar systems in which the variables involved are flow quantity Q, vorticity c, depth H, outlet diameter d, kinematic viscosity ν and the gravitational acceleration g. On forming the dimensional

matrix for M, L and T it is found to be of order two, so that the π theorem gives the result that, for N variables, there are N-2 numerics.

We have therefore, $\frac{Q}{g^{\frac{1}{2}}d^{5/2}}$, $\frac{H}{d}$, $\frac{c}{g^{\frac{1}{2}}d^{3/2}}$, $\frac{c}{\nu}$.

The last two of these will be seen to be a form of the Froude number and Reynolds number respectively. The equation for flow quantity is therefore of the form:

$$\frac{Q}{g^{\frac{1}{2}}d^{5/2}} = \phi\left(\frac{H}{d}, \frac{c}{g^{\frac{1}{2}}d^{3/2}}, \frac{c}{\nu}\right). \qquad ..(6)$$

In the experimental investigation, if two of the numerics on the right hand side are held constant, the effect of the third numeric can be studied. If, for instance, the flow were independent of Froude number, then for the same values of $\frac{H}{d}$ and $\frac{c}{\nu}$ in model and prototype the value of $\frac{Q}{g^{\frac{1}{2}}d^{5/2}}$ would also be the same. Similarly, if the flow is independent of Reynolds number similar values of $\frac{H}{d}$ and $\frac{c}{g^{\frac{1}{2}}d^{3/2}}$ should give identical values of $\frac{Q}{g^{\frac{1}{2}}d^{5/2}}$. It may well be that both Froude number and Reynolds number are significant in which case similar values of $\frac{Q}{g^{\frac{1}{2}}d^{5/2}}$ and $\frac{H}{d}$ will yield different values of Reynolds number and Froude number, from which the velocity scale for similarity may be determined. An experimental study of these numerics will be made to determine the correct scale relationship.

FIG. 2

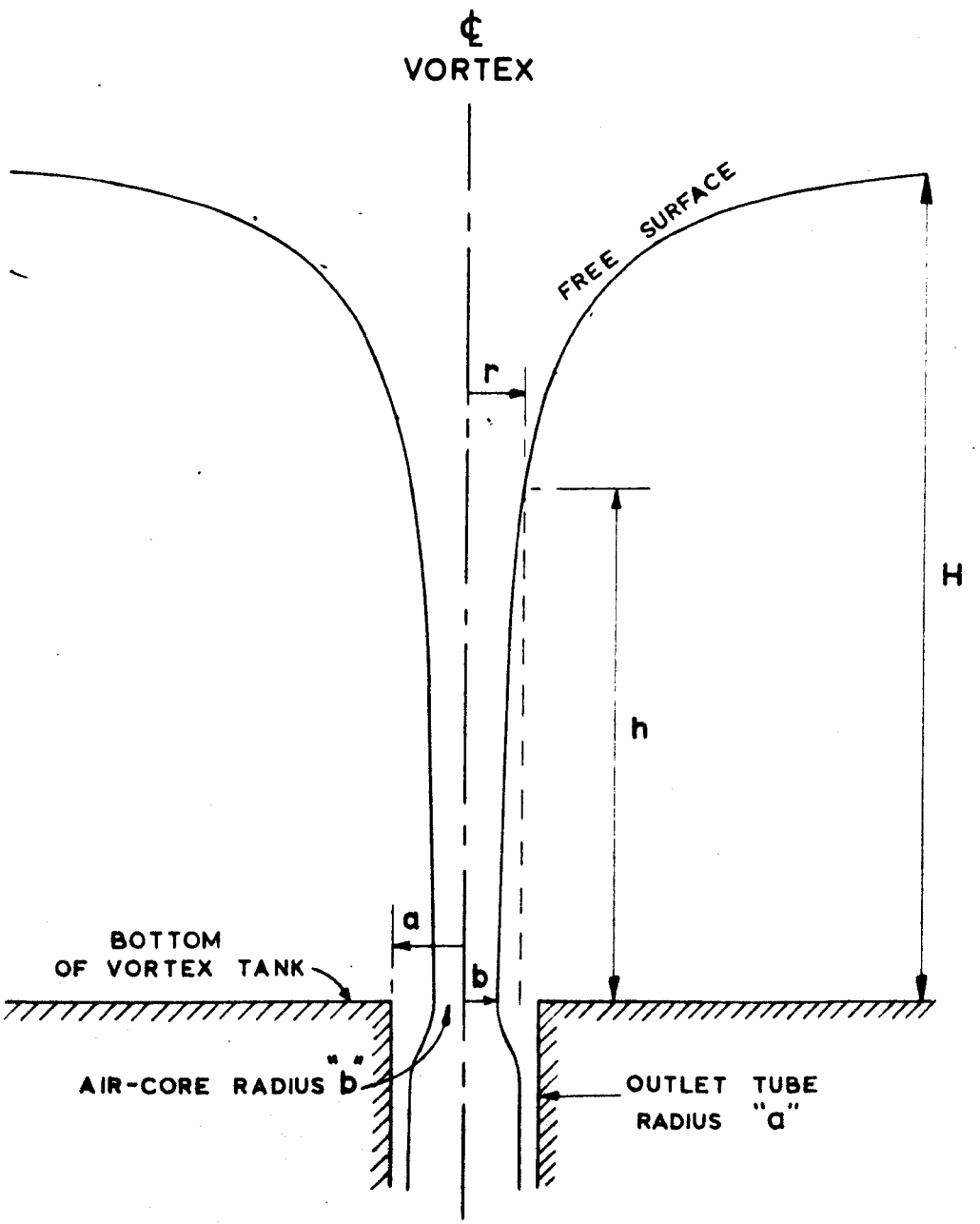

DIAGRAM TO ILLUSTRATE ANALYSIS OF FREE SPIRAL VORTEX.

2. Ideal Fluid Analysis of the Free Spiral Vortex.

The analysis that follows was first derived by A.M.Binnie and G.A.Hookings[4] for the discharge of a swirling fluid through a trumpet shaped outlet. It assumes that at the outlet section the only significant velocities are the vertical velocity and the swirl velocities, the radial velocity being insignificant. In the present work it has been assumed that even for a sharp edged orifice the radial velocities are still negligible and the same analysis is applicable. The analysis depends on the condition that for stability of flow the quantity of outflow is a maximum, a condition identical with that of minimum energy.

Referring to the diagram of a free spiral vortex, Fig.2, Bernoulli's equation is applied at a radius r where $b < r < a$ and it is also applied at a large radius where the depth is H and the swirl velocity can be considered as being negligibly small. For non-viscous flow these two values of Bernoulli's equation will be equal and this gives,

$$h + \frac{v^2}{2g} + \frac{c^2}{2gr^2} = H \qquad ..(7)$$

4. A.M.Binnie and G.A.Hookings. Proc.Roy. Soc.A 194 p.398, 1948.

where h is the water depth at radius r, v is the vertical velocity through the outlet, and c is the value of the swirl, w.r.

Bernoulli's equation can also be applied at the outlet at radius r and on the core surface, radius b. The vertical velocity v through the outlet is assumed to be constant and therefore,

$$h + \frac{v^2}{2g} + \frac{c^2}{2gr^2} = 0 + \frac{v^2}{2g} + \frac{c^2}{2gb^2} .$$

$$\text{Therefore} \quad h = \frac{c^2}{2g}\left(\frac{1}{b^2} - \frac{1}{r^2}\right) \qquad ..(8)$$

Substituting in Eqn.(7) for h,

$$\frac{v^2}{2g} + \frac{c^2}{2gb^2} = H$$

$$\text{Therefore} \quad v = \left(2.g.H - \frac{c^2}{b^2}\right)^{\frac{1}{2}} \qquad ..(9)$$

The value of the discharge, Q, will be given by multiplying this vertical velocity by the flow area.

$$\text{Therefore } Q = \pi(a^2 - b^2)(2gH - \frac{c^2}{b^2})^{\frac{1}{2}} \qquad ..(10)$$

For stability the discharge must be a maximum, i.e.,

$\frac{\partial Q}{\partial b} = 0$, and $\frac{\partial^2 Q}{\partial b^2}$ should be nagative.

$$\frac{\partial Q}{\partial b} = -2.\pi.b.(2.g.H - \frac{c^2}{b^2})^{\frac{1}{2}} + \frac{\pi}{2}(a^2 - b^2)(2.g.H - \frac{c^2}{b^2})^{-\frac{1}{2}}(-\frac{2c^2}{b^3}).$$

Equating to zero and re-arranging terms,

$$4.g.H.\ b^4 - c^2.b^2 - c^2.a^2 = 0$$

Solving for b^2,

$$b^2 = \frac{c^2 \pm \sqrt{c^4 + 16.c^2.a^2.g.H.}}{8.g.H.} \qquad ..(11)$$

The negative solution is not possible and the positive solution makes $\frac{\partial^2 Q}{\partial b^2}$ negative so that the condition of maximum discharge is fulfilled.

Combining Eqns.(10) and (11),

$$Q = \pi\left(a^2 - \frac{c^2+\sqrt{c^4+16.c^2.a^2.g.H}}{8.g.H}\right)\left(2.g.H - \frac{8.g.H.c^2}{c^2+\sqrt{c^4+16.c^2.a^2.g.H}}\right)^{\frac{1}{2}} \qquad ..(12)$$

Binnie and Hookings considered that this analysis was only applicable when the radial component of flow at the outlet was negligible. They therefore thought that it would only apply to outlets of a trumpet shape in which radial velocities are suppressed. However, the experiments to be described were carried out using sharp edged orifices or tubes with sharp entrances and even with these unfavourable outlet conditions the radial velocities have not proved to be significant.

FIG 3.

The Small Vortex Apparatus.

FIG. 4

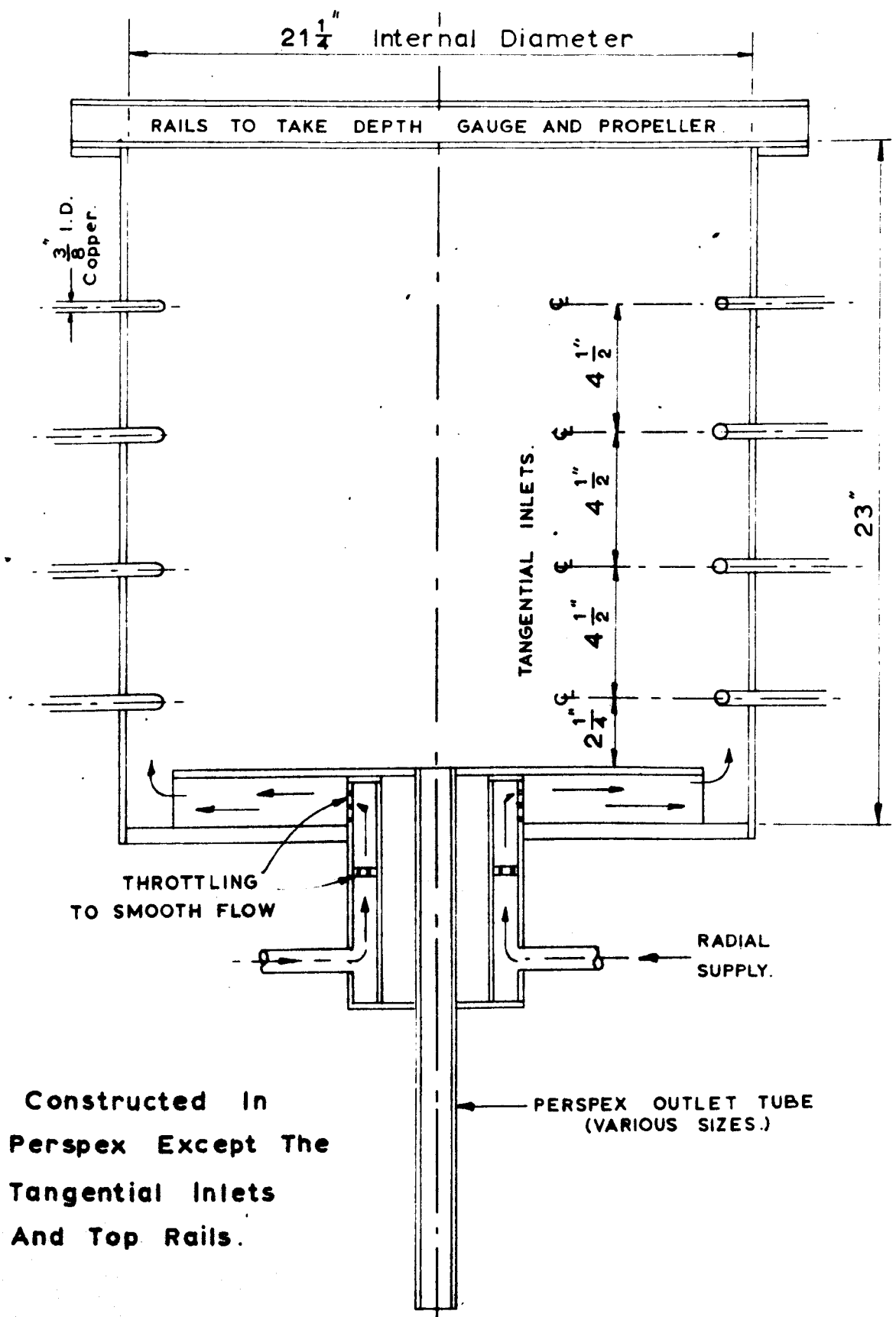

Constructed In Perspex Except The Tangential Inlets And Top Rails.

SMALL TANK : SECTION ON ℄ .

FIG 5

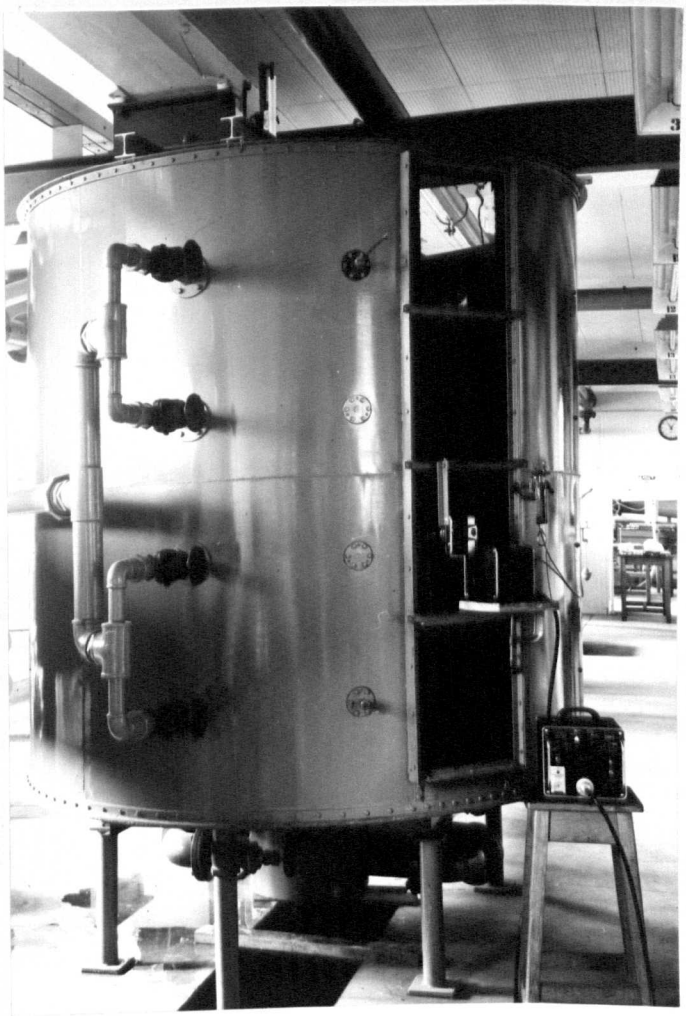

The Large Vortex Apparatus.

CHAPTER III

EXPERIMENTAL STUDY OF THE FREE SPIRAL VORTEX

1. Small Vortex Tank

To study the free spiral vortex in detail it is necessary to obtain steady conditions, and the apparatus must therefore be symmetrical about a central vertical axis and the flow conditions should be axisymmetric. It is also important to make conditions uniform throughout the depth of the tank so that the tangential velocity distribution only varies radially and not with depth. Conditions will then be as nearly as possible those assumed in the analysis of the free spiral vortex. To obtain these conditions the design of tank adopted was as shown in Figs. 3 and 4. This is similar to that used by A. M. Binnie except for the tangential inlets. It was thought that if all the tangential supply entered at the bottom of the tank a secondary circulation might be generated as the water passed upwards to the remainder of the tank. Various possible arrangements were considered that finally adopted consisted of eight tangential supply pipes, four one side of the tank and four diametrically opposite, spaced evenly throughout the depth of the tank and vertically above each other. The supply to these eight tangential supply pipes was branched symmetrically so that each pipe

received an equal supply. This supply was both axially symmetrical and also proved to be uniform with respect to depth. If the tank was to be operated at a depth ~~lower~~ less than maximum, the tangential supply pipes which were then above the water surface were disconnected to prevent the issuing jet of water impinging on the free surface and causing disturbance.

Measurements were made of flow quantity, surface profile and the velocity distribution throughout the tank. It was proposed to use photographic methods to measure both velocities and core profiles and therefore it was essential to be able to view the vortex through the sides of the tank. The view through the top free surface would be distorted both by the curvature of the surface and by surface ripples. The small vortex tank was therefore constructed entirely of perspex and this enabled the vortex to be studied not only in the tank but also in the outlet. The tank itself was a 21 inch internal diameter cylinder two feet high moulded from $\frac{1}{4}$ inch perspex sheet. A $\frac{1}{2}$ inch thick rim $1\frac{1}{2}$ inches wide was cemented around the top to prevent distortion. This tank was mounted on a triangular levelling frame. The radial supply arrangement is shown in Fig. 4. This system is not ideal because all the radial supply is at the bottom of the tank, but a system giving radial supply equally at all depths would have entailed

building another supply tank outside the vortex tank, and requiring considerable screening and vaning to make the flow uniform and radial. This would have made it impossible to observe events in the tank as thoroughly as with the system used. The effect of non-uniformity of radial supply is small compared with that of the tangential supply because the maximum radial velocities are only about $\frac{1}{3}$ inch per second compared with about 26 inches per second for the tangential supply. Axial symmetry of the radial supply was obtained by passing it through throttling rings of equally spaced holes and by using radial guide vanes underneath the baffle plate.

The 21 inch perspex cylinder, when filled with water, acted as a large lens, distorting the appearance of anything within the tank. To counter this distortion a chamber with two flat plate glass sides at right angles to each other was sealed on to the outside of the perspex tank and the intervening space was filled with water. This reduced distortion to a negligible amount.

On top of the vortex tank rails were fitted to carry a depth gauge, propeller meter and other such measuring devices. These rails were accurately levelled and graduated in inches from the centre of the tank. At the outlet from the tank provision was made either to fit sharp edged orifices or outlet tubes of suitable diameter. Below the outlet was a calibrated measuring tank.

2. Velocity Measurements

The non-viscous analysis of a free spiral vortex shows that the quantity of water flowing out from the tank is a function of both the water depth at a large radius where velocity energy is negligible, and the value of the vorticity c. It is assumed that vorticity is constant which implies that the tangential velocity w varies inversely with the radius. As far as is known, no velocity measurements have been made in a free spiral vortex structure and so it has not been established whether the assumption of constant vorticity for a real, viscous fluid is true or false, or whether it is a reasonable approximation. Before the ideal analysis can be used it must be shown not only that the assumption of constant vorticity is reasonable, but also that the distribution of tangential velocity is uniform with depth. Superimposed on the tangential velocities will be radial and vertical velocities and these should become more significant as the flow approaches the outlet. Consideration will now be given to the problems of measuring velocities in various parts of the flow and the methods of velocity measurement most likely to be successful.

In the small vortex tank, at radii greater than about two inches from the core centre line, the velocities

to be measured varied from about 12 inches per second to 2 inches/sec. This order of velocity gives a small dynamic head when using a Pitot Tube and entails very accurate measurement of head. A small propeller meter will work satisfactorily over this range, though the response may become sluggish at velocities below 3 or 4 inches/sec. unless great care is taken to minimise bearing friction. The speed of rotation can be measured with a stroboscope or at very low speeds, less than 120 r.p.m., the propeller speed can be found by visual counting.

The disadvantages of a propeller meter are that it averages velocities across its swept area and it may disturb delicate flow patterns. Therefore near the core of the vortex, where there is a steepening velocity gradient and where the flow pattern was found to be very susceptible to disturbances, the propeller meter is no longer suitable for measuring velocities. Despite the higher velocities to be measured in this region, a Pitot Tube is also unsuitable because it too, will destroy the pattern it is required to measure.

A method of velocity measurement is required which will take energy from the flow and which will give the velocity at a particular point in the flow. The only method which does this exactly is that used by Fage in which he used an ultramicroscope to follow minute particles in the water. This method would not have been practicable

in this instance because of intervening fluid layers, but a similar type of method can be used. Some small pellets of wax, loaded with lead stearate to bring their specific gravity to unity, can be added to the flow. Being of the same density as the water which they displace, they will experience the same forces as the water and will therefore follow the flow pattern in detail. Their movement over a short interval of time can be recorded as a streak on a photograph and if the camera shutter speed is known the mean velocity along the path traced out can be found. In this investigation the flow pattern is three dimensional, whilst the method of recording velocities photographically is two dimensional. Therefore, to determine the flow two simultaneous photographs are required in directions at right angles.

As previously mentioned, a water filled chamber with two perpendicular plate glass sides fastened to the outside of the vortex tank allowed distortion free viewing of the vortex. A mirror system, shown diagrammatically in Fig.6, reflected these two views into one camera thus giving the information for each reading on one photograph. This method avoided the complication of having to synchronise two cameras. First attempts to obtain readings by this method showed that the water between the core region and

the camera scattered so much light into the camera that the pellet images were obscured. Photographs were, therefore, taken at night with no lighting except for intense illumination of the core region. Details of the illumination method and film development are given in Appendix I and typical photographs obtained are shown in Figs. 9 and 10. At first an electronic flash gun was used to give a bright spot at the beginning of each streak but later it was found possible to deduce the direction of travel from the photographs and so the flash was omitted.

3. Interpretation of Photographs

The camera, through its mirror system, views the vortex as if it were viewing from A and B (Fig. 7a). These directions are the x and y axes respectively. The z axis is the centre line of the core.

The photographs do not give x, y and z directly because the scale for y and z in the left hand photograph is dependent on the value of x. Similarly, x from the right hand photograph, depends on the value of y. This is clear by considering the lengths ℓm, no, pq in Fig.7a, for on the photograph each of these differing lengths will appear to be the same length if the camera distortion is linear.

FIG. 6

SMALL TANK

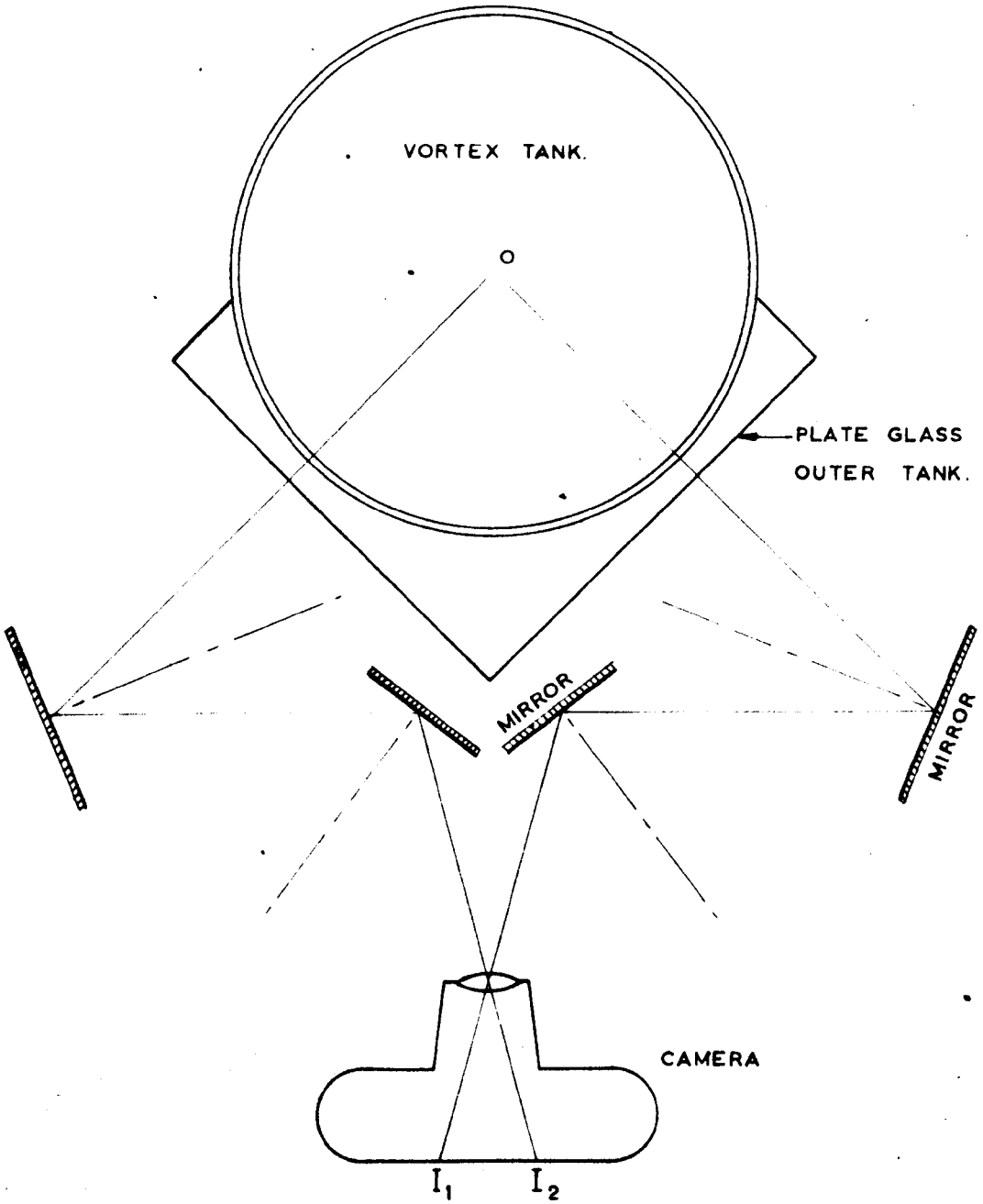

MIRROR AND CAMERA ARRANGEMENT FOR BEAD PHOTOGRAPHS.

FIG . 7

SMALL TANK : PHOTOGRAPHIC INTERPRETATION.

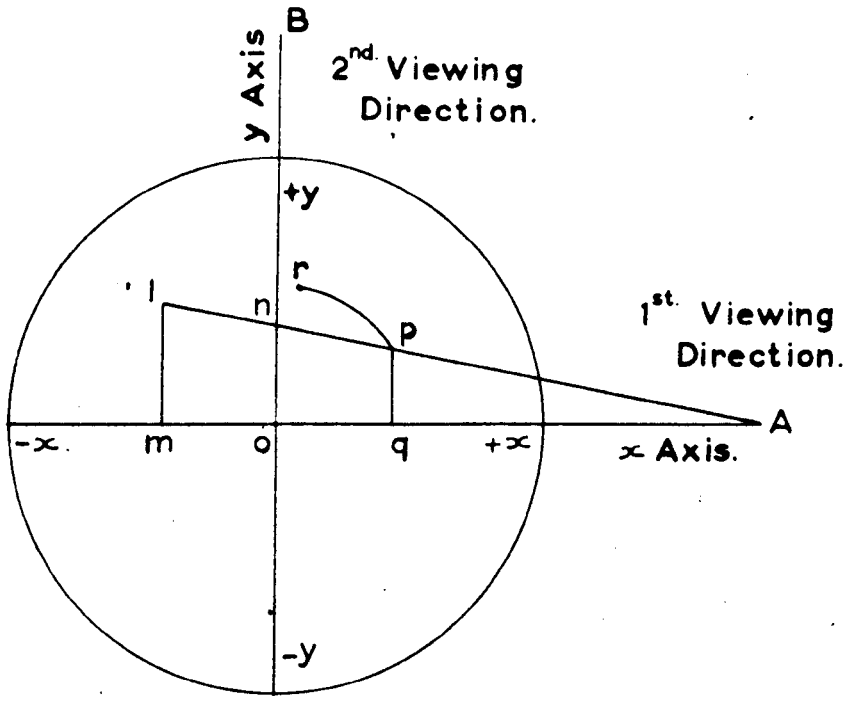

PLAN VIEW OF TANK.

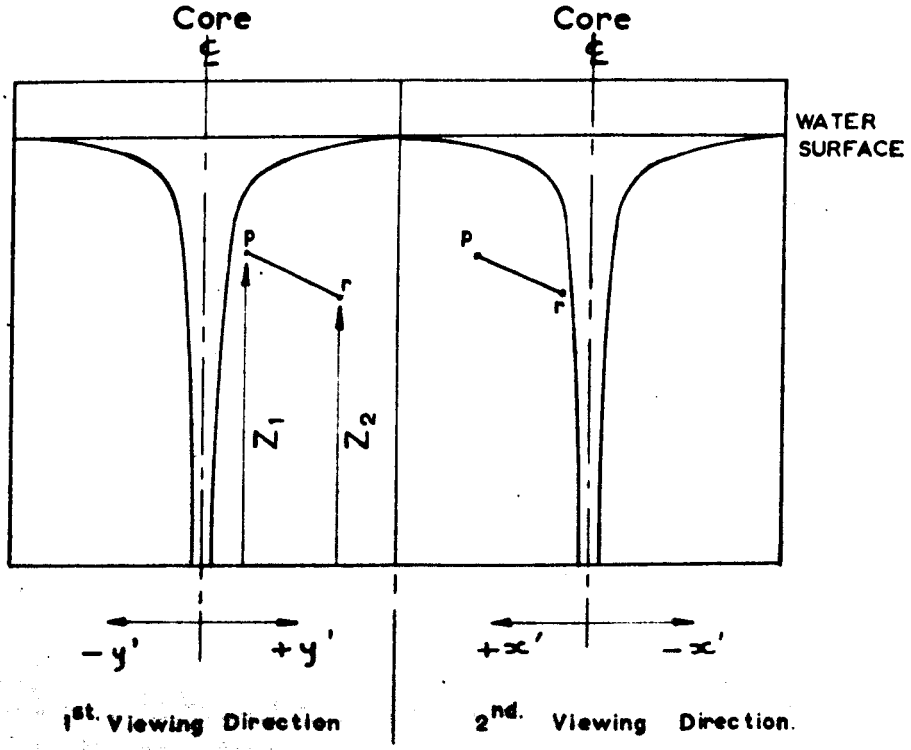

DIAGRAM OF TYPICAL PHOTOGRAPH TO SHOW MEASUREMENTS MADE.

FIG. 8

a) Determination Of Scale Factors : Small Tank.

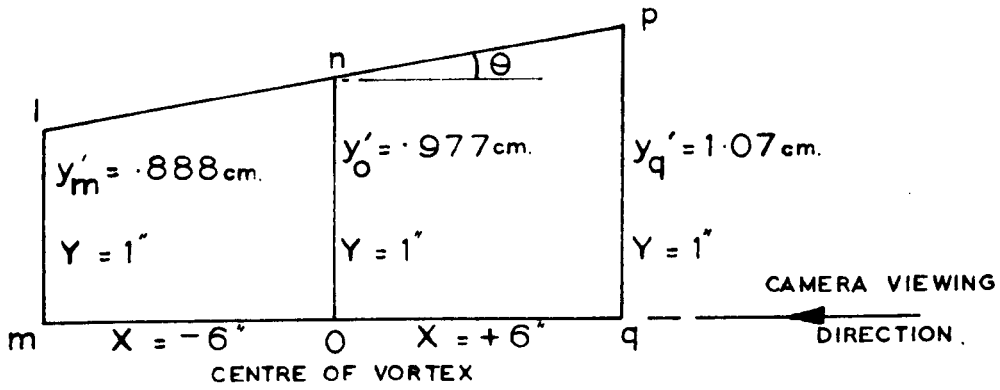

$Y = r.y'_o$ $\qquad$ $y = y'(1 - xs)$

$\therefore r = 5.2$ $\qquad$ $\therefore s = \tan\theta = 0.081$

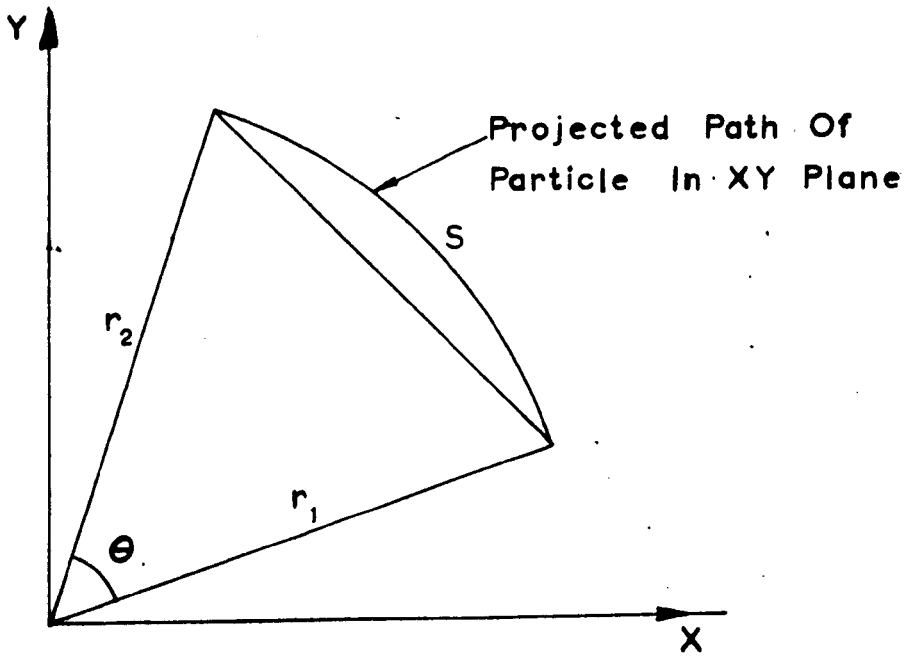

b) From Rectangular Coordinates To Polar Notation.

Let x', y', z', be the co-ordinates measured from the photographs.

Let x, y, z, be co-ordinates from photographs if there were no distortion.

Now suppose x is not zero and introduce a distortion scale factor, s, so that,

$$y = y' (1 - x.s) \qquad 1$$

If OA = OB we have two similar expressions for x and z (to be measured from left hand photograph), because s will apply to both photographs.

Therefore $x = x' (1 - y.s)$ 2

and $z = z' (1 - x.s)$ 3

These equations satisfy the condition that when $x' = 0$, $x = 0$, $y' = 0$, $y = 0$ and $z' = 0$, $z = 0$.

Combining equations 1 and 2 and solving for x,

$$x = x' [1 - y' (1 - xs)s]$$

$$x = x' \frac{(1 - y's)}{1 - x'y's^2} \qquad 4$$

Let X, Y, Z be the full-scale co-ordinates and let r be the scale factor such that,

$$X = rx \qquad 5$$

Then $$X = rx' \frac{(1 - y's)}{1 - x'y's^2} \qquad 6$$

Similarly $$Y = ry' \frac{(1 - x's)}{1 - x'y's^2} \qquad 7$$

$$Z = rx' \frac{(1 - x's)}{1 - x'y's^2} \qquad 8$$

This equation 8 assumes that z' is taken from the left hand photograph.

As will be shown later, the value of s for the small vortex tank and for the standardised position of the camera is 0.0805.

$$s^2 = 0.0065$$

Also the values of x' and y' never exceed 0.5, so that $x'y's^2$ is always less than 0.0016. Therefore, the term $1 - x'y's^2$ is considered negligible.

Equations 6, 7 and 8 become

$$X = rx' (1 - y's) \qquad 9$$

$$Y = ry' (1 - x's) \qquad 10$$

$$Z = rz' (1 - x's) \qquad 11$$

The co-ordinates (X_1, Y_1, Z_1) and (X_2, Y_2, Z_2) of the beginning and end of each streak were determined from equations 9, 10 and 11. These co-ordinates were then used to determine the vertical velocity Z and the circumferential velocity $r\theta$; the radial component from observation was negligible, or at least not measurable.

Let the shutter speed be t

$$Z = \frac{Z_2 - Z_1}{t} \qquad 12$$

Considering projection of motion in XY plane to find $r\theta$, see Fig. 8b.

$$r_1 = (X_1^2 + Y_1^2)^2$$

$$r_2 = (X_2^2 + Y_2^2)^2 \quad , \qquad 13$$

Equation 13 was averaged to give a mean radius r.

The chord length ℓ is given by

$$\ell = \{ (X_2 - X_1)^2 + (Y_2 - Y_1)^2 \}^{\frac{1}{2}} \qquad 14$$

The value of θ was computed from

$$\sin \frac{\theta}{2} = \frac{\ell}{2r}$$

so that

$$\theta = 2 \sin^{-1} \frac{\ell}{2r} \qquad 15$$

$$r\theta = \frac{2r}{t} \sin^{-1} \frac{\ell}{2r} \qquad 16$$

If the bead had completed more than half a turn or several turns the value of θ obtained from eqan. 15 was always the minimum value. For instance, if the bead had completed an arc of $\frac{3\pi}{2}$ radians the value obtained for θ would be $\frac{\pi}{2}$. Therefore, the approximate value of θ had to be obtained by inspection and given in the form $2\pi N \pm \theta$.

The scale factors r and s were determined by photographing a rectangular plate 20 inches high and 12 inches wide which had been painted black and then scribed horizontally and vertically with lines 2 inches apart. This square meshwork of scratchmarks showed

bright against the black paint. Three photographs were taken from each viewing direction, one with the plate at the centre of the tank and then two more 6 inches nearer and further from the camera. When these photographs had been printed, using a known and constant setting of the enlarger, the scale factors could be determined as illustrated in Fig. 8a. The lengths ℓm, no, pq all represent a length of 1 inch on the three photographs. The factor r is determined directly from the length no and s is found from tan θ. It is also possible to check that the scale factor is reasonably linear over the range required and it was found that for distances not greater than 6 inches from the core centre line the scale factor was linear within 2%. This degree of accuracy was better than the accuracy with which measurements from the photographs could be made and is not therefore significant.

4. Large Vortex Tank

To investigate the scale relationship between different sizes of geometrically similar vortex apparatus, a second and much larger tank was required. The maximum size of apparatus that could be accommodated in the laboratory was one with dimensions four times those of the small tank previously described. This large tank would therefore be seven feet in diameter and would hold about eight tons

of water. Before building this large size apparatus the small tank was constructed and tested to check that the design was satisfactory and then the dimensions of the small tank were scaled up four times to obtain the dimensions for the large tank.

Again it was considered essential to be able to observe events within the tank but with this large apparatus this could best be done through glass panels let into the tank wall. A photograph of this tank is given in Fig. 5. The large tank was constructed of 16 gauge sheet steel welded and rolled into a seven foot diameter cylinder. This thin sheet was then kept in shape by rolled steel angle hoops at the top and bottom and an $\frac{1}{8}$ inch thick steel base plate bolted to the lower angle. The base plate was braced with welded 2 inch channels and angles and was then supported on a square subframe carried on four legs.

Two plate-glass panels $\frac{3}{8}$ inch thick were let into the sides of the tank. The plate-glass windows are one foot across and run the full depth of the tank. The cylinder hoop stresses arising from the internal water pressure are carried across the windows with 1 inch angle tie bars.

The only part of the apparatus not scaled exactly from the smaller apparatus was the radial supply inlet chamber. This chamber was made from two concentric pipes

of 9 inches and 18 inches diameter instead of 16 inches and 24 inches if the true scale factor had been used. Because this chamber is only used to give an even distribution of water and is not the final inlet into the tank it was not considered that this would affect the functioning of the apparatus.

The size of the apparatus made it inconvenient to insert propeller meters from the top. Four water-tight glands were therefore fitted in the tank wall and through these glands the propeller meter could be moved into any required position. Because of the higher velocities to be measured a pitot-static tube was made which could be inserted through the same glands. Rails were again positioned across the top of the tank and a depth gauge made for measuring surface profiles. A micrometer type of depth gauge was found too slow for this work and a depth gauge reading to an accuracy of 0.01 inches and with a rapid friction drive for raising and lowering was constructed.

Quantity measurement was by orifice plate meters placed in the radial and tangential supply lines. Various combinations of orifice plate sizes and air-water or water-mercury differential gauges gave a complete coverage of both high and low supply rates. The measured meter constants were in agreement with B.S.1088.

5. Velocity Measurements in the Large Vortex Tank

In the large vortex tank the velocities to be measured were generally higher than those in the small tank and the methods of velocity measurement found satisfactory in the small tank were used, sometimes in a modified form, in the large tank. In the outer regions of the tank velocity measurements were again made with a propeller and it was confirmed, by observing the path followed by beads of unit specific gravity that the flow mainly followed horizontal circular paths at these greater radii. Nearer the core, for stronger vortices, the velocities were sometimes high enough for a pitot tube to be used. Close to the core of the vortex the flow became three dimensional in character and this variable direction of flow near the core made it impossible to use a pitot tube in this region; the photographing of beads was again used.

With this much larger tank it was not possible to use mirrors as had been possible with the small tank because the image of the beads would have been too small, the camera being some 16 feet from the core. Two cameras were therefore used, one at each window and only 3 feet from the vortex core. Larger beads were obtained, made of a plastic somewhat less dense than water, and were brought to the correct density by drilling holes in them and ballasting with plasticene.

The problem now to be overcome was that of synchronising the two cameras. It was realised that precise synchronisation of the shutters was almost impossible and so a method was devised which depended on approximate synchronisation of the shutters.

The method depended on using a stroboscope set at a known flashing rate in conjunction with a small amount of general illumination. The camera shutters were opened for about half a second and were known to be synchronised to within about a $\frac{1}{20}$th of a second. The photographs obtained showed a streak for the path of the bead and on this streak were bright spots, instantaneous photographs of the bead whenever it was illuminated by the high intensity light of the stoboscope. Typical examples of these photographs are given in Figs. 19 and 20. The two photographs were therefore accurately synchronised by the stroboscope. Each stroboscope flash gave a bright picture of the bead on each photograph and from the stroboscope flashing rate the time interval between any two bead images was determined. The co-ordinates of corresponding images together with the time interval between them could be used to determine velocities in a manner exactly similar to that used for the small tank.

It was found necessary to use two synchronised stroboscopes, one triggered by the other, in order to obtain

sufficient intensity of illumination. One stroboscope was placed alongside each camera. The camera shutters were synchronised by using cable releases which led to a common trigger. The synchronisation was adjusted firstly by listening to the click of the shutters and was checked by setting the shutter speed of one camera to a $\frac{1}{10}$th of a second and triggering an electronic flash from the other camera; a second photograph was taken with the shutters set at $1/_{25}$ of a second. If the shutters were synchronised to within $\frac{1}{10}$ or $\frac{1}{25}$th of a second a flash photograph was obtained on both cameras. It was found possible to synchronise consistently within $\frac{1}{10}$th of a second and sometimes to a $\frac{1}{25}$th.

The stroboscope flashing rate was set at 420 flashes per minute for an exposure time of $\frac{1}{2}$ second. This ensured that at least three, and at most four, stroboscope flashes appeared on every photograph: more flashes would have been confusing while less would not have sufficied because some images are hidden behind the vortex core. It was found that the photographic conditions were very critical; too much general lighting blotted out the stroboscopic images while too little general lighting gave no streak to connect up the stroboscopic images so that the path of the bead could not be traced. To record bead images either when the beads were illuminated by the

stroboscopes or the general lighting only, a very fast film was required and special development had to be given. Details of the various films and developers used are given in Appendix 1.

The interpretation of these photographs was exactly the same as for the small tank except that measurements were now made of corresponding stroboscope flash images. The scale factors were also determined in a similar fashion.

FIG 9

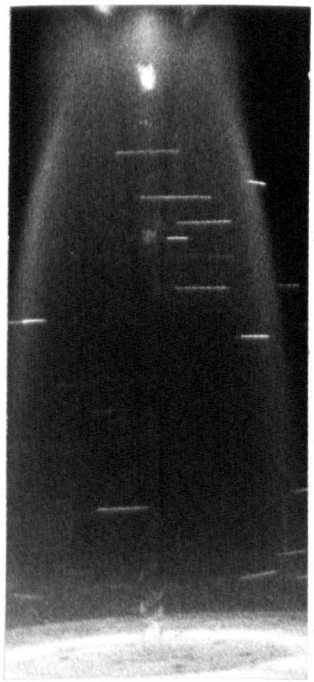

1st Viewing Direction

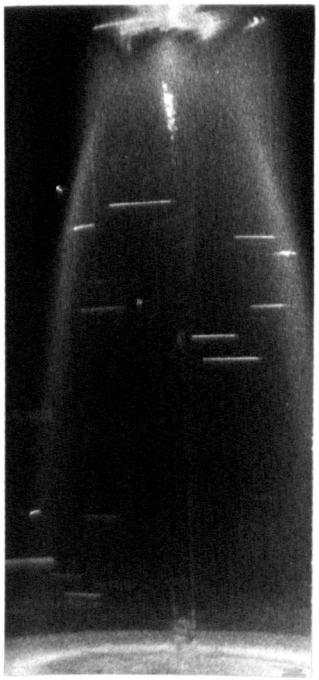

2nd Viewing Direction

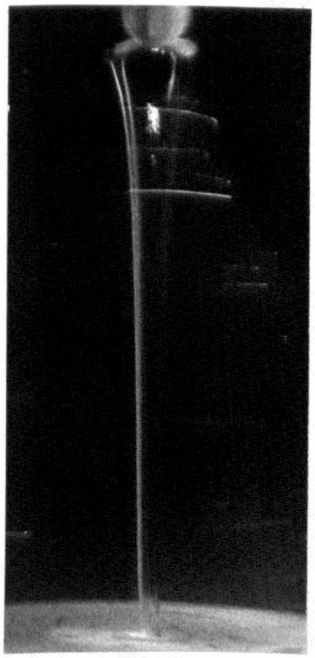

SMALL TANK: TYPICAL VELOCITY TRACES

FIG 10

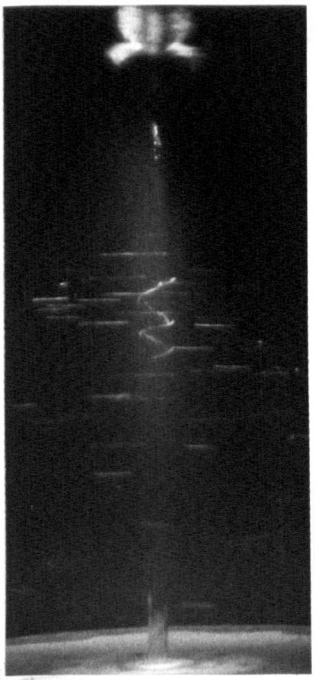

1st Viewing Direction

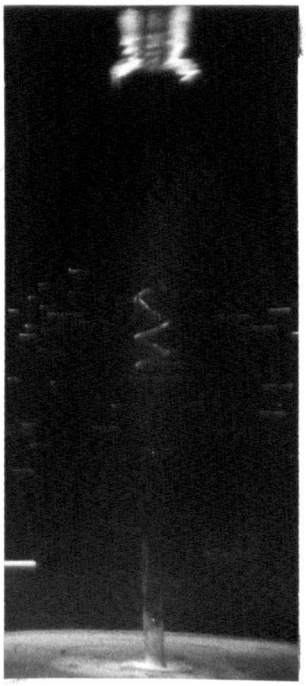

2nd Viewing Direction

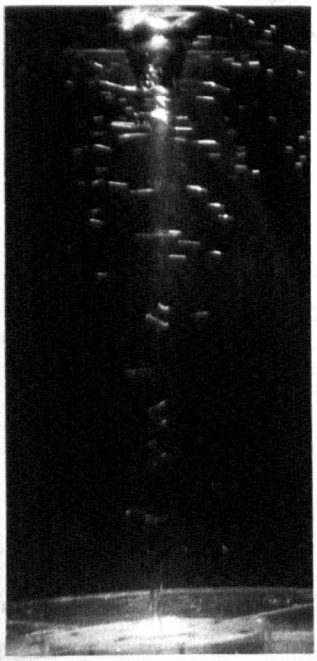

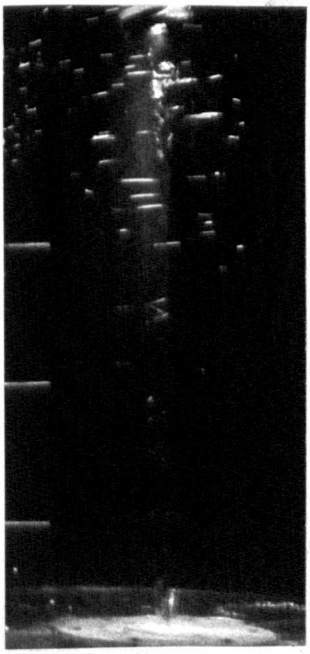

SMALL TANK: TYPICAL VELOCITY TRACES

SMALL TANK : C = 44 INS.²/SEC.

FIG.11

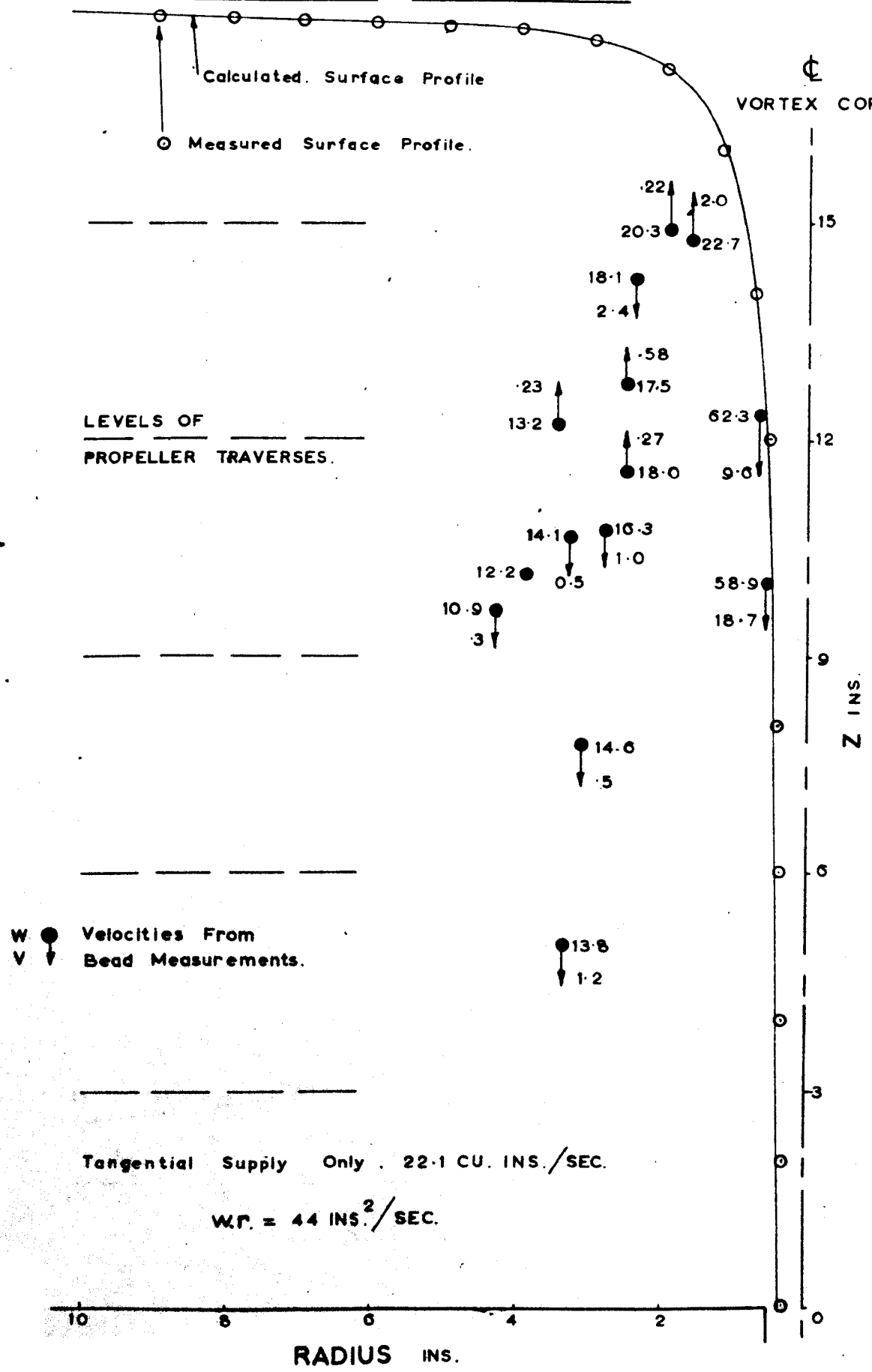

FIG.12

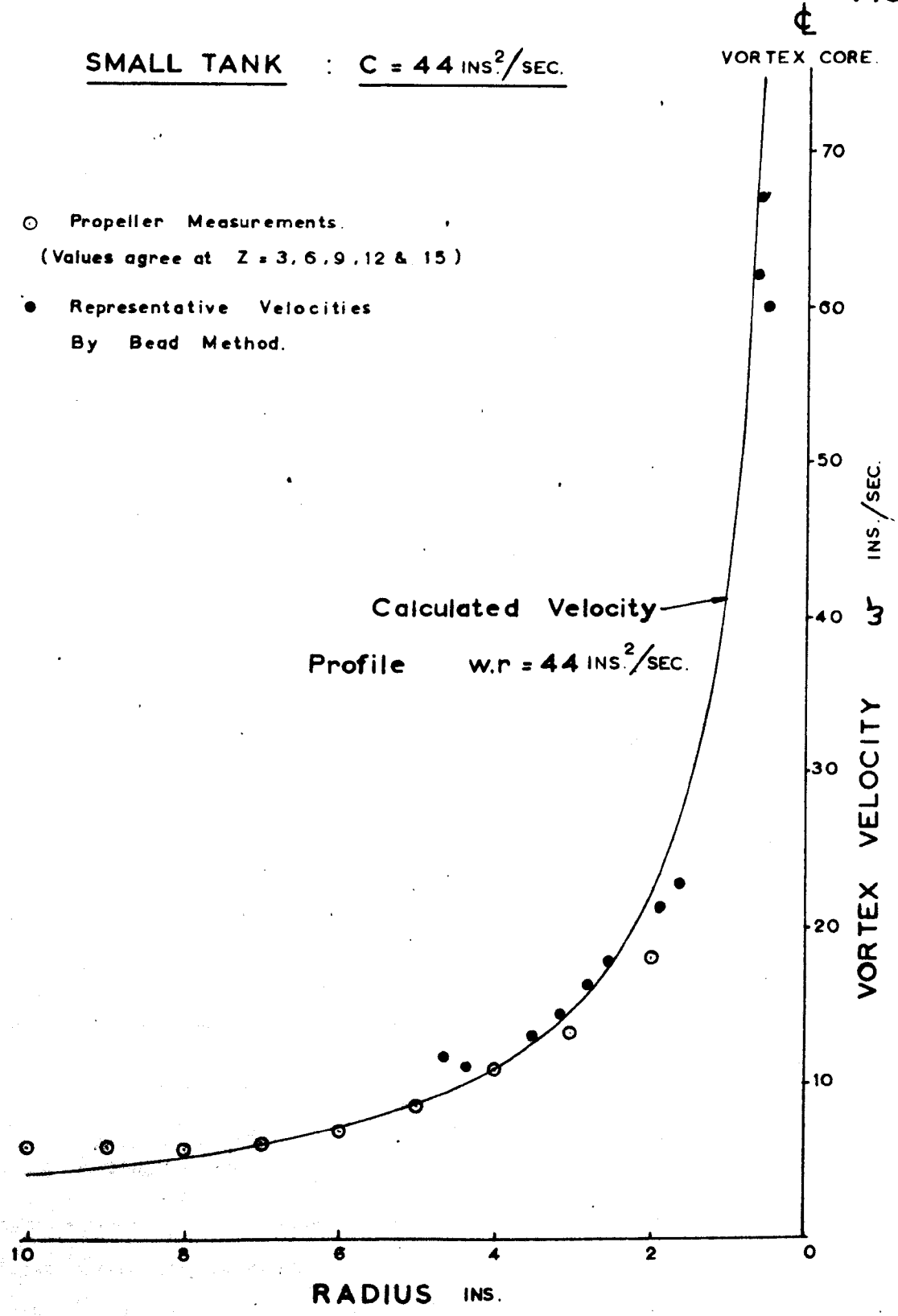
SMALL TANK : C = 44 INS.²/SEC.
℄
VORTEX CORE.
⊙ Propeller Measurements.
(Values agree at Z = 3, 6, 9, 12 & 15)
● Representative Velocities
By Bead Method.
Calculated Velocity
Profile w.r = 44 INS.²/SEC.
70
60
50
40
30
20
10
VORTEX VELOCITY w INS./SEC.
10
8
6
4
2
0
RADIUS INS.

FIG.13

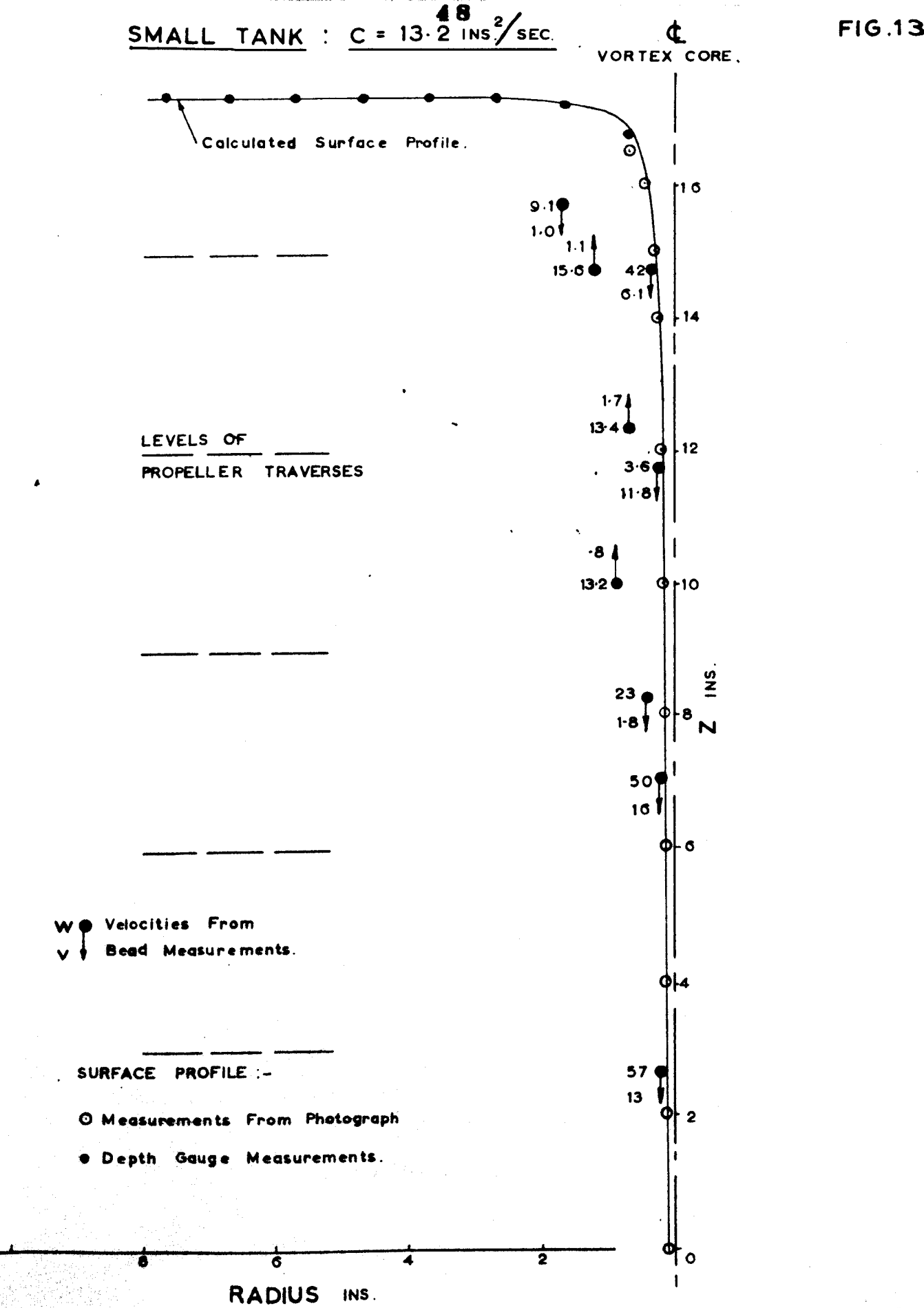
SMALL TANK : C = 13·2 INS²/SEC.
℄ VORTEX CORE.
Calculated Surface Profile.
LEVELS OF PROPELLER TRAVERSES
W Velocities From
V Bead Measurements.
SURFACE PROFILE :-
O Measurements From Photograph
● Depth Gauge Measurements.
9·1
1·0
1·1
15·6
42
6·1
1·7
13·4
3·6
11·8
·8
13·2
23
1·8
50
16
57
13
16
14
12
10
8
6
4
2
0
Z INS.
8
6
4
2
RADIUS INS.

FIG. 14

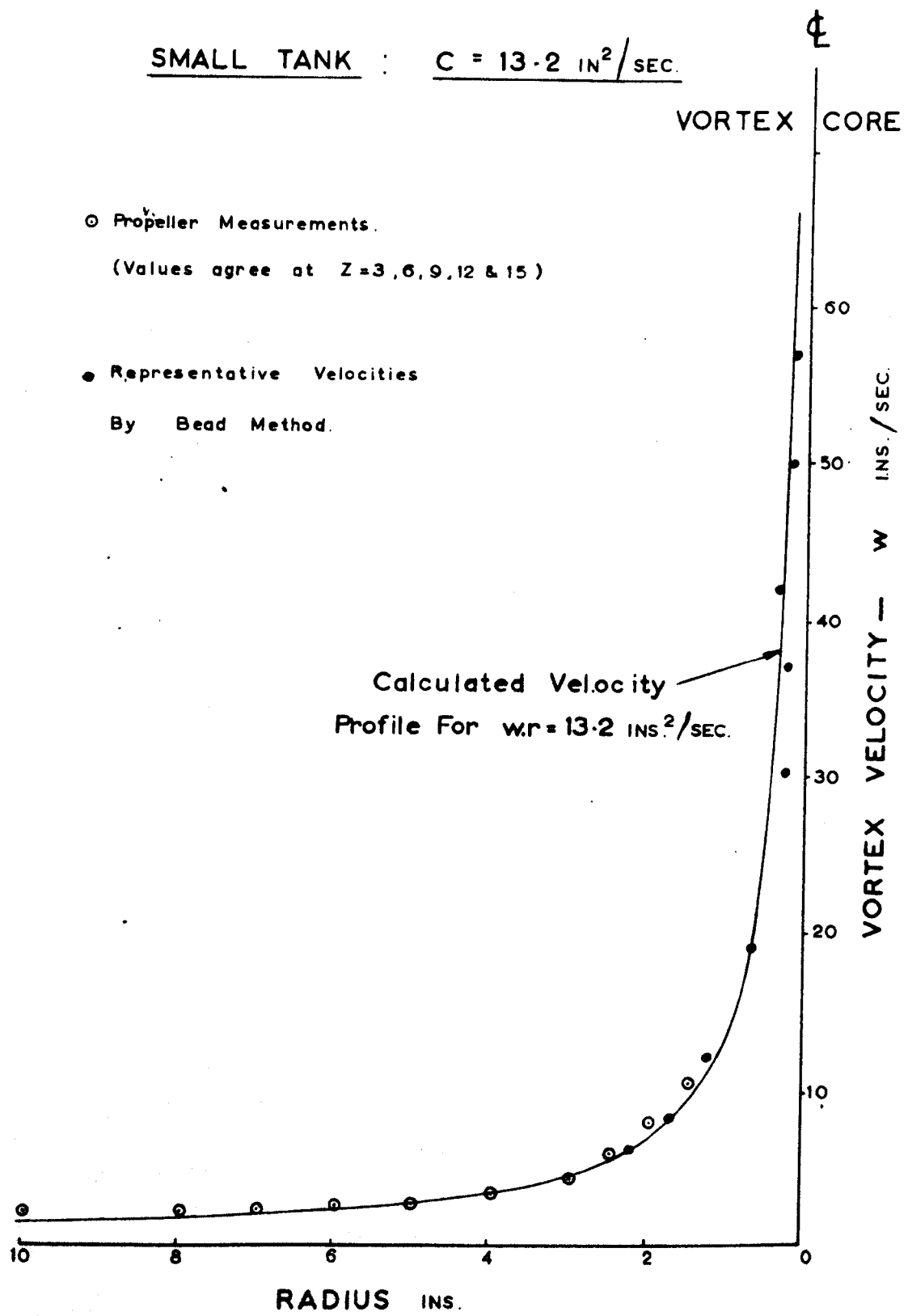
SMALL TANK : C = 13·2 IN²/SEC.
℄
VORTEX CORE
⊙ Propeller Measurements.
(Values agree at Z = 3, 6, 9, 12 & 15)
● Representative Velocities
By Bead Method.
Calculated Velocity
Profile For w.r = 13·2 INS.²/SEC.
60
50
40
30
20
10
VORTEX VELOCITY — w INS./SEC.
10
8
6
4
2
0
RADIUS INS.

FIG. 15

SMALL TANK : C = 13·2 IN.^{2}/SEC.

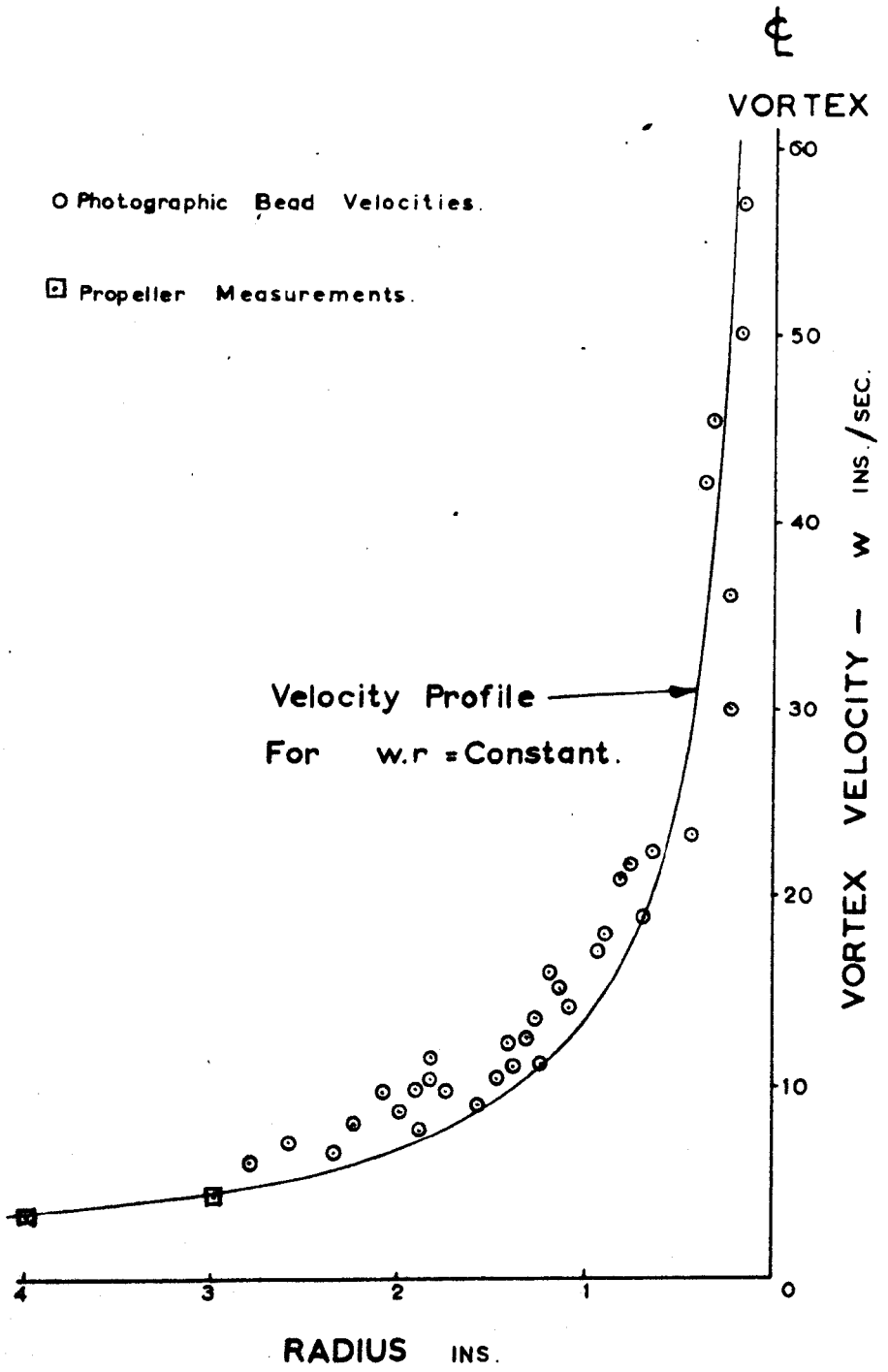

SMALL TANK : C = 8·4 INS.²/SEC

FIG. 16

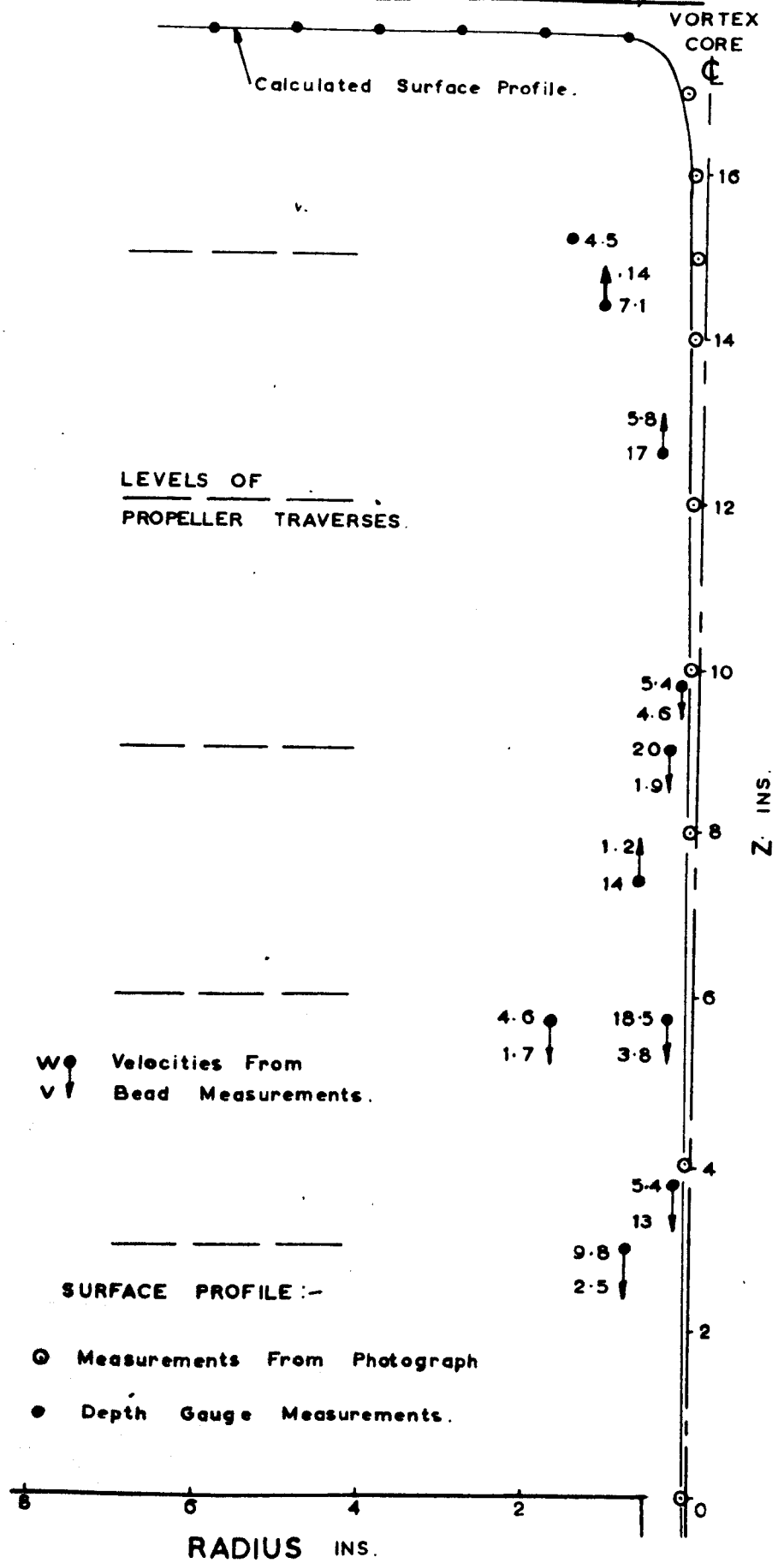

FIG.17

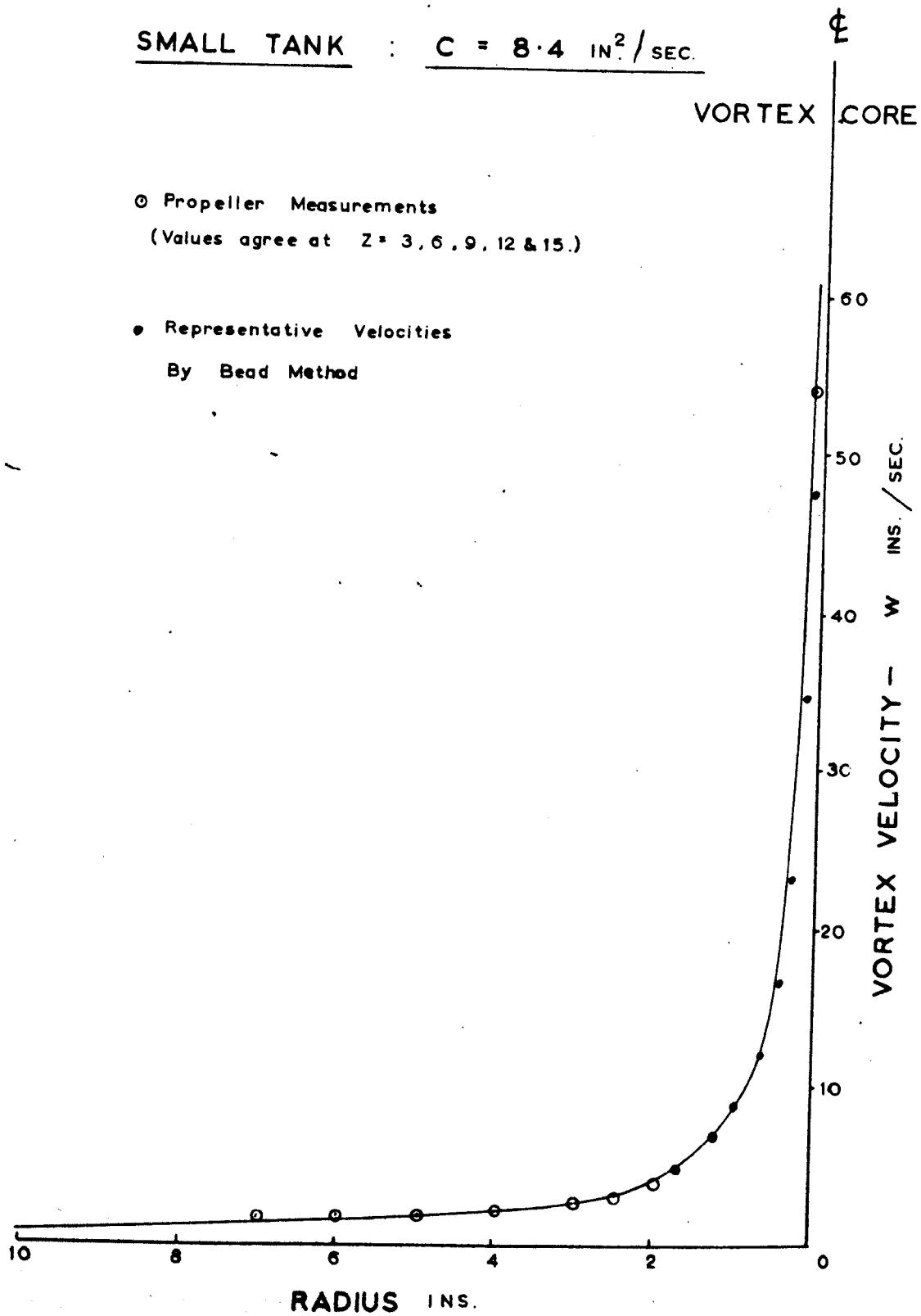
SMALL TANK : C = 8·4 IN.²/SEC.
℄
VORTEX CORE
⊙ Propeller Measurements
(Values agree at Z = 3, 6, 9, 12 & 15.)
• Representative Velocities
By Bead Method
60
50
40
30
20
10
0
VORTEX VELOCITY — W INS./SEC.
10
8
6
4
2
0
RADIUS INS.

FIG.18

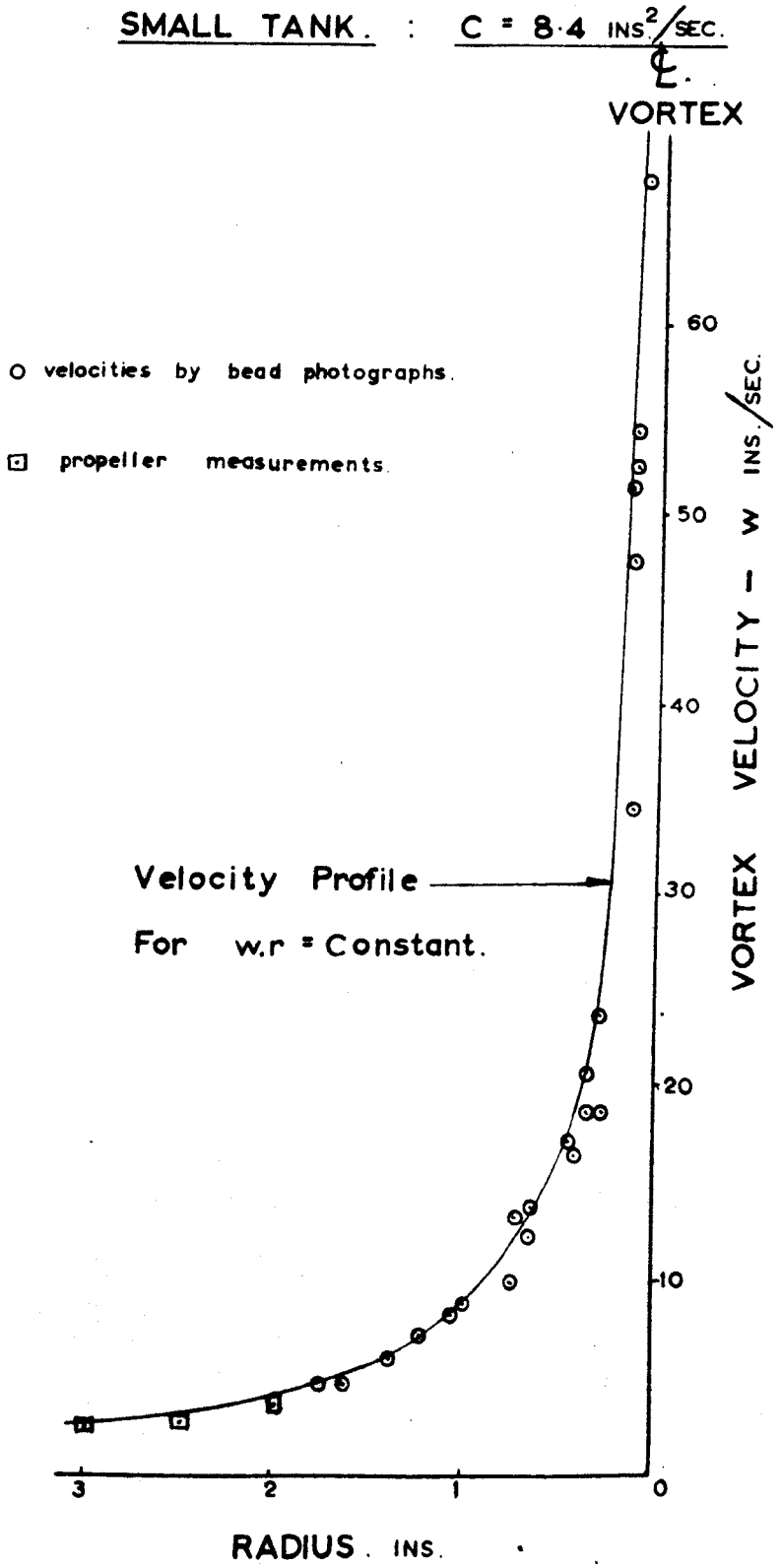
SMALL TANK. : C = 8·4 INS.²/SEC.
℄.
VORTEX
O velocities by bead photographs.
⊡ propeller measurements.
Velocity Profile
For w.r = Constant.
VORTEX VELOCITY - W INS./SEC.
60
50
40
30
20
10
0
3
2
1
RADIUS. INS.

FIG 19

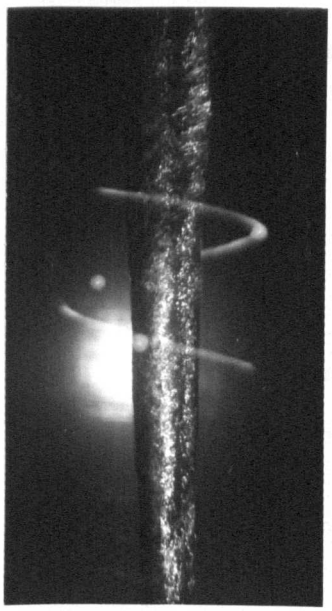

1st Viewing Direction

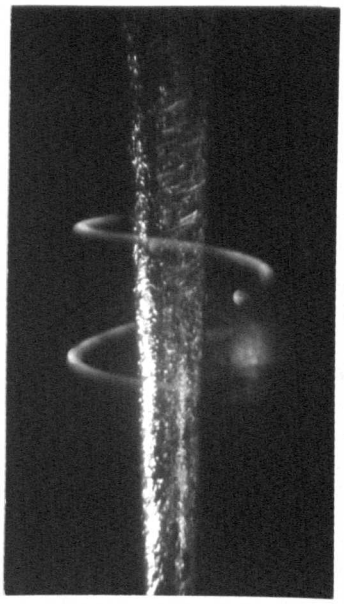

2nd Viewing Direction

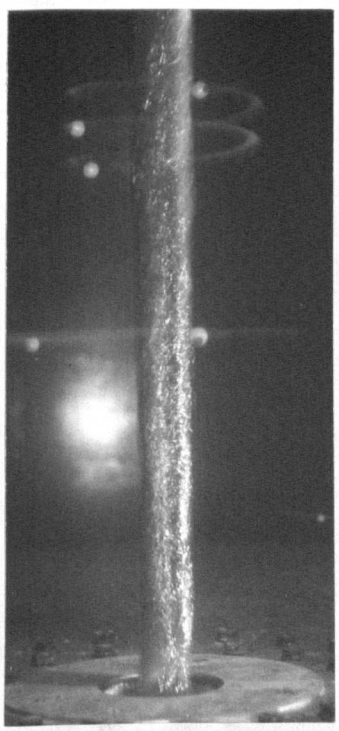

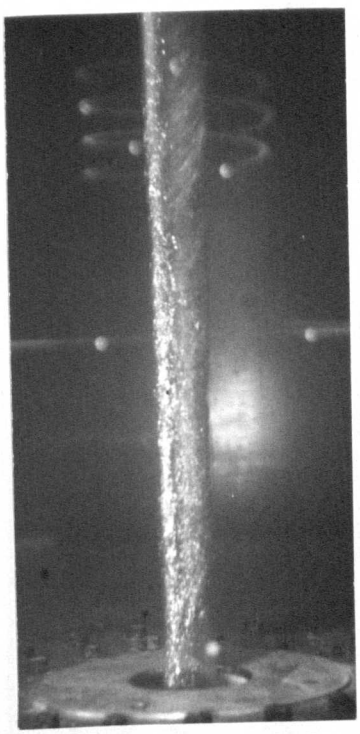

LARGE TANK: TYPICAL VELOCITY TRACES

Stroboscopic images of beads are seen joined by feint streaks.

FIG 20

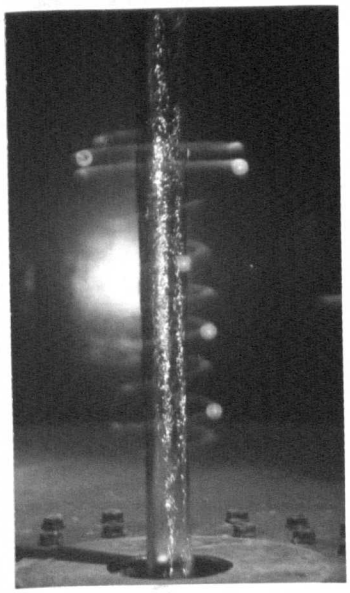

1st Viewing Direction

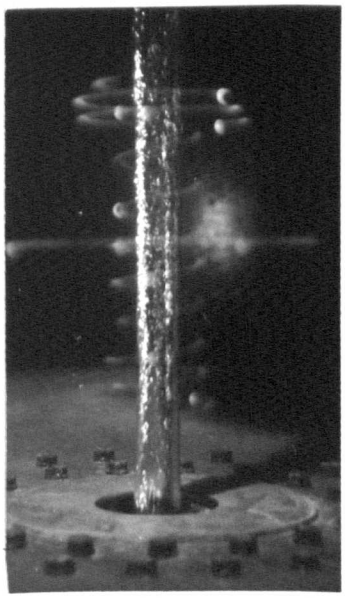

2nd Viewing Direction

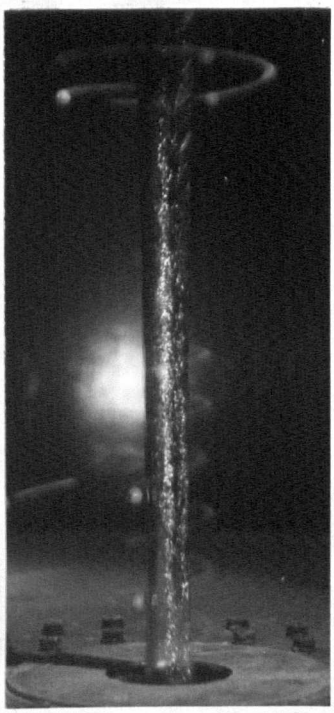

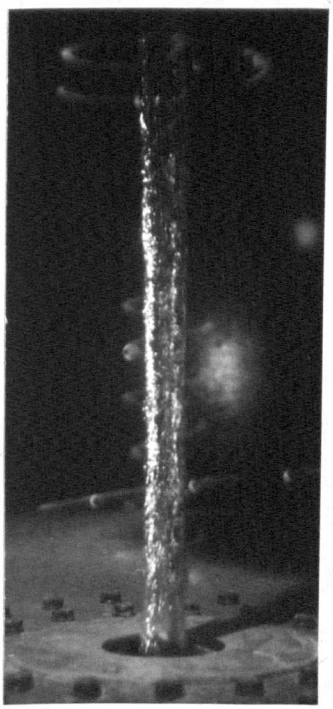

LARGE TANK: TYPICAL VELOCITY TRACES.
Stroboscopic images of beads are seen joined by feint streaks.

FIG. 21

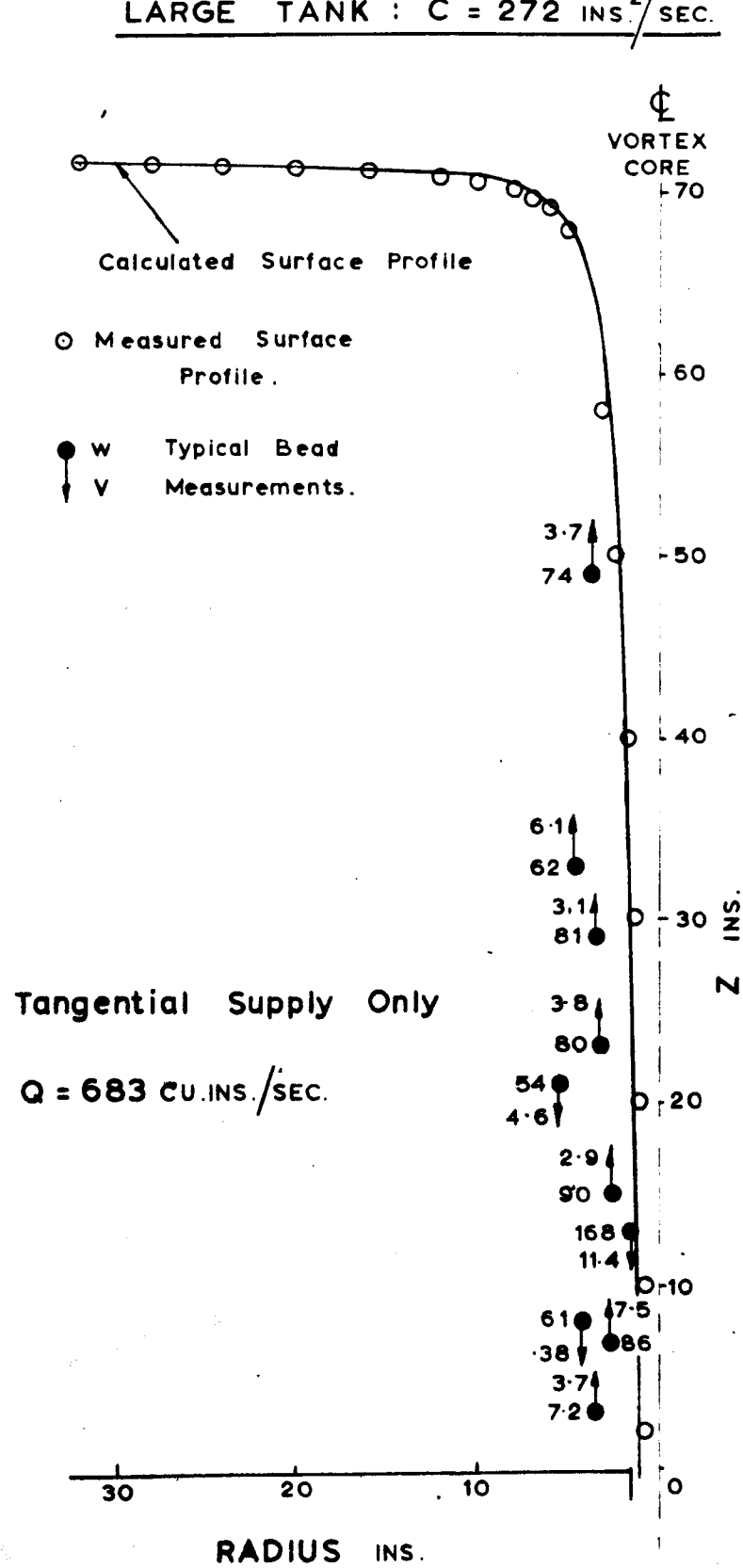
LARGE TANK : C = 272 INS.²/SEC.
℄
VORTEX CORE
Calculated Surface Profile
Measured Surface Profile.
W Typical Bead
V Measurements.
Tangential Supply Only
Q = 683 CU.INS./SEC.
3·7
7·4
6·1
6·2
3·1
8·1
3·8
8·0
5·4
4·6
2·9
9·0
16·8
11·4
7·5
6·1
8·6
3·8
3·7
7·2
70
60
50
40
30
20
10
0
Z INS.
30
20
10
RADIUS INS.

FIG.22

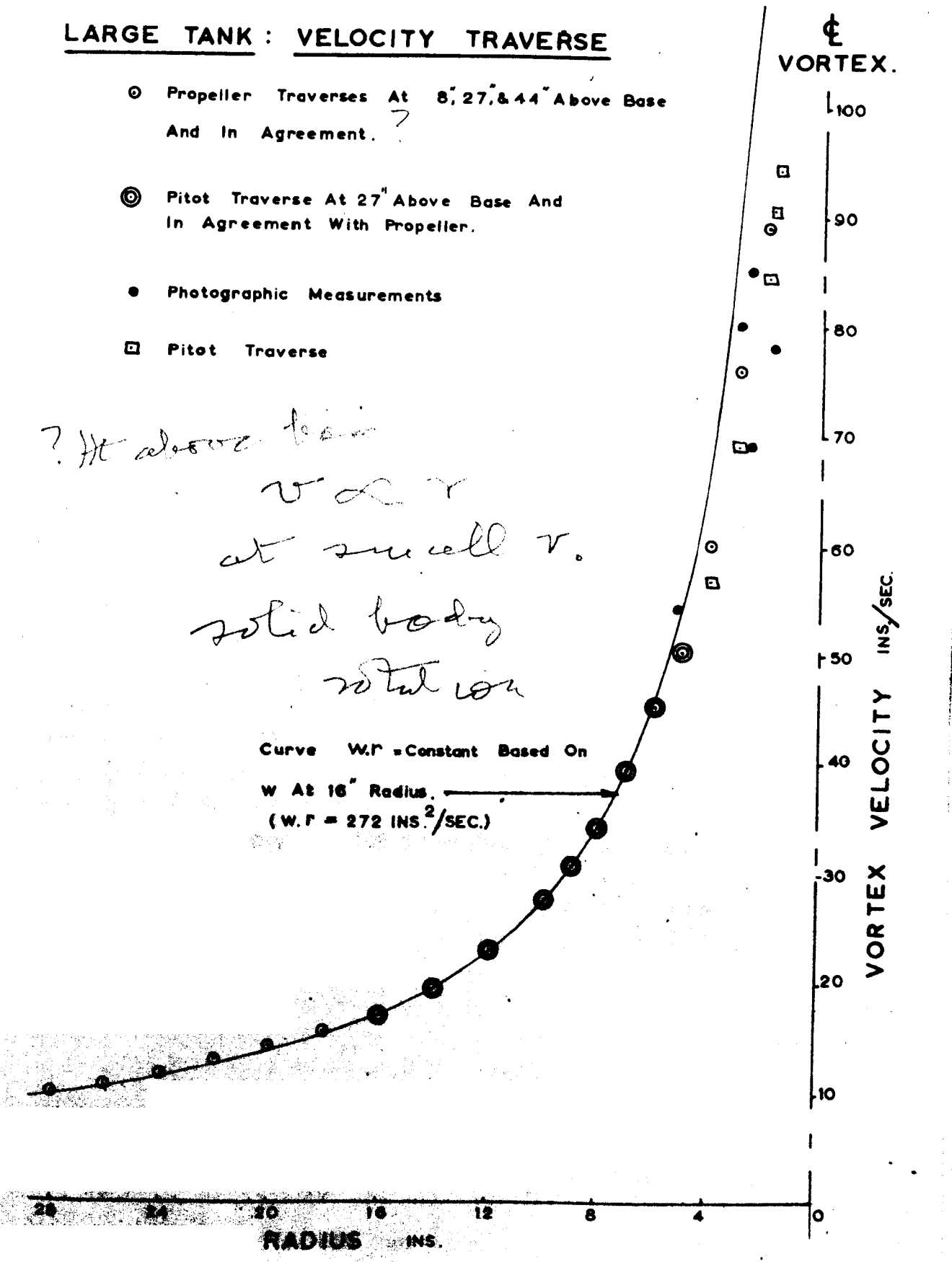
LARGE TANK : VELOCITY TRAVERSE
Propeller Traverses At 8", 27", & 44" Above Base And In Agreement.
Pitot Traverse At 27" Above Base And In Agreement With Propeller.
Photographic Measurements
Pitot Traverse
? Ht above bin
v ∝ r
at small r.
solid body rotation
Curve W.r = Constant Based On W At 16" Radius.
(W.r = 272 INS.²/SEC.)
℄ VORTEX.
100
90
80
70
60
50
40
30
20
10
0
VORTEX VELOCITY INS/SEC.
28
24
20
16
12
8
4
RADIUS INS.

FIG.23

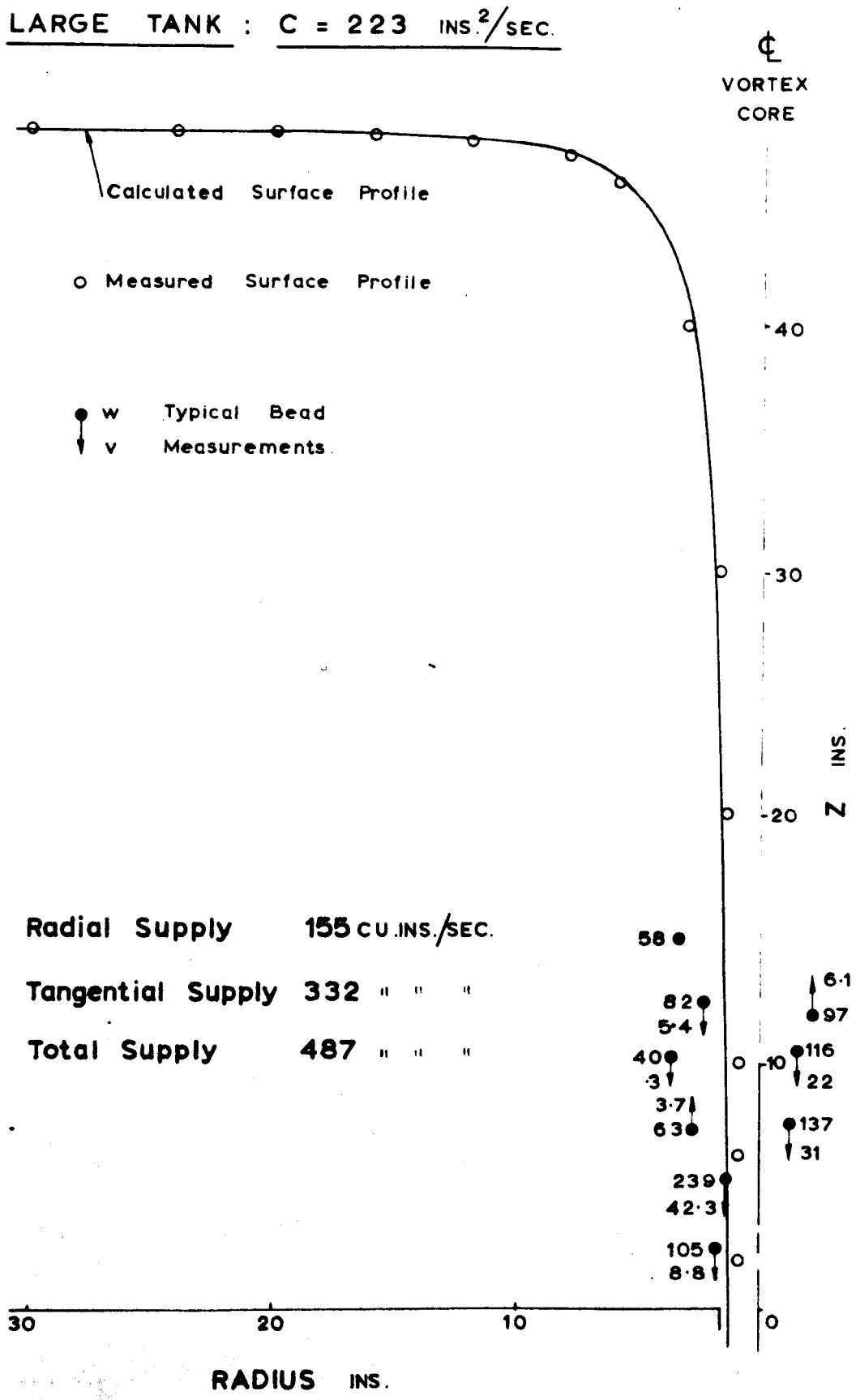
LARGE TANK : C = 223 INS.²/SEC.
℄
VORTEX
CORE
Calculated Surface Profile
Measured Surface Profile
w Typical Bead
v Measurements
40
30
20
Z INS.
Radial Supply 155 CU.INS./SEC.
Tangential Supply 332 " " "
Total Supply 487 " " "
58
82
5·4
40
·3
3·7
63
239
42·3
105
8·8
6·1
97
116
22
137
31
10
0
30
20
10
0
RADIUS INS.

FIG. 24

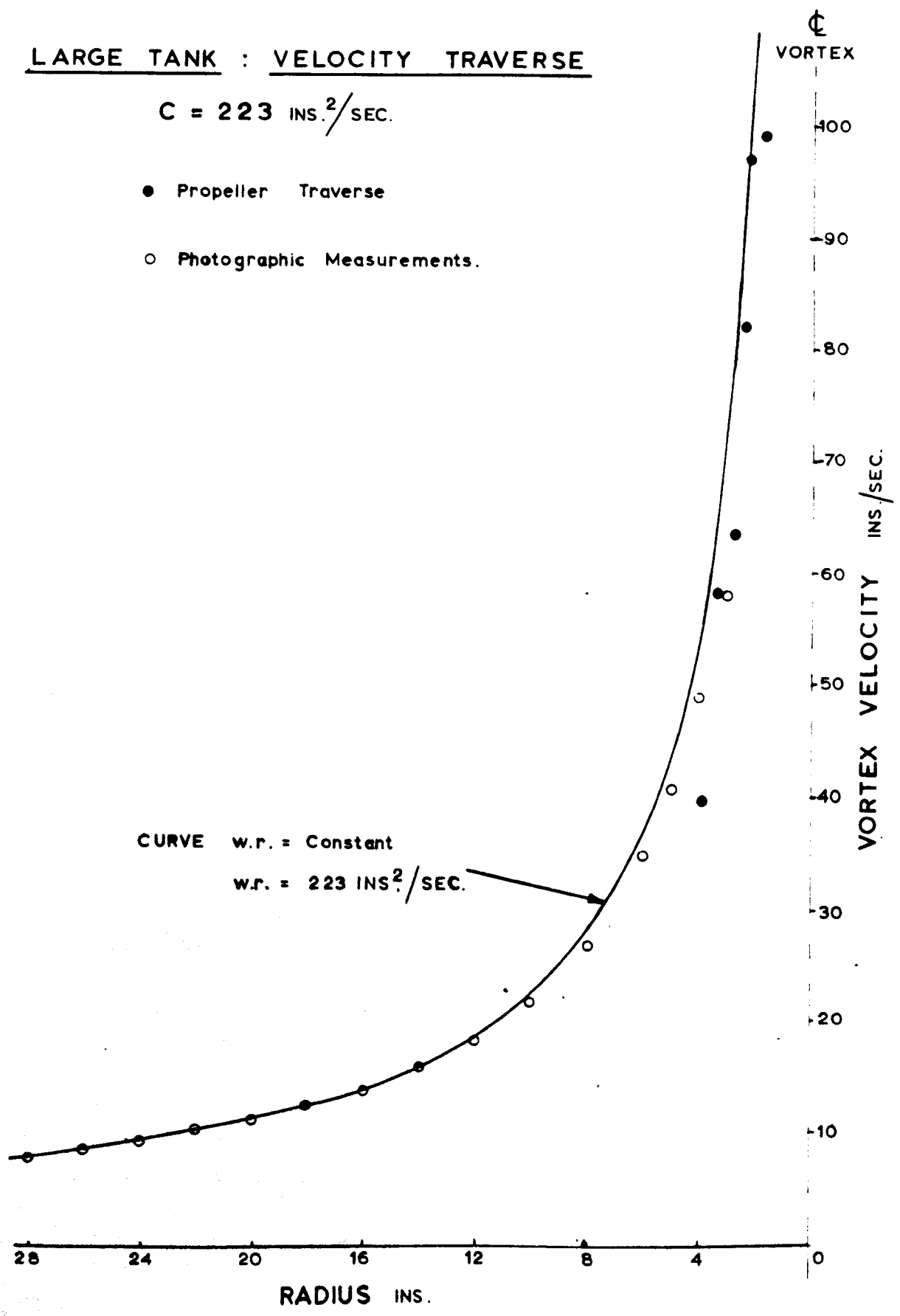
LARGE TANK : VELOCITY TRAVERSE
C = 223 INS.²/SEC.
● Propeller Traverse
○ Photographic Measurements.
℄ VORTEX
CURVE w.r. = Constant
w.r. = 223 INS.²/SEC.
VORTEX VELOCITY INS./SEC.
400
90
80
70
60
50
40
30
20
10
0
28
24
20
16
12
8
4
RADIUS INS.

FIG. 25

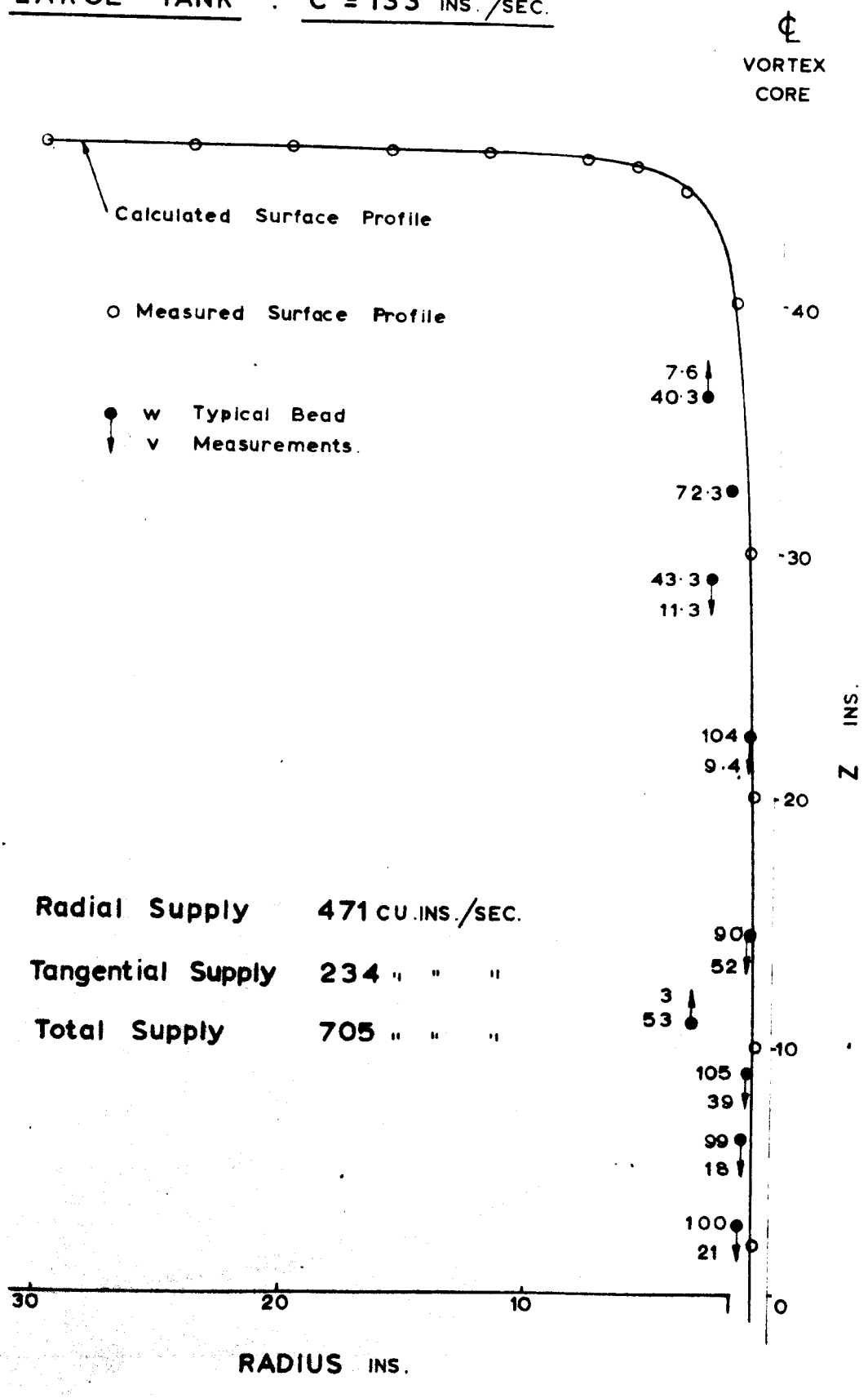
LARGE TANK : C = 133 INS.²/SEC.
℄
VORTEX
CORE
Calculated Surface Profile
Measured Surface Profile
w Typical Bead
v Measurements.
7·6
40·3
72·3
43·3
11·3
104
9·4
90
52
3
53
105
39
99
18
100
21
Radial Supply 471 CU.INS./SEC.
Tangential Supply 234 " " "
Total Supply 705 " " "
40
30
20
10
0
Z INS.
30
20
10
0
RADIUS INS.

FIG. 26

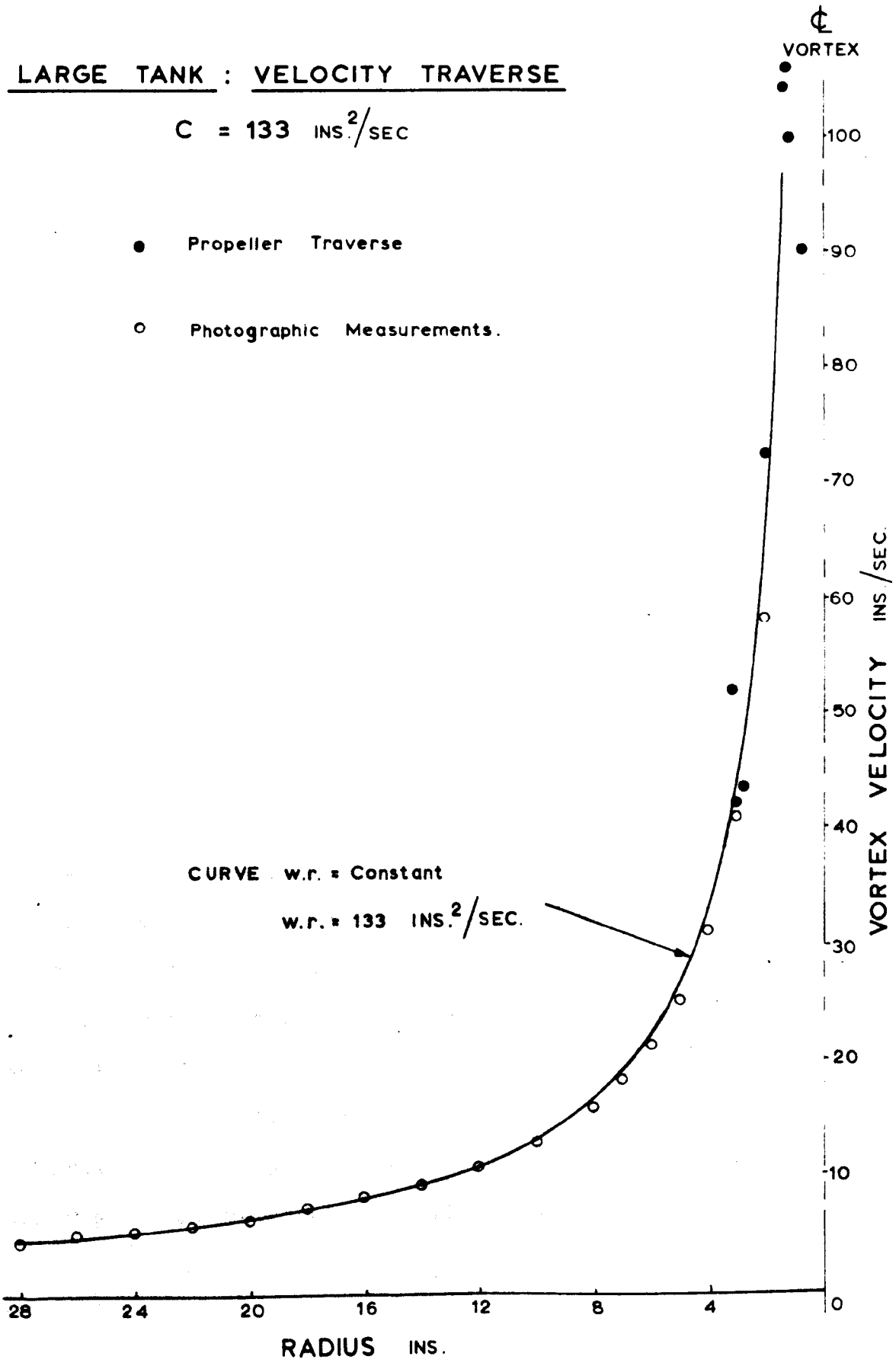
LARGE TANK : VELOCITY TRAVERSE
C = 133 INS.²/SEC
Propeller Traverse
Photographic Measurements.
CURVE w.r. = Constant
w.r. = 133 INS.²/SEC.
℄ VORTEX
100
90
80
70
60
50
40
30
20
10
0
VORTEX VELOCITY INS./SEC.
28
24
20
16
12
8
4
RADIUS INS.

CHAPTER IV

THE RESULTS OF THE FREE SPIRAL VORTEX EXPERIMENTS

1. Velocity Measurements

In discussing the purposes of the investigation of the free spiral vortex it was shown that a first requirement was a study of the velocity distribution within the vortex structure. The design and construction of apparatus suitable for this purpose and the velocity measuring techniques to be used have been described in the previous chapter. The measured velocities were then used to study the velocity distributions of several different strengths of vortex for both the small and the large sizes of apparatus. Where possible an overlap of readings by the various methods was obtained to give an additional check on the accuracy of the methods used.

The measurements of velocity obtained are plotted in Figs 11 to 18 and 21 to 26. In Figs.11,13,16,21,23 and 25 representative readings are plotted in the positions in which they were taken, except that it is assumed that there is axial symmetry; without this assumption it is not possible to plot the results on a two dimensional diagram. The readings given in these figures indicate the general coverage of the observations throughout the depth of the tank. They show the two components of velocity measured, the swirl velocity and the vertical velocity ; the direction upwards or downwards of the vertical velocity being indicated by an arrow.

It should be pointed out that efforts were made to measure the third component, the radial velocity, but this component was found to be so small in comparison with the other velocities that it could not be measured.

The swirl velocities from these same readings are then plotted against radius, no account being taken of the depth at which they were made. From these figures it is apparent that the swirl velocity profile is independent of the depth at which it is taken. In these figures the full line drawn in has been obtained by taking a measured value of the vorticity, swirl velocity multiplied by radius, at a certain radius and then calculating velocities at all other radii by assuming that velocity varies inversely with radius. This line is therefore the velocity profile to be expected from the non-viscous theory. For the small tank this curve has been based on the velocity measured at a radius of four inches because this was considered to be the position nearest to the centre line of the vortex at which reliable measurements could be made with the propeller meter. In the larger tank measurements of tangential velocity were made at a radius of sixteen inches, the geometrically similar position in this tank, and velocity curves assuming constant vorticity were drawn based on the values of velocity obtained at this station.

The figures in which swirl velocity is plotted against radius show that the swirl velocity profile is, firstly, independent of the depth at which it is taken and, secondly, it approximates very closely to the lines of constant vorticity.

There is a slight divergence of the ideal curve of velocities and the measured values near the centre of the tank where the velocity gradient is steep and where the viscous losses must be significant. Even in these central regions the deviation from the ideal free vortex velocity distribution is not great. It would therefore appear that the assumption of velocity varying inversely with radius is accurate to within a small distance from the core surface and even in this region it is still approximately true.

It will be seen that three strengths of vortex have been studied for each size of tank. These three vortices are considered to be representative of a weak, a moderate and a strong vortex and were chosen because it was thought that different strengths of vortex might vary in their approximation to the ideal velocity distribution. This was considered possible because the shear gradients, and therefore the energy losses, are higher in a strong vortex than in a weaker vortex: this energy loss in a strong vortex might also be accentuated by the comparatively lower flow and therefore lower rate of supply of energy.

However, the results show that the approximation to the ideal velocity distribution is as good for the stronger vortices as it is for the weaker ones and it is therefore concluded that the assumption of constant vorticity is approximately correct for all strengths of vortex.

FIG. 27

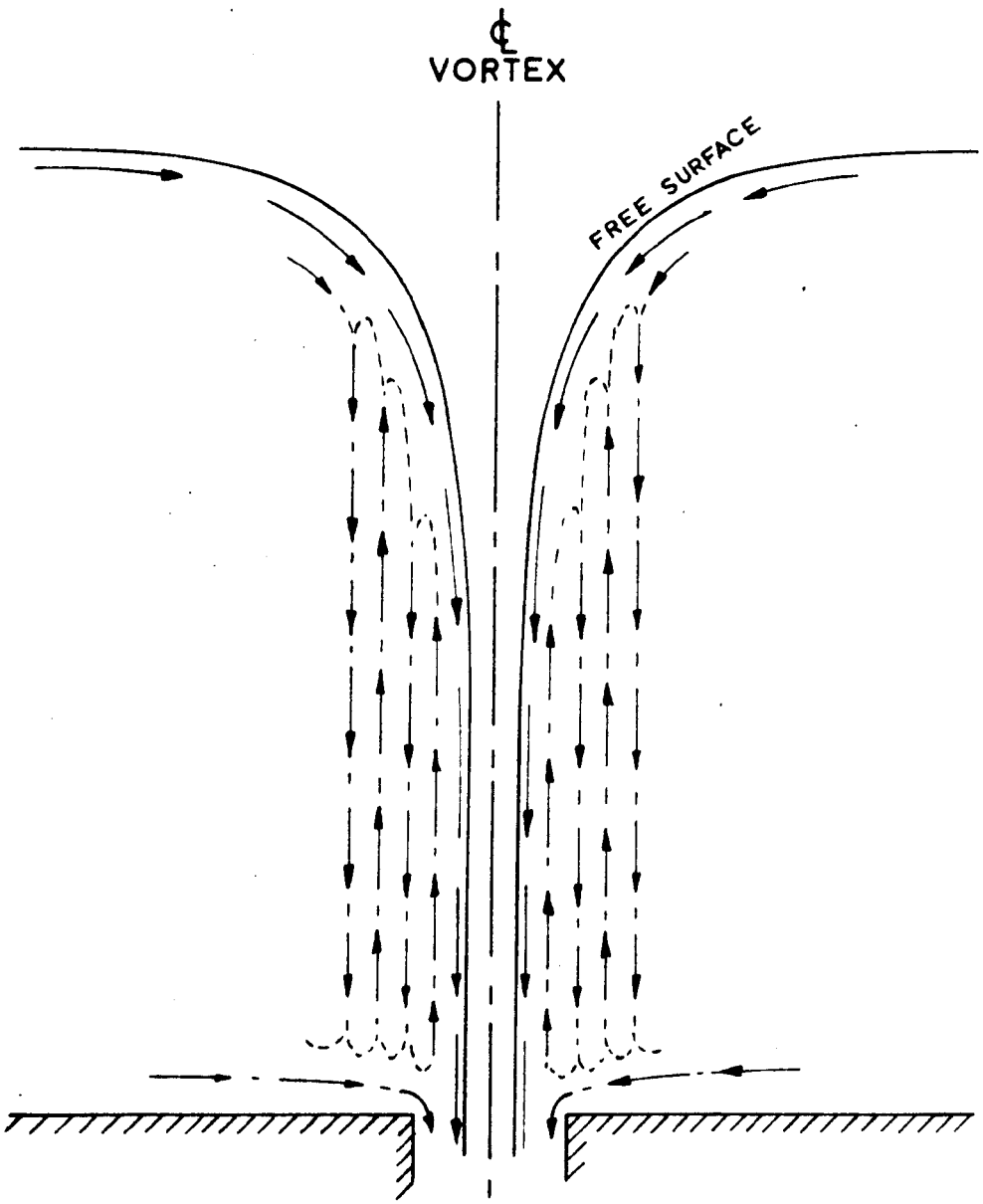

SKETCH OF OBSERVED RADIAL AND VERTICAL VELOCITY PATTERN NEAR CORE OF VORTEX.

FIG. 28.

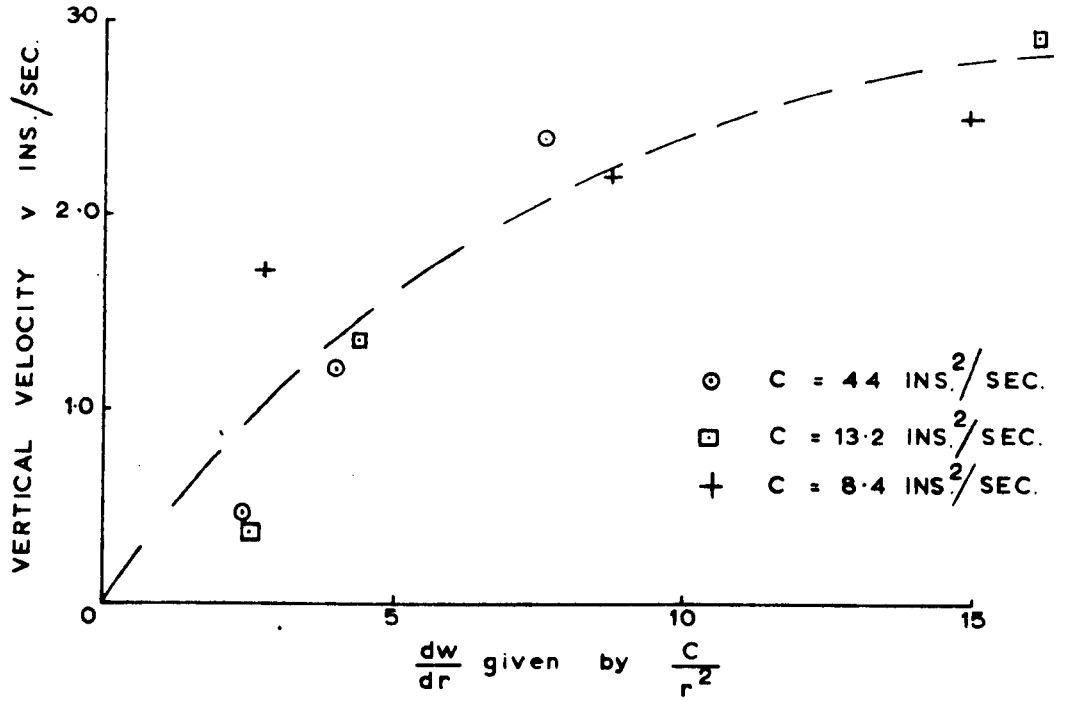

MAXIMUM DOWNWARDS VERTICAL VELOCITIES PLOTTED AGAINST SWIRL VELOCITY GRADIENT.

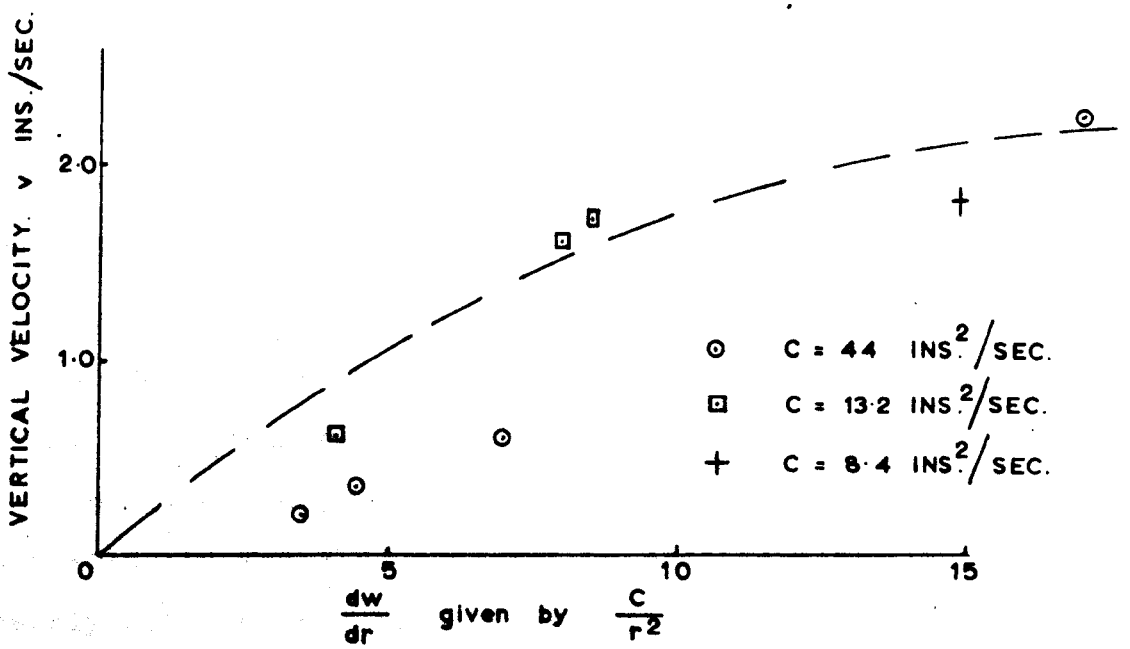

MAXIMUM UPWARDS VERTICAL VELOCITIES PLOTTED AGAINST SWIRL VELOCITY GRADIENT.

2. The Vertical and Radial Velocity Components.

Using beads with specific gravity equal to that of water it was possible to study not only the tangential velocity component but also the radial and vertical components. In Chapter III it has been shown how the various velocity components can be derived from photographic traces of the bead movements, although the radial component has been omitted because it was observed that throughout the whole region of flow the radial velocities were too low to be measured. Radial flow must exist to satisfy the continuity condition, but when the flow is distributed throughout the tank the radial velocities need only be a fraction of an inch per second and this is too low to be measured, especially when comparatively high tangential velocities are present.

A study of vertical velocities again showed that in the outer regions of the tanks the vertical velocities were immeasurably small. Nearer the core, perhaps within $1\frac{1}{2}$ inches radius in the small tank and 6 inches radius in the large tank, the vertical velocities became significant and an interesting pattern of velocity became apparent. In the surface of the core itself the velocity was always downwards and increased approximately with the square root of the depth.

At a slightly larger radius the beads were sometimes observed to move upwards in a helical path; with increasing radius alternate layers of upward and downward moving fluid were found. Some representative values obtained at various radii are shown plotted in Figs. 11,13,16,21,23 and 25 and direction is also indicated. Unfortunately the beads do not follow the flow perfectly because of slight variations in their specific gravity from that of the water and also,because of the velocity gradient,they must be subject to slight "lift" forces. It was not therefore possible to watch a particular bead follow a flow path for any length of time, but, observing isolated parts of the flow and by considerations of continuity, the flow pattern sketched in Fig.27 has been built up. The main observable radial flow occurred at the surface and the bottom of the tank: elsewhere little or no flow was observed radially. The significance of this observation will be discussed later.

It is apparent that the regions in which vertical velocities are significant are also regions in which the swirl velocity has a high gradient. There being, apparently, no appreciable radial component of velocity except near the surface and the bottom it is reasonable to assume that the vertical flow is supplying fresh energy to replace the energy losses caused by the swirl velocity gradient and its resultant shear stresses. A plot of vertical velocity components against swirl velocity gradient was therefore made to investigate a possible correlation.

The vertical velocities have been shown to occur in alternate layers of upward and downward flow. Therefore there will be, over a small radial distance, a variation from a certain maximum upwards flow to a certain maximum downwards flow and all possible intermediate values will also be present. When velocity readings are made using the bead method only a few of the values will happen to give maximum upward or downward velocity components; there will be many of the intermediate values. To draw the graph of vertical velocities against shear gradient, only the maximum vertical velocities at any given radius have been used and they have been plotted against the ideal value of the swirl velocity shear gradient, $\frac{dw}{dr}$ given by $\frac{c}{r^2}$. Because the final outflow is downwards the downwards velocities were always found to be higher than the upwards velocities and therefore two graphs have been drawn, one for the upward and one for the downward vertical velocities; they are shown in Fig.28. The number of readings available for these graphs was not sufficient to be conclusive, but it is significant that readings taken from three different strengths of vortex show agreement when plotted on this basis. More evidence would be needed to prove or disprove this apparent correlation between vertical velocities and swirl velocity gradient.

FIG. 29

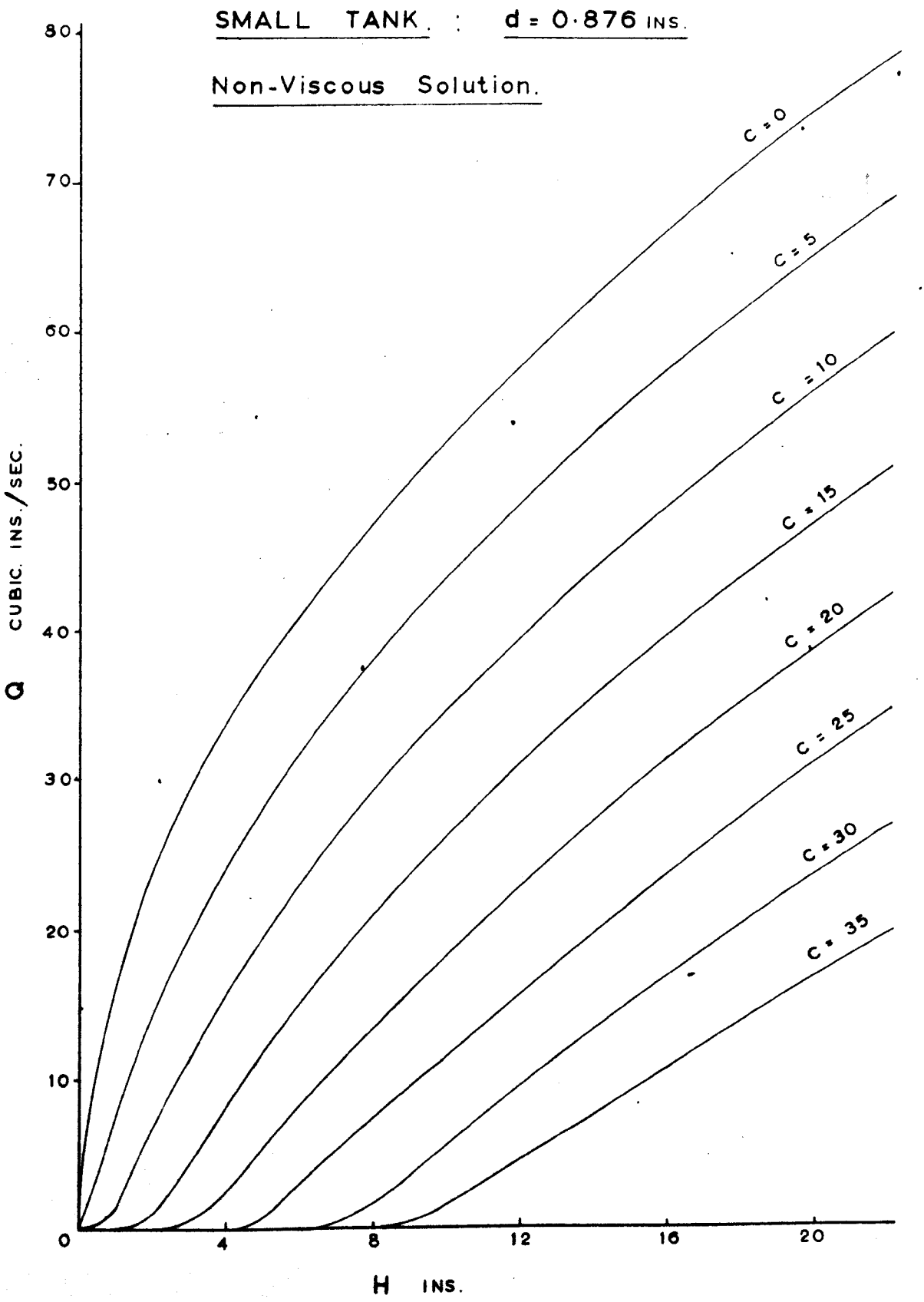
SMALL TANK : d = 0·876 INS.
Non-Viscous Solution.
C = 0
C = 5
C = 10
C = 15
C = 20
C = 25
C = 30
C = 35
Q CUBIC. INS./SEC.
H INS.
0
10
20
30
40
50
60
70
80
4
8
12
16
20

FIG.30

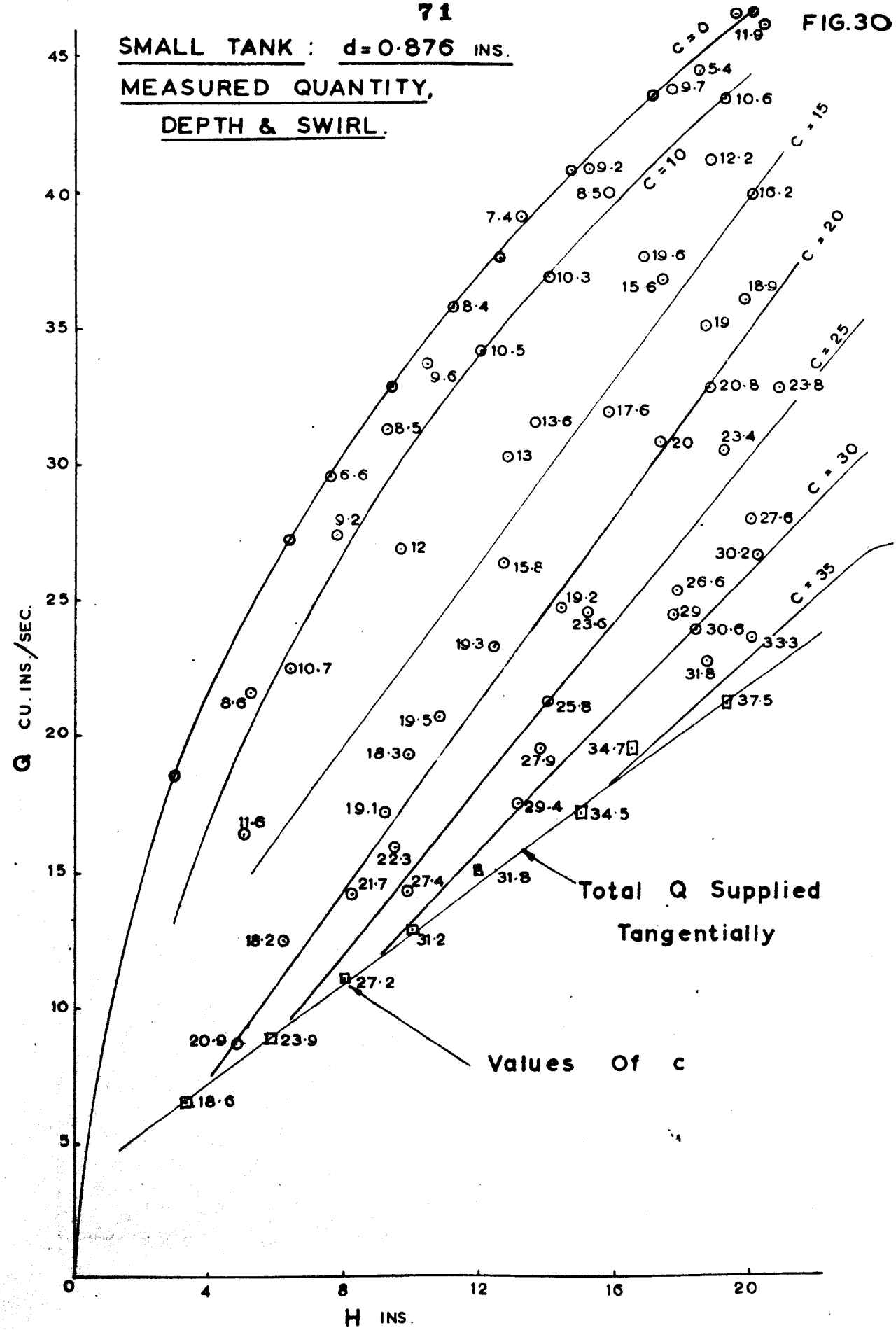
SMALL TANK : d=0·876 INS.
MEASURED QUANTITY,
DEPTH & SWIRL.
C=0
C=10
C=15
C=20
C=25
C=30
C=35
Q CU. INS./SEC.
H INS.
0
4
8
12
16
20
5
10
15
20
25
30
35
40
45
Total Q Supplied Tangentially
Values Of c
11·9
5·4
9·7
10·6
9·2
8·50
12·2
7·4
16·2
19·6
10·3
15 6
18·9
8·4
19
10·5
9·6
20·8
23·8
8·5
13·6
17·6
6·6
13
20
23·4
9·2
12
27·6
15·8
30·2
26·6
19·2
23·6
29
19·3
30·6
33·3
10·7
31·8
8·6
25·8
37·5
19·5
18·30
34·7
27·9
19·1
29·4
34·5
11·6
22·3
21·7
27·4
31·8
18·2
31·2
27·2
20·9
23·9
18·6

FIG .31

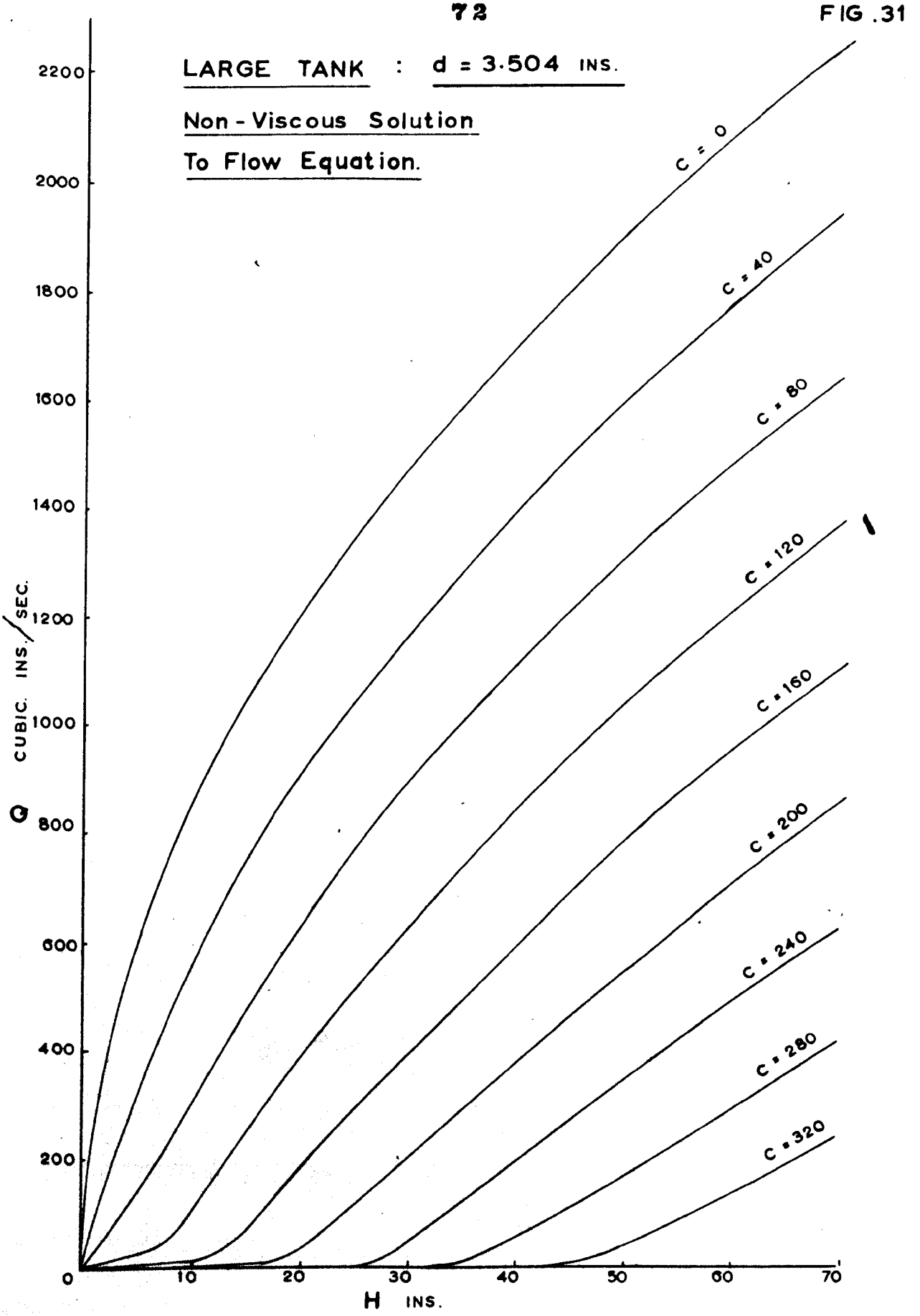
LARGE TANK : d = 3.504 INS.
Non - Viscous Solution
To Flow Equation.
C = 0
C = 40
C = 80
C = 120
C = 160
C = 200
C = 240
C = 280
C = 320
Q CUBIC. INS./SEC.
2200
2000
1800
1600
1400
1200
1000
800
600
400
200
0
10
20
30
40
50
60
70
H INS.

FIG. 32

LARGE TANK : d = 3·54 INS.

MEASURED QUANTITY, DEPTH & SWIRL.

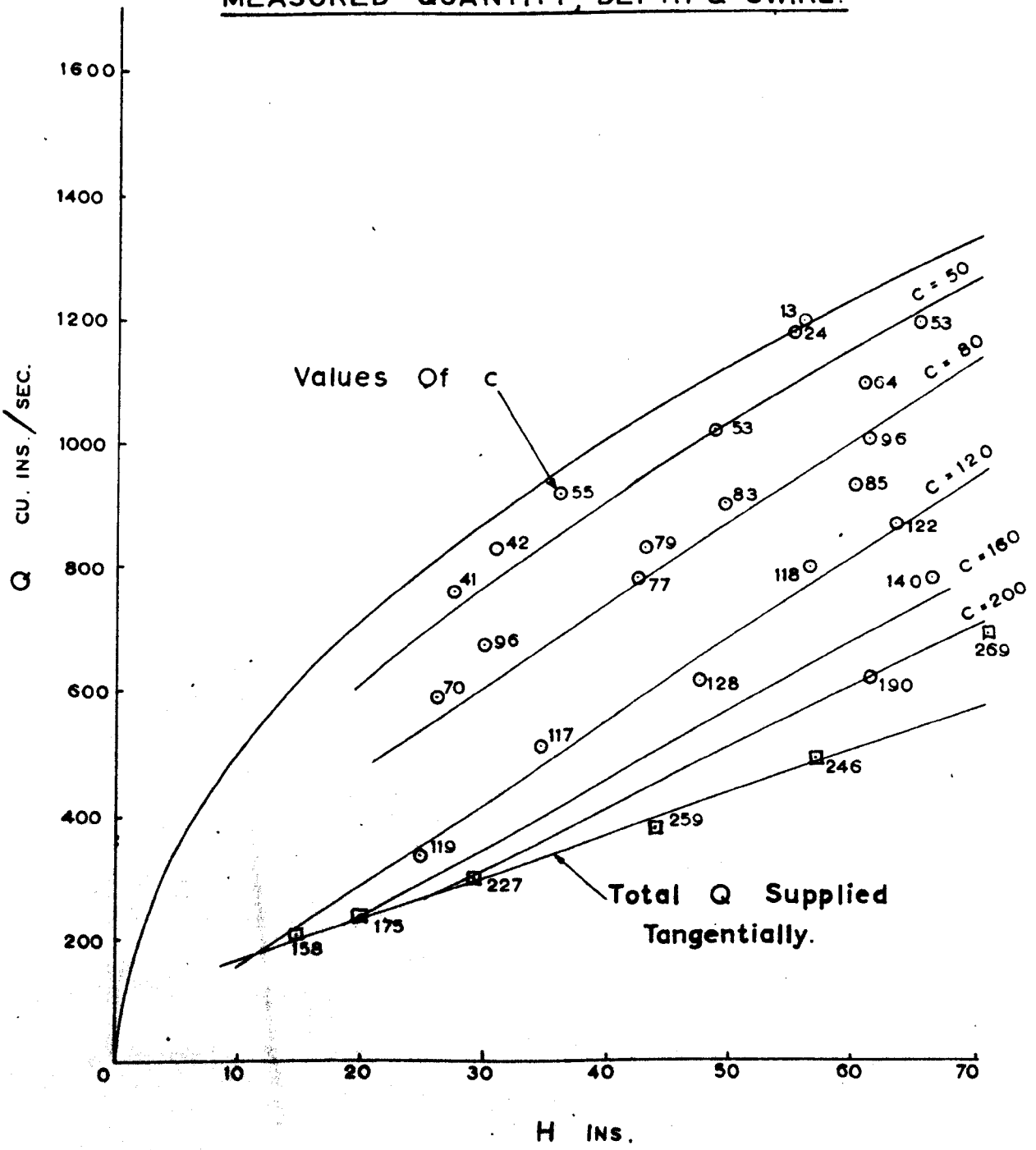

FIG.33

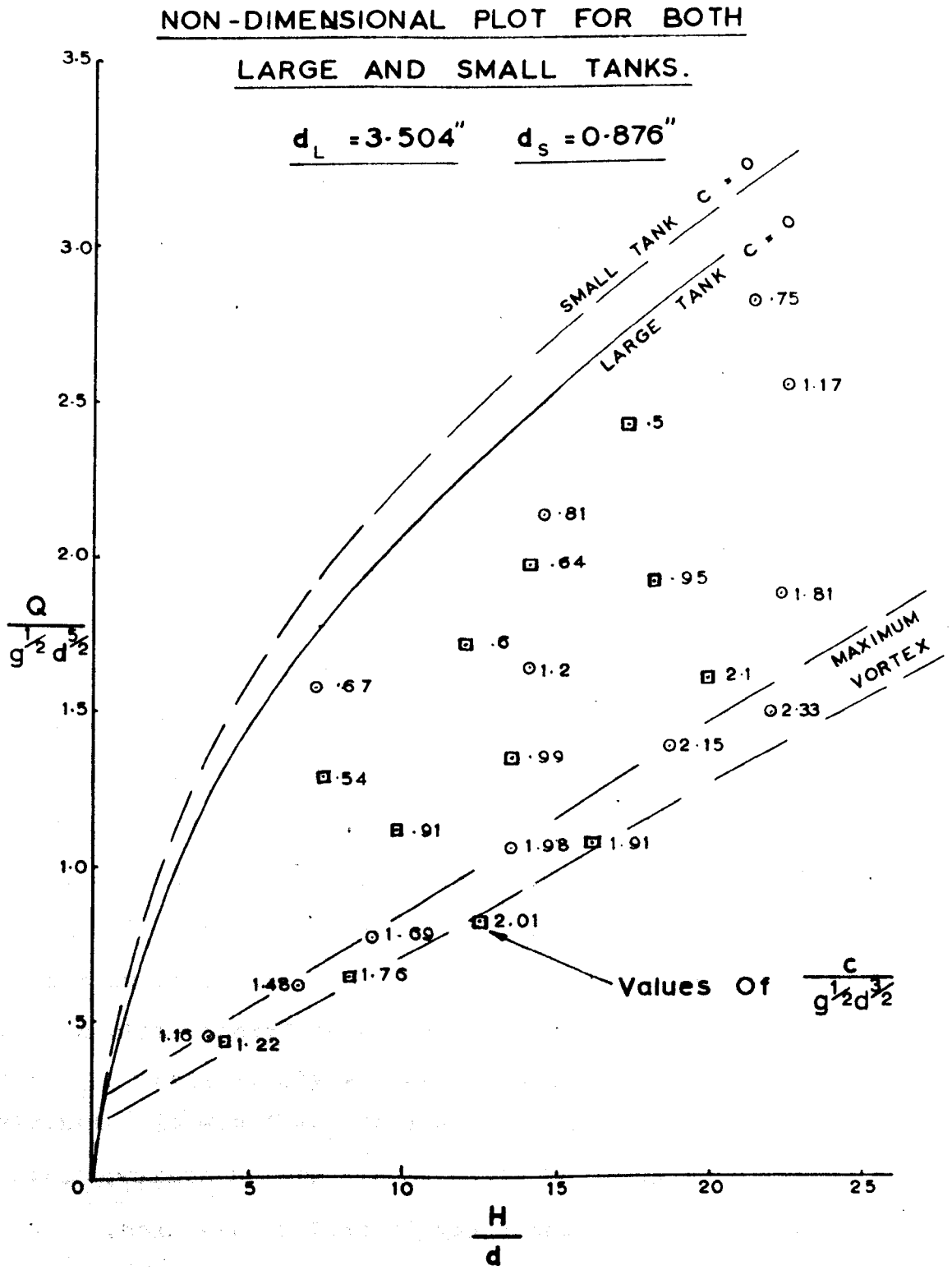
NON-DIMENSIONAL PLOT FOR BOTH
LARGE AND SMALL TANKS.
d_L = 3·504" d_S = 0·876"
SMALL TANK C = 0
LARGE TANK C = 0
MAXIMUM VORTEX
Values Of $\frac{C}{g^{1/2}d^{3/2}}$
$\frac{Q}{g^{1/2}d^{5/2}}$
$\frac{H}{d}$
3·5
3·0
2·5
2·0
1·5
1·0
·5
0
5
10
15
20
25
·75
1·17
·5
·81
·64
·95
1·81
·6
1·2
2·1
·67
2·33
2·15
·99
·54
·91
1·98
1·91
2·01
1·69
1·48
1·76
1·16
1·22

3. Experiments to measure Quantity, Depth and Swirl.

Having established that the swirl velocity pattern is independent of depth and also that swirl velocity follows the ideal constant vorticity curve almost perfectly it was possible to proceed with experiments relating quantity, depth, and swirl.

The first series of tests were carried out in the small tank with an outlet orifice of 0.876 inches diameter. It was considered important to cover the whole range from zero vorticity to maximum vorticity and from low depth to maximum depth to discover whether the behaviour of the vortices followed a definite pattern or whether there was anomalous behaviour under some conditions. With three variables, quantity, head and vorticity, a considerable number of readings are required to cover the whole range adequately. The vorticity can be altered by changing the ratio of tangential to radial supply: if all the supply is radial then the vorticity is zero and if all the supply is tangential then the vorticity is a maximum. When a given proportion of radial and tangential supply has been set and the flow quantity therefore determined, conditions will gradually stabilise until steady values of quantity, depth and swirl are obtained. It was found necessary to make about one hundred sets of measurements before Fig.30 could be fully constructed and for each of these sets a time of about two hours was required to obtain steady flow conditions.

In Fig.30 quantity has been plotted against head and the value of the vorticity has been written against each experimental point. When enough points were obtained lines of equal vorticity could be sketched in. It will be seen that the upper limit of the vortex region is formed by the line c = o and corresponds to an orifice freely discharging under a head of h. It will also be seen that there is a lower limit to the region. This lower limit is set by the maximum vorticity it was found possible to generate at any given depth; for these readings the whole quantity was supplied tangentially. It is interesting to note that the locus of these points of maximum vorticity is a straight line.

This same procedure was now repeated for the large vortex tank with an orifice four times the diameter of that used in the small tank, namely 3.504 inches. Fewer readings were taken but these were carefully distributed so that the whole range of quantity, head and vorticity was adequately covered. The readings obtained are shown plotted in Fig.32.

Fig. 33 was then constructed by plotting together some of the results from both the small and large vortex tanks on a non-dimensional basis. Instead of Q, H and C, the parameters used were $Q/g^{1/2}.d^{5/2}$, H/d and $c/g^{1/2}.d^{3/2}$, where d was the respective outlet diameter. It is seen that there is approximate agreement between the results obtained from the two sizes of apparatus. It is especially interesting to note that even the maximum vorticity that can be generated in the two sizes

of apparatus corresponds. One apparently anomalous result is the slight divergence of the lines of zero swirl. It was found that the large vortex tank gave a coefficient of discharge of 0.59 while the small tank gave 0.63, values which are in good agreement with measurements made by Hamilton Smith, Strickland and several other investigators. Values interpolated from their results would give a value of 0.592 for the coefficient of discharge for the large tank and 0.628 for the small tank.

In the discussion of the dimensional analysis it has been pointed out that a plot of H/d against $Q/g^{\frac{1}{2}}d^{5/2}$ will reveal the degree to which Froude or Reynolds Numbers effect the flow. It has been stated that if readings from two sizes of apparatus are plotted on this basis and it is found that the corresponding values of $c/g^{\frac{1}{2}}d^{3/2}$ agree, then it can be concluded that Reynolds Number does not influence the flow. The flow is then controlled by gravitational forces alone, represented by the Froude Number. Consideration of the results plotted in Fig.33 show that the values plotted from the two sets of apparatus are in approximate agreement; the maximum divergence of values of $c/g^{\frac{1}{2}}d^{3/2}$ is of the order of 12%. It should be pointed out that the Reynolds Numbers corresponding to similar readings from the two tanks differ by 800%, so that it is reasonable to conclude that Reynolds Number plays only a minor part and similarity is obtained by operating at similar Froude Numbers in model and prototype.

FIG. 34

SMALL TANK : MAXIMUM SWIRL FOR DIFFERENT OUTLET DIAMETERS PLOTTED NON-DIMENSIONALLY.

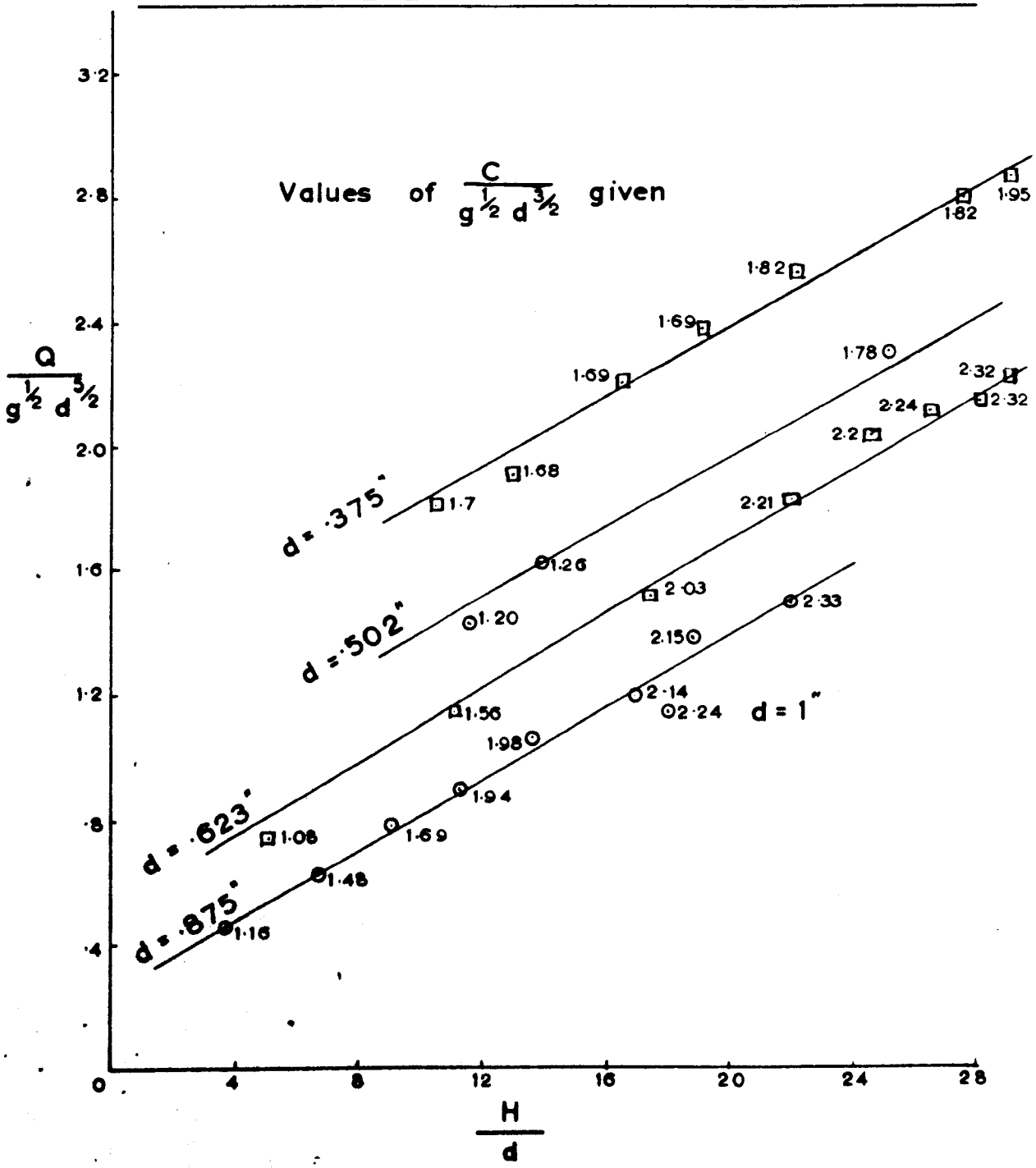

FIG.35

SMALL TANK : MAXIMUM SWIRL VALUES FOR DIFFERENT OUTLET DIAMETERS.

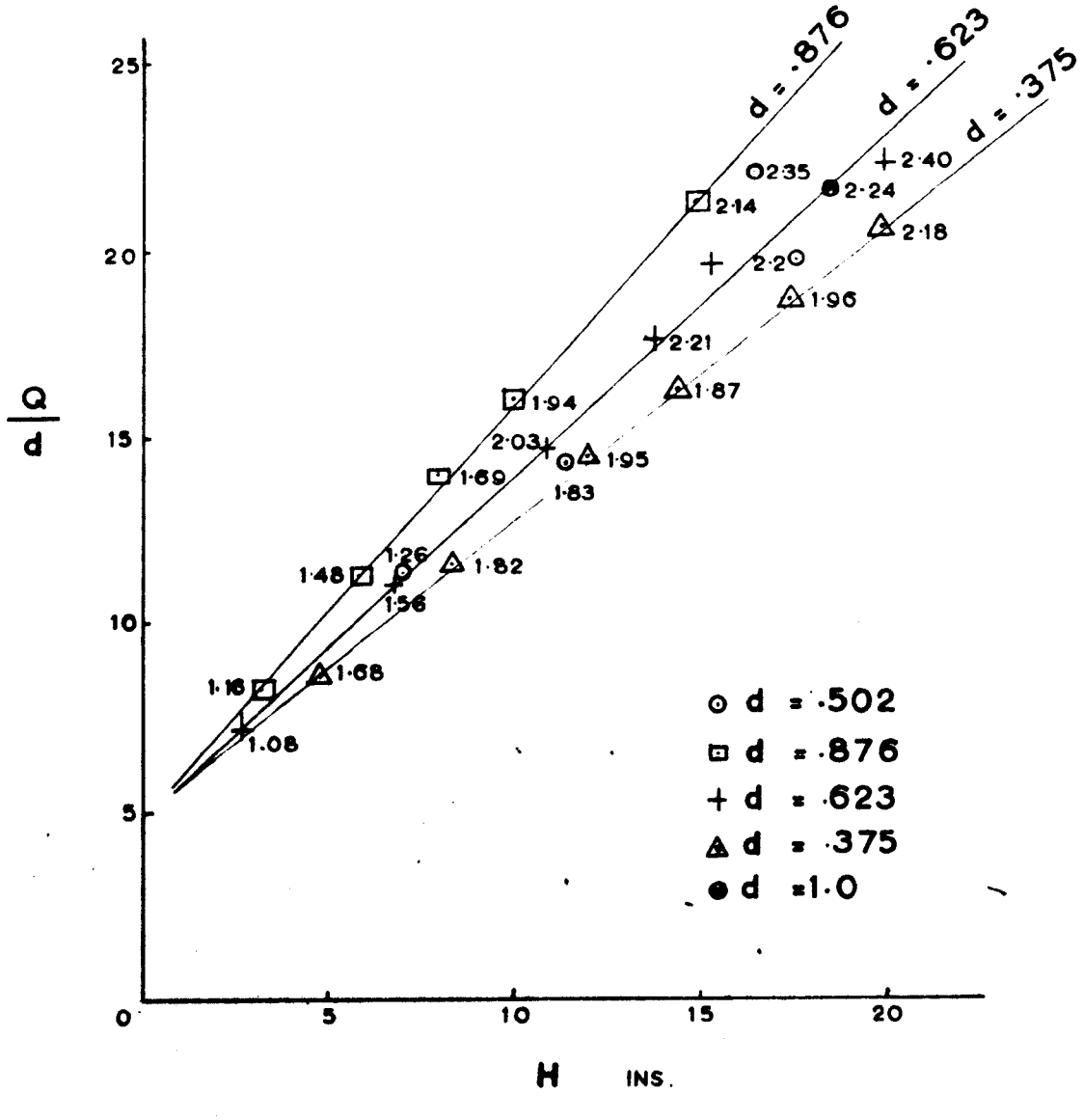

4. Experiments for non-geometrically similar systems.

Having established the scale relationship between geometrically similar systems it was then proposed to study whether a similar scale relationship could be found when a particular geometrical distortion of one system is made. In the non-viscous analysis of the free spiral vortex the only dimension of the apparatus which is introduced is the diameter of the outlet. This suggests that the outlet diameter is the only important dimension and that other dimensions of the apparatus may be varied without altering the relationship between quantity, depth and swirl. An alternative way of approaching this is to say that for a given set of apparatus the outlet diameter may be altered but the results obtained will still be in agreement when plotted on the non-dimensional basis of $\frac{Q}{g^{\frac{1}{2}}d^{\frac{5}{2}}}$ against $\frac{H}{d}$ for known values of $\frac{C}{g^{\frac{1}{2}}d^{\frac{3}{2}}}$. If this were proved to be correct it would allow geometrical distortion of the outlet diameter of a model without destroying similarity. Thus a model could be designed so that the velocities in the flow approaching the outlet represented similarity of Reynolds Number, while by choosing a suitable size of outlet similar Froude Number could be obtained at outlet.

The reason for wishing to operate a model so that there is similarity of Reynold's Number in the approaching flow will be discussed later, but it might be said at this point that while Froude Number represents similarity once the swirl has been generated, it will later be shown that certain types of vorticity will only arise if the Reynolds Number is sufficiently large and is not too far removed from its value in the prototype.

This theory has been tested by altering the outlet diameter in the small tank and making a series of readings of quantity, swirl and depth. These readings were made with the total quantity supplied tangentially, which is the condition for generating maximum swirl. The outlet diameters used varied from 0.375 inches to 1.0 inches and the values obtained are plotted non-dimensionally in Fig.34. It is quite clear from this plot that the results are not in agreement and the outlet diameter is not the only significant dimension. Dynamic similarity cannot therefore be maintained once the geometry of the apparatus has been distorted in this way.

It was noticed, however, that if the non-dimensional form for the swirl, $\frac{c}{(gd)^{\frac{1}{2}}}$, was retained and then the quantity Q divided by the outlet diameter, d, was plotted against h, then the results from the several different sizes of outlet diameter showed quite good agreement:

they are plotted in Fig. 35. At present no theoretical basis has been produced for this empirical result. If it can be substantiated for a wide range of outlet diameters it should be possible to alter the outlet diameter in the model and yet interpret from the result obtained the corresponding conditions in the prototype.

5. Comparison of theoretical and experimental results.

Having shown that there is similarity between the experimental results for the two sizes of apparatus, comparison was then made between the experimental results and the predictions of the non-viscous theory. The diagrams of quantity, depth and swirl found experimentally show some resemblance to the corresponding diagrams found from the theory: the experimental values for the two tanks are plotted in Figs. 30 and 32 while the theoretical values are plotted in Figs. 29 and 31.

Comparison of the experimental and theoretical results was made by selecting a certain value of the depth of flow H and reading off the experimental and theoretical values of the quantity for each value of the swirl . The ratio of experimental and theoretical quantities gave values of Cd , the coefficient of discharge for each value of the swirl. Some of the results obtained are plotted in Figs. 36 and 37, in which the coefficient of discharge is plotted against the swirl

for both sizes of apparatus and for constant values of H. The graphs obtained indicate that the coefficient of discharge Cd increases at first only slightly and linearly with increase of swirl but at high swirl the increase in Cd becomes non-linear and is considerable. It will be seen that this non-linear portion occurs when the swirl approaches its maximum value.

The reason for this increase in Cd can be seen by considering the conditions near the exit to the vortex tank. When the swirl, C, increases the core diameter, b , also increases but the velocity of outflow, v , is decreased. The non-viscous theory gives

$$b^2 = \frac{c^2 + \sqrt{c^4 + 16c^2a^2gH}}{8gH}$$

and $$v = \sqrt{2gH - \frac{c^2}{b^2}}$$

Therefore at the exit to the vortex tank an increase in the value of the swirl must produce a greater tangential velocity gradient and a correspondingly greater loss of energy. The true value of the swirl, c, at the exit must therefore be somewhat less than that measured at a distance from the outlet, which is the value of the swirl used to calculate the theoretical quantity. The theoretical quantity is therefore underestimated, so that the coefficient of discharge appears to increase. When the maximum value of the swirl is reached the energy losses are presumably considerable so that the rise in Cd is correspondingly greater.

Figs. 36 and 37 show that when Cd is plotted against $\frac{c}{g^{\frac{1}{2}}d^{\frac{3}{2}}}$ there is approximate agreement between the results from the two sizes of apparatus, but the coefficient of discharge for the small tank increases slightly more rapidly than that for the large tank. Therefore agreement between the non-viscous analysis and the experimental results can only be obtained by introducing a coefficient of discharge which is a function of the swirl.

FIG.36

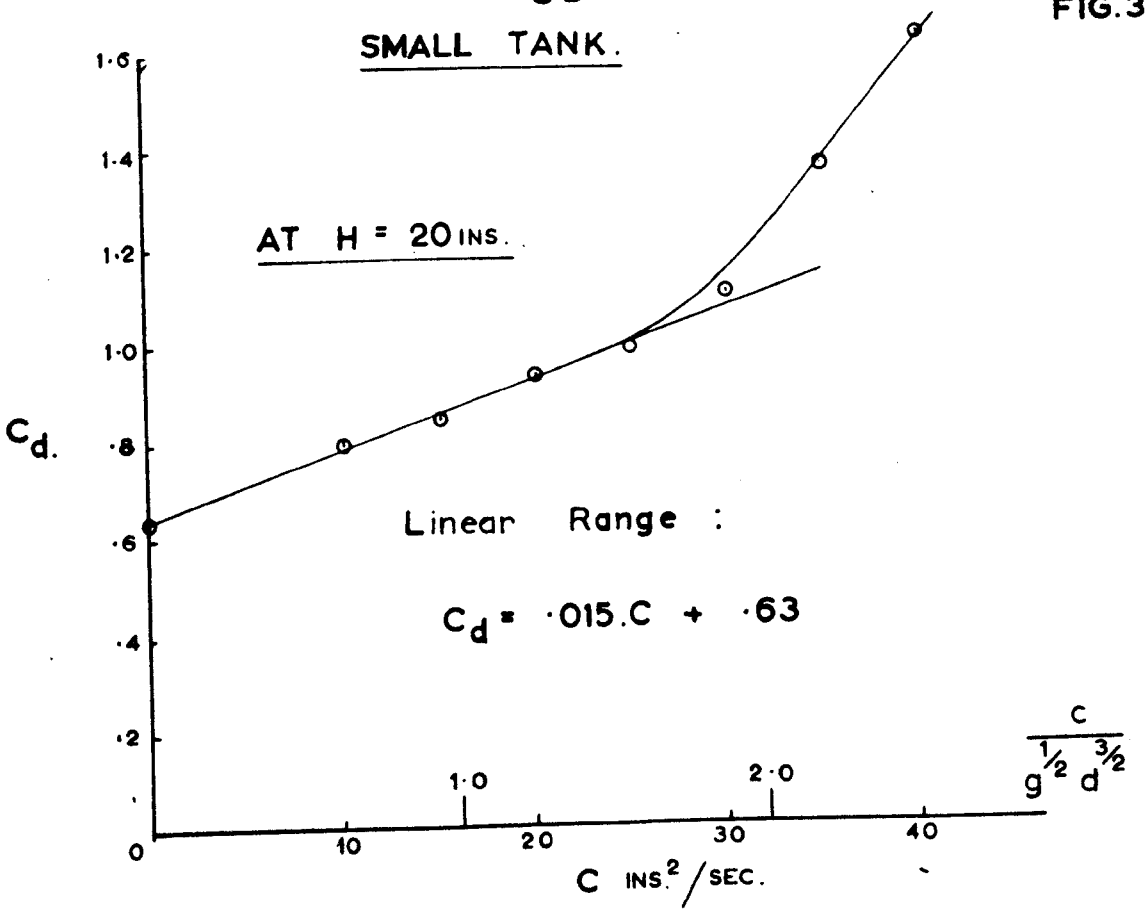
SMALL TANK.
AT H = 20 INS.
Linear Range :
$C_d = .015.C + .63$
C_d.
1·6
1·4
1·2
1·0
·8
·6
·4
·2
0
1·0
2·0
10
20
30
40
C INS.^{2}/SEC.
$\frac{C}{g^{1/2} d^{3/2}}$

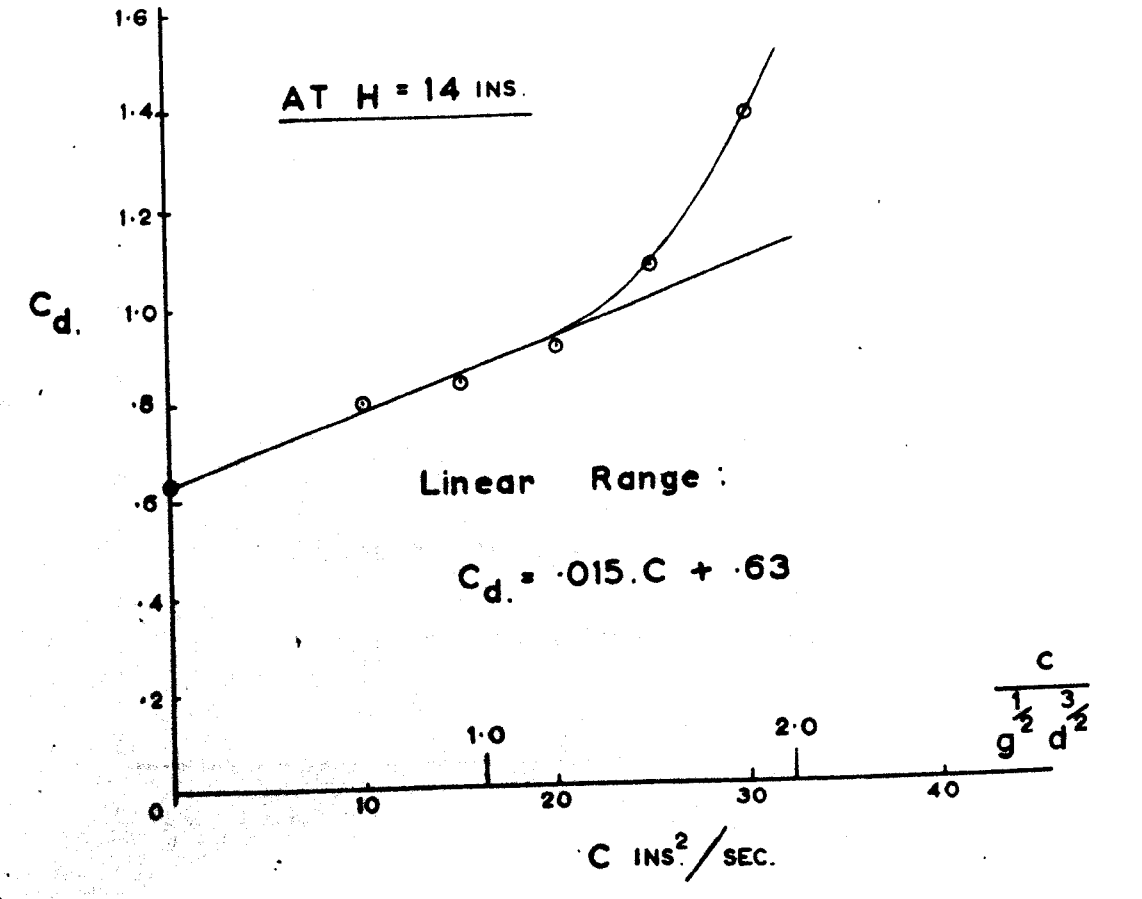
AT H = 14 INS.
Linear Range :
$C_d = .015.C + .63$
C_d.
1·6
1·4
1·2
1·0
·8
·6
·4
·2
0
1·0
2·0
10
20
30
40
C INS.^{2}/SEC.
$\frac{C}{g^{1/2} d^{3/2}}$

FIG. 37

LARGE TANK : COEFFICIENT OF DISCHARGE.

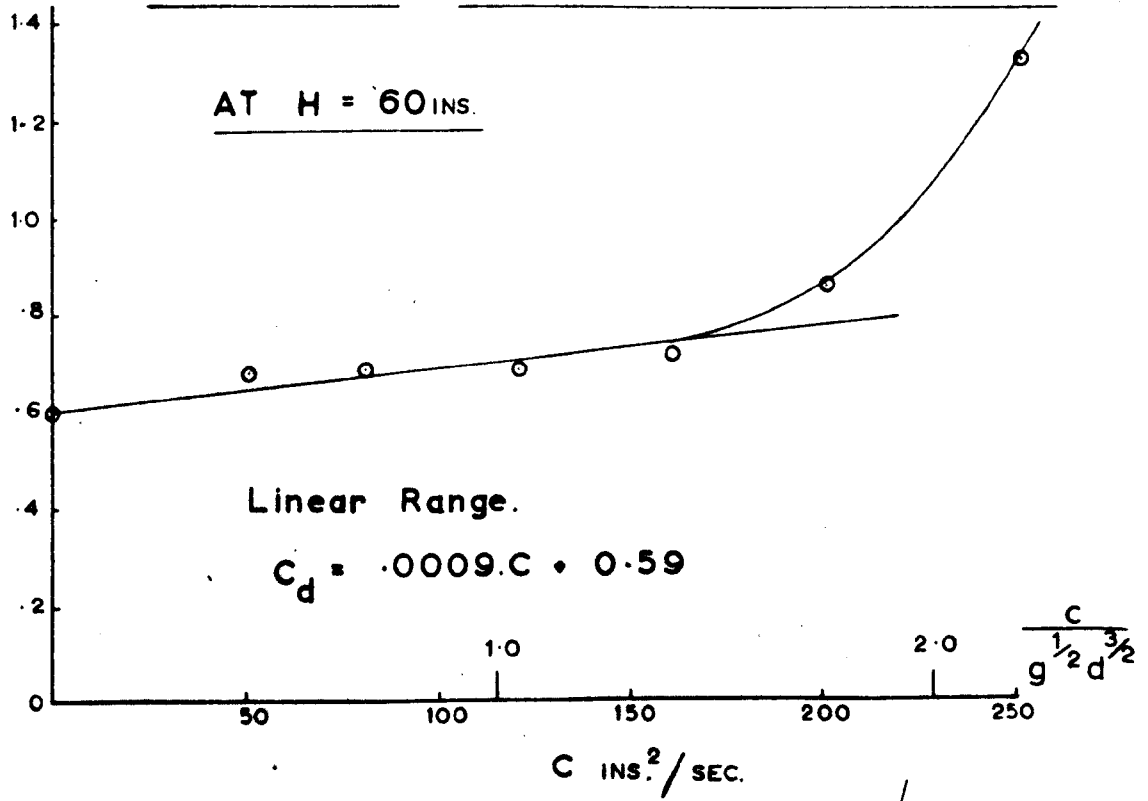

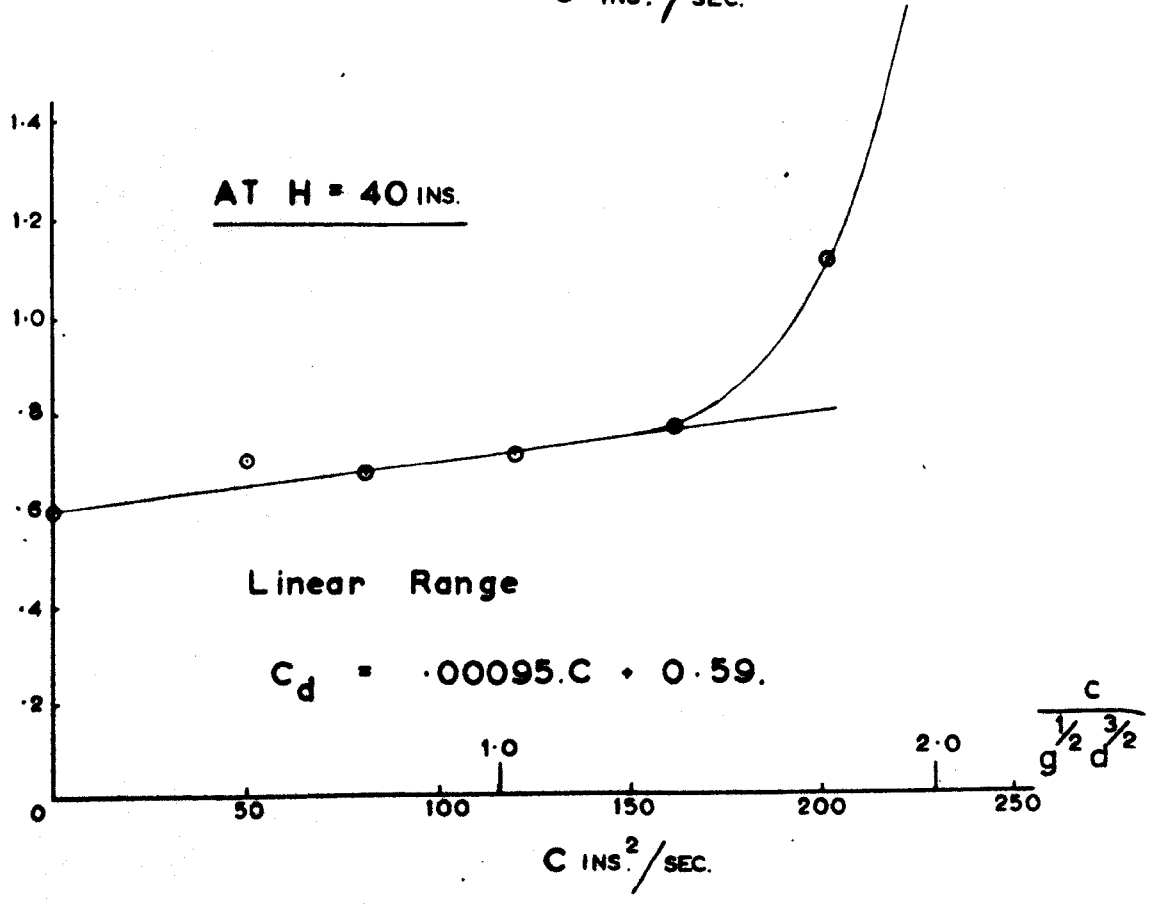

FIG 38

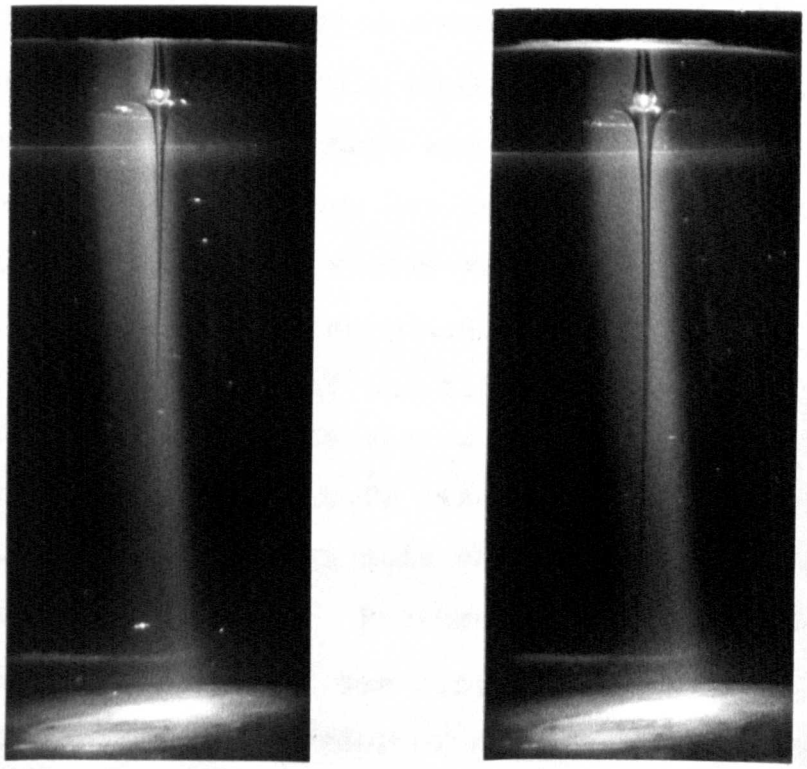

LIMITING SWIRL

The swirl is less than the minimum for the cores to reach the tank outlet.

6. The minimum swirl to produce a vortex core.

While studying the variation of quantity, depth and swirl to obtain the required values for Figs. 30 and 32 it was noticed that a vortex core existed at very low values of the swirl even when there were considerable depths of water. It was also quite conclusively shown that, with all the water supplied radially so that there was zero swirl, no vortex core formed at any depth; at very low depth the outlet behaved as a circular weir, but no vortex was present. When a small proportion of the flow was supplied tangentially, a proportion as small as 7% of the total supply was sufficient to produce an extremely thin vortex core. In both sizes of apparatus this limiting core size appeared to be of the same order, and measurements made of core diameter ranged from .04 to .02 of an inch. Because of the smallness of this core exact measurement was difficult but the above measurements indicate the order of size. If the tangential supply was now decreased even slightly the vortex core stopped short of the tank exit. Some experiments were made to determine the value of this limiting swirl for several depths and for both sizes of apparatus For the small tank with a depth of 18 inches, if the swirl was only 6 ins^2/sec the core did not extend as far as the outlet, but at a depth of 16 inches a swirl of 8.5 ins^2/sec gave a complete vortex core. At a low depth of 7 inches a swirl of 4.2 ins^2/sec was

sufficient to give a core. In the large tank for a depth of 56 inches a swirl of 24 ins^2/sec gave a complete core, but when this swirl was reduced to 13 ins^2/sec for the same depth the core was incomplete. For depths in the two tanks that are comparable, namely H_2 being four times H_1 it was found that the limiting values of the swirl only differed by a factor of between two and three instead of a factor of eight for Froude Number similarity.

Various factors were now considered which might control this limiting core size. One possibility that was considered is that waves are sometimes formed on the vortex cores, especially on the large ones, and it was thought that the breaking of the core might be due to these wave crests touching. Observation was made of some of the very smallest cores and it was found that no waves were observable and this theory was therefore discarded. For a small core it was thought that surface tension forces might be significant and were probably responsible for the collapse of the core. To investigate this possibility, a small amount of detergent was dropped into the vortex core when the swirl was so weak that the core only extended through part of the depth of the tank. If the core had stopped short of the tank outlet because of surface tension force, then the lowering of surface tension by the detergent should cause the core to reform: the core did reform for

a brief time and it was therefore concluded that surface tension was responsible for the core closing.

Since surface tension did appear to be responsible for the collapse of the core an analysis of this limiting condition was attempted. Considering an elementary ring of fluid bounded on its inner side by the free surface of the air core, the following conditions can be stated. Arising from the motion of the water in a circular path,

$$\frac{dp}{dr} = \rho.\frac{W^2}{r} \qquad ..(1)$$

and assuming that there is a free vortex distribution such that $w.r = K$ this equation becomes,

$$\frac{dp}{dr} = \rho.\frac{K^2}{r^3} \qquad ..(2)$$

Due to surface tension, there is a pressure change across the free surface where

$$p_T \; 2r = 2T$$

$$\therefore \; p_T = \frac{T}{r} \qquad ..(3)$$

At large radii the value of p is clearly negligible and it is only as r becomes small that p is likely to be large enough to have any effect. If the vortex core is

in equilibrium at a core radius r it is possible to study the stability of the core by considering the effect of a small change in radius. Suppose that the core radius is slightly diminished by δr, then due to the free vortex flow the pressure in the surface will decrease by δp where

$$\delta p = -\rho \frac{K^2}{r^3} \delta r \qquad ..(4)$$

Since this pressure is now lower than that of the air core, the air pressure will tend to restore the core to its original radius.

In addition, there is the effect of the surface tension, and by differentiating equation 3 it will be seen that the change in pressure arising from surface tension is

$$\delta p_T = -\frac{T}{r^2} (-\delta r) = \frac{T \delta r}{r^2} \qquad ..(5)$$

From equations 4 and 5 when r^2 is very small the decrease in pressure $\rho \frac{K^2 \delta r}{r^3}$ is much greater than the increase $\frac{T \delta r}{r^2}$ and so the core cannot become unstable from the action of surface tension forces. However, it is known from observation that, because of the very high shear stress near the vortex core, the free vortex pattern breaks down and w does not change inversely with the radius.

Suppose that the velocity distribution near the core is such that $w.r^n = C$, a constant.

Then equation 1 becomes:

$$\frac{dp}{dr} = \frac{C}{r^{1+2n}} \qquad ..(6)$$

Comparing this equation with equation 5 it is apparent that if 1 + 2n is less than two, then at very small radii $\frac{dp}{dr}$ will change more rapidly than $\frac{dp}{dr}$ so that the core can become unstable and will collapse. The limiting core radius will be given by,

$$\frac{dp}{dr} = \frac{dp}{dr} \qquad ..(7)$$

i.e. $$\frac{T}{r^2} = \rho.\frac{C}{r}^{1+2n}$$

Therefore the limiting value of the core radius is,

$$r = \left(\frac{T}{\rho C}\right)^{\frac{1}{1-2n}} \qquad ..(8)$$

Equation 8 will only give solution for r which lies in the correct region if 1-2n is positive, which implies that n is less than a half. Using experimental values to calculate the value of n, if r is 0.015 inches, the swirl 8 ins^2/sec and the surface tension 0.176 pdls./ft., the value of n is found to be o.49.

From this theory it is therefore possible to calculate the velocity distribution very close to the core of the limiting vortex and it is found that, approximately, $w.r.^{.49}$ is equal to a constant.

FIG 39

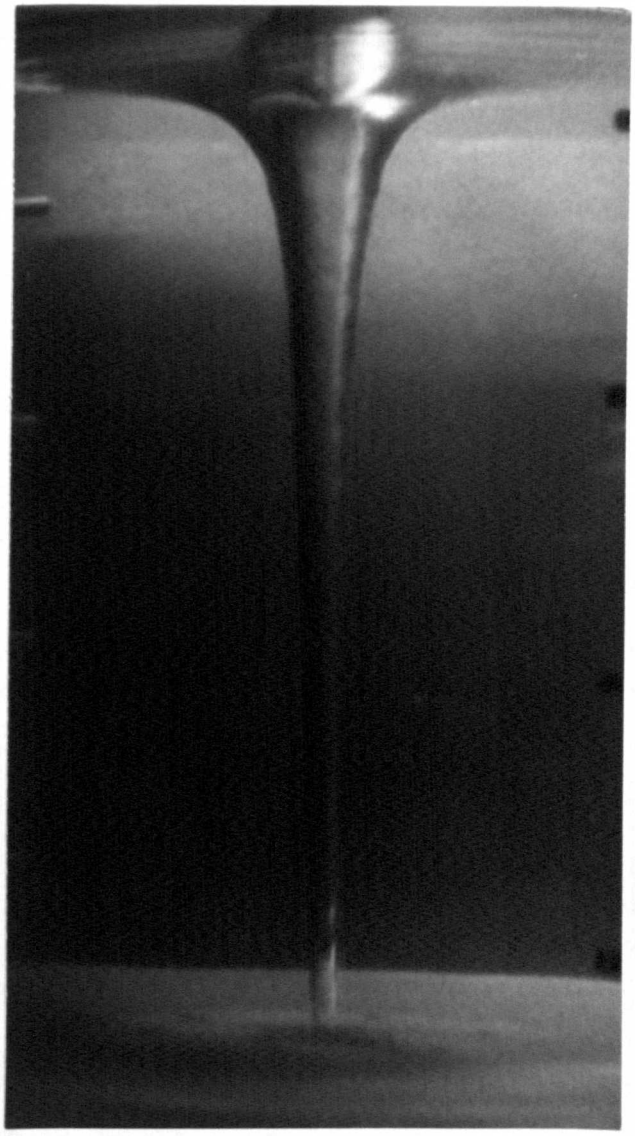

RESTRICTED OUTLET.

A strong vortex, but the core stops abruptly at exit to tank.

FIG. 40

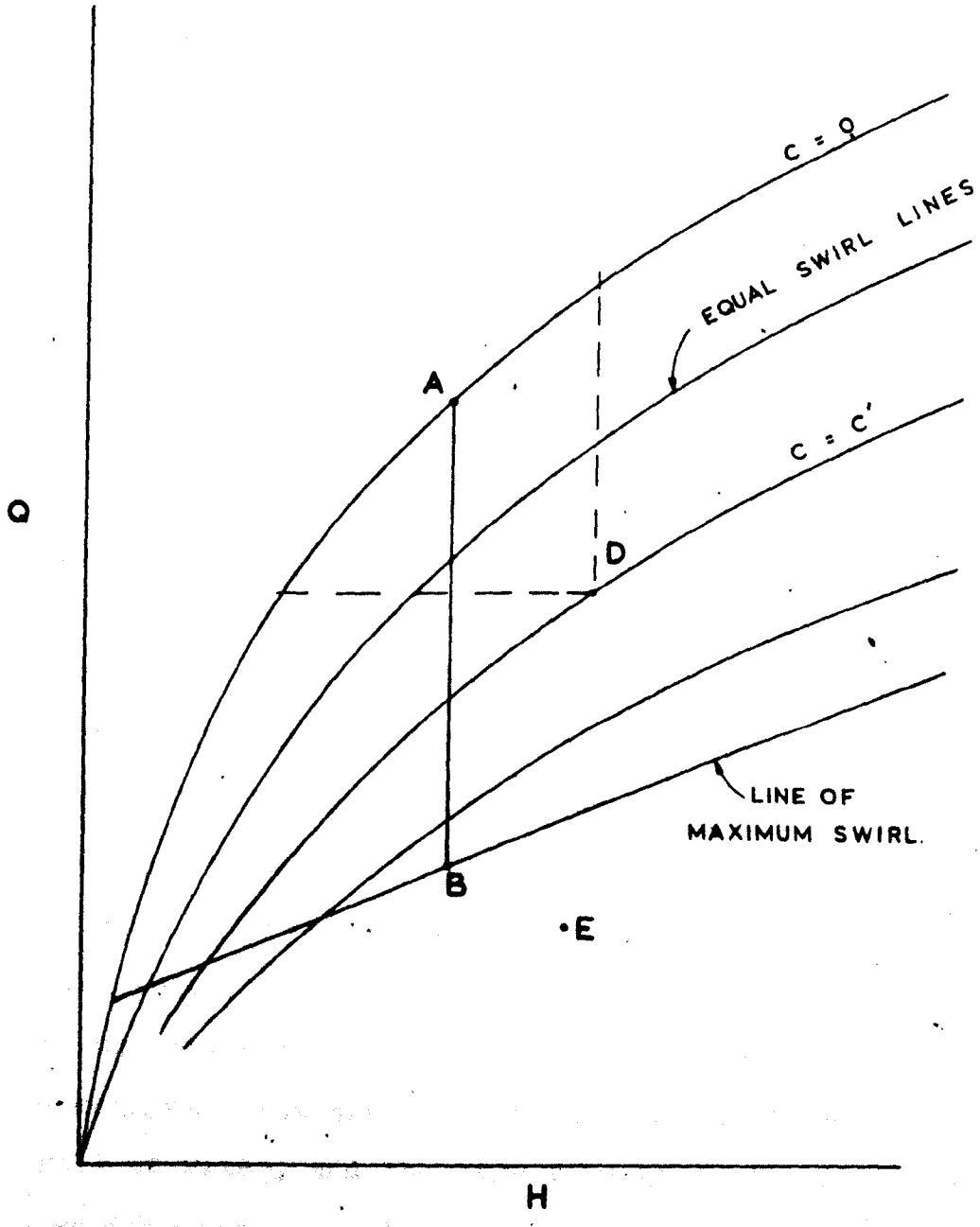

DIAGRAM TO ILLUSTRATE BEHAVIOUR WHEN OUTLET IS RESTRICTED.

CHAPTER V

FURTHER ANALYSIS AND EXPERIMENTS

1. Restriction of the Outlet.

In the experiments so far described the water was allowed to discharge freely under gravity from the tank outlet. Fig.40 is a diagrammatic version of the graphs relating quantity, head and swirl. The outlet to the tank is assumed to be an orifice, so that the total head available is the depth of water in the tank. If no swirl is present, the outflow will be represented by the c = 0 line for any particular depth, a typical example is point A. Similarly for any given swirl the outflow can be determined from the known value of the swirl and the depth of water in the tank; for constant depth and increasing swirl the quantity will diminish, following the line AB. It will be now assumed that an outlet tube with the same diameter as the orifice is fitted. When a vortex core is present the outflow with the tube fitted will be the same as for the orifice, because, as the vortex theory has shown, the outlet is a control section through which the velocity is critical and the quantity a maximum. But when no vortex is present the tube will run full of water, and the effective head will increase, producing an increase in outlet velocity and quantity.

Suppose, now, that the outflow for a given depth and zero swirl is restricted to the value represented by point D, Fig.40. If a small amount of swirl, less than the value c', is now induced, it will be impossible for a vortex core to form unless either the depth decreases or the quantity increases, these variations being represented by the dotted line through D. This variation in depth or quantity could well be a combined variation of both factors. Therefore, when the outflow is restricted a considerable swirl may have to be induced before a vortex core can form. If the flow is restricted so that point E represents the outflow it will be impossible to induce sufficient swirl to produce a vortex, point E being below the line of maximum swirl.

This was checked experimentally in the small apparatus. The restriction to the outlet was made by fitting a valve to the end of the outlet tube so that any required amount of restriction could be obtained. A certain swirl was produced in the tank by supplying some of the water tangentially and then the outlet was restricted by closing the valve until the vortex core was just prevented from entering the outlet tube. The values of swirl, depth and quantity were then compared with the values which would be expected from Fig.30, and were found to be in agreement. This procedure was repeated for a number of different depths and swirls. When the experimental values corresponded to a point such as E in

Fig.40 it proved impossible to generate sufficient swirl to produce a vortex core in the outlet. The photograph in Fig.39 shows a strong vortex extending to the outlet, yet with the restriction of quantity, the vortex core did not extend into the outlet tube and only a few very small bubbles of air passed into it.

These results can best be explained by considering the energy of the outflow. Considering point D again, Fig.40, if a core is to form for a swirl less than c' the quantity must increase if the depth in the tank is to remain constant; alternatively if the quantity is to remain constant the depth must decrease which implies that the resistance to flow must decrease. The first of these conditions demands an increase in the energy of flow while the second condition requires that less energy be dissipated in the outlet.

For a downwards outlet from a vessel, a critical velocity of outflow for the formation of vortices can now be determined. If the velocity in the outlet is greater than $\sqrt{2.g.H}$, where H is the depth of water in the vessel, then any sustained swirl in the region of the outlet will produce a vortex core. If the outlet velocity is less than $\sqrt{2.g.H}$ a certain minimum value of swirl must be present before a vortex core can form, and if the velocity is much less than $\sqrt{2.g.H}$ the conditions may correspond to a point such as E and no vortex core can form because swirl of sufficient strength cannot be generated.

With a downwards outlet, therefore, two conditions can be stated for which no vortex cores can form, firstly, when there is no swirl in the flow approaching the outlet and secondly, when the outlet velocity is restricted to a value less than $\sqrt{2gH}$ and any swirl present is less than c', the minimum value necessary to produce a vortex. If the maximum possible swirl is being generated, to prevent a vortex forming, it may be necessary to restrict the outlet velocity to about $\frac{1}{2}\sqrt{2gH}$, but probably, for most conditions a restriction to $\frac{3}{4}\sqrt{2gH}$ would be sufficient. If an outlet is fitted which tapers slowly from a large diameter to the final outlet pipe diameter the velocity at outlet will probably be made less than $\sqrt{2gH}$ at the critical section; an increase in velocity after this section is probably not detrimental.

2. Vortex Theory.

There are several theorems concerning the potential vortex in a non-viscous fluid and some of these theorems have been extended for viscous fluid flow. Lagrange's theorem states that if a velocity potential exists at one time in a motion of an inviscid, incompressible fluid, subject to conservative extraneous force, it exists at all past and future times. An alternative and simpler statement is that once a motion is irrotational it is always so. This fundamental theorem of hydrodynamics has been extended by

St.Venant to potential vortex flow in a viscous, incompressible fluid. According to his theorem vorticity cannot be generated in the interior of a viscous incompressible fluid but is necessarily diffused inwards from the boundaries. This was taken one step further by Boussinesq and Duhem who showed that although vorticity cannot be generated within a viscous incompressible fluid, if already present, it will decay.

These theorems are in agreement with the results of the many experiments made to study the formation of vortices, all of which indicate that vorticity is induced in the approaching fluid either by the form of the inlet to the sump or by vortices shed from sharply curved contours on the boundaries. Sketches of three types of flow in which swirl is generated are given in Fig.46, Fig.46a showing a general swirl caused by an asymmetrical inlet while Figs. 46b and c show vortices being shed from boundaries.

Some investigators have thought that swirl could arise from the inside of an outlet, either from secondary flow in corners and bends or from spin coming back from a pump. This implies that vorticity is transmitted back upstream through the oncoming flow, but this transmission of vorticity within a fluid is contrary to the theorems already stated, which show that vorticity cannot be generated within a viscous fluid, but can only decay. Therefore if vortices are to form at the exit from a vessel the necessary vorticity must be generated at the boundaries of the flow before it reaches the outlet.

For non-viscous flow there are two theorems concerning vortex tubes which have been shown by experiment to be only modified slightly by viscous effects. The first theorem states that no flow crosses a vortex tube, the second that the circulation has the same value for all closed curves embracing the vortex tube, and this has the implied corollary that vortex tubes must either form closed rings or else begin and end on a boundary of the flow. Applying these theorems to the experimental results, the free spiral vortex must begin at the free surface and end at the base of the tank or at the outlet, thus satisfying the requirements of the second theorem. The requirement that no flow should cross a vortex tube implies that there should be no radial flow, but only vertical flow within a vortex tube. With viscous flow there must be fresh vorticity to make good the energy losses and therefore there must be a radial flow. It is interesting to note from the experimental velocity measurements that radial velocities were generally not observable except at the surface and at the base of the tank; elsewhere there were vertical velocities, both upwards and downwards. It might therefore appear that flow only enters or leaves a vortex tube at the free surface or, at the base of the tank or at the outlet. This qualitative agreement between theory and experiment can only be checked by solving the Navier-Stokes equations, which was not found possible

for three dimensional flow. A particular solution was obtained for two dimensional flow, which lends support to this idea.

3. A Particular Solution of the Navier-Stokes Equations.

Starting from the complete Navier-Stokes equations in cylindrical polar coordinates, r, θ, z and corresponding velocity components u, w and v, certain simplifying assumptions were made until it was possible to obtain a particular solution. The Navier-Stokes equations in cylindrical polar form are:

$$\rho\left(\frac{\partial u}{\partial t} + u\frac{\partial u}{\partial r} + \frac{w}{r}\frac{\partial u}{\partial \theta} + v\frac{\partial u}{\partial z} - \frac{w^2}{r}\right) = -\frac{\partial}{\partial r}(p + \rho\Omega) + \mu\left(\nabla^2 u - \frac{u}{r^2} - \frac{2}{r^2}\frac{\partial w}{\partial \theta}\right).$$

$$\rho\left(\frac{\partial w}{\partial t} + u\frac{\partial w}{\partial r} + \frac{w}{r}\frac{\partial w}{\partial \theta} + v\frac{\partial w}{\partial z} + \frac{u.w}{r}\right) = -\frac{1}{r}\frac{\partial}{\partial \theta}(p + \rho\Omega) + \mu\left(\nabla^2 w + \frac{2}{r^2}\frac{\partial u}{\partial \theta} - \frac{w}{r^2}\right)$$

$$\rho\left(\frac{\partial v}{\partial t} + u\frac{\partial v}{\partial r} + \frac{w}{r}\frac{\partial v}{\partial \theta} + v\frac{\partial v}{\partial z}\right) = -\frac{\partial}{\partial z}(p + \rho\Omega) + \mu\nabla^2 v$$

$$\nabla^2 = \frac{\partial^2}{\partial r^2} + \frac{1}{r}\frac{\partial}{\partial r} + \frac{1}{r^2}\frac{\partial^2}{\partial \theta z} + \frac{\partial^2}{\partial z^2}$$

Ω is the force potential.

The continuity equation is

$$\frac{\partial(u.r.)}{r.\partial r} + \frac{\partial w}{r\partial \theta} + \frac{\partial v}{\partial z} = 0$$

It was assumed that the flow was steady and therefore independent of time. Also it was assumed that the flow was

axially symmetrical and therefore independent of θ. Lastly, it was found necessary to assume the flow to be confined to the r,θ plane so that the vertical velocities, v, are everywhere zero. The flow therefore consists of an axially symmetrical flow with velocity components u, radially and w, tangentially. With these simplifications the equations become

$$\rho\left(u\frac{\partial u}{\partial r} - \frac{w^2}{r}\right) = -\frac{\partial}{\partial r}(p + \rho\Omega) + \mu\left(\nabla^2 u - \frac{u}{r^2}\right) \qquad ..(1)$$

$$\rho\left(u\frac{\partial w}{\partial r} + \frac{uw}{r}\right) = \mu\left(\nabla^2 w - \frac{w}{r^2}\right) \qquad ..(2)$$

$$\nabla^2 = \frac{\partial^2}{\partial r^2} + \frac{1}{r}\frac{\partial}{\partial r}.$$

The continuity equation becomes

$$\frac{\partial(ur)}{r\partial r} = 0. \qquad ..(3)$$

Eqn.(3) gives ur = constant = K and Eqn.(2) then becomes an equation in w and r which can be solved. Substituting for u in Eqn.(2):-

$$\rho\frac{K}{r}\frac{\partial w}{\partial r} + \rho\frac{Kw}{r^2} = \mu\frac{\partial^2 w}{\partial r^2} + \frac{\mu}{r}\frac{\partial w}{\partial r} - \frac{\mu w}{r^2} \qquad ..(4)$$

It is worth noting here if μ is made zero the resulting equation is independent of K and gives

$$\frac{\partial w}{\partial r} + \frac{w}{r} = 0 \qquad ..(5)$$

Eqn. (5) gives the solution that w.r. is constant and shows that the vortex flow is independent of the radial flow, and similarly the vertical flow, for a non-viscous fluid.

To return to the viscous solution, re-arranging terms,

$$\frac{\partial^2 w}{\partial r^2} + \left(\frac{\nu - K}{\nu r}\right) \frac{\partial w}{\partial r} - \left(\frac{\nu + K}{\nu r^2}\right) w = 0 \qquad ..(6)$$

Frobenius' method of solution will now be used and it will be assumed that.

$$w = r^c (a_o + a_1 r + a_2 r^2 + \ldots) \qquad ..(7)$$

Differentiating:

$$\frac{\partial w}{\partial r} = a_o c r^{c-1} + a_1 (c + 1) r^c + a_2 (c + 2) r^{c+1} + \ldots \qquad ..(8)$$

$$\frac{\partial^2 w}{\partial r^2} = a_o c (c - 1) r^{c-2} + a_1 (c + 1) c r^{c-1} + \ldots \qquad ..(9)$$

Substituting in Eqn.(6) and equating successive powers of r to zero, for r^{c-2} :

$$a_o c(c - 1) + \left(\frac{\nu - K}{\nu}\right) a_o c - \left(\frac{\nu + K}{\nu}\right) a_o = 0$$

$$\text{i.e.} \left[c - \left(1 + \frac{K}{\nu}\right)\right][c + 1] = 0 \qquad ..(10)$$

This indicial equation gives, if $a_o \neq 0$, that $c = -1$ or $1 + \frac{K}{\nu}$.

Similar comparison of coefficients shows that a_1, a_2 etc. are all zero. The particular solution obtained is, therefore:

$$w = a r^{1 + \frac{K}{\nu}} + b r^{-1} \qquad ..(11)$$

Two boundary conditions would be needed to obtain values for the non-zero constants a and b, This result can, however, be discussed in general terms. It has been shown in Eqn.(5) that when μ is zero the solution obtained is $w = br^{-1}$ when b is a constant. Therefore in the solution obtained when μ is not equal to zero the expression $ar^{\frac{1}{\nu}+\frac{K}{\nu}}$ represents the distortion of the velocity profile by the viscous shear forces. Experiment has shown that w.r is approximately constant and certain implications can therefore be drawn from the equation for w, Eqn.(11).

Considering Eqn.(11), if K is positive, the radial velocity is outwards and $1 + \frac{K}{\nu}$ is positive and greater than one. Eqn.(11) shows that the resulting equation for w will be far removed from the non-viscous solution. Alternatively, if K is negative and large compared with ν, implying a moderate inwards radial velocity, then $1 + \frac{K}{\nu}$ becomes negative and large. At small radii the distortion of the swirl velocity profile will again be considerable. Lastly, if K is negative and has a value approximately equal to that of ν , $1 + \frac{K}{\nu}$ tends to zero and the equation for w becomes:

$$w = a + \frac{b}{r} ,$$

which could well be a close approximation to the ideal vortex velocity distribution. This particular solution does not prove that radial velocities have a certain value, but it does show that near agreement with the ideal velocity distribution is possible when the radial velocity is extremely

small and directed inwards. This result may give support to the observed lack of radial flow except near the surface and outlet.

4. The Solution of Axially Symmetric Flow by Relaxation Analysis

Experiment has shown that the velocity distribution and the free surface differ only slightly from those to be expected by the non-viscous theory. Despite this approximate agreement, the quantity measured at a higher value of swirl differs considerably from the non-viscous value, as can be seen from the non-linear portion of Figs. 36 and 37. It has already been suggested that this lack of agreement is caused by the high shear stresses near the outlet and the consequent losses. If this is so there should be a measurable difference between the ideal free surface and the measured free surface at the outlet to the tank. The only analysis at present available for calculating the ideal free surface profile is a relaxation method; this method was used and was compared with measurements made photographically at the outlet to the tank.

Consider a set of cylindrical coordinates r, θ and z, such that O_z is directed downwards and u, w and v are the velocity components in these three directions: u is then the radial velocity, w the tangential velocity and v the vertical velocity. For an ideal, non-viscous flow which

has complete axial symmetry about Oz, then a stream function ψ and a potential function ϕ must exist such that:

$$u = -\frac{1}{r}\frac{\partial\psi}{\partial z} \qquad ..(1)$$

$$v = \frac{1}{r}\frac{\partial\psi}{\partial r} \qquad ..(2)$$

The tangential velocity distribution w must also be symmetrical about the Oz axis so that at a given radius the velocity w must be constant. Such a flow pattern, if it is also to be irrotational, must be a potential vortex so that w.r. is constant. The total flow pattern is then irrotational and can be described by a potential function ϕ and stream function ψ.

Lord Rayleigh showed that the irrotational motion in the r,z plane is unaltered by a potential vortex motion, w.r equals a constant. This result was first used by Binnie and Davidson for a relaxation analysis of the free spiral vortex. Although the flow is not directly affected, the Bernoulli equation for the free surface is modified and this must be allowed for when determining the free surface.

Taking the free water surface at a large radius as the datum level for z,Bernoulli's equation for the free surface becomes:

$$\frac{u^2 + v^2 + w^2}{2g} - z = 0 \qquad ..(3)$$

In addition there are two more boundary conditions, firstly, ψ is constant on a boundary and, secondly, the

velocity on a boundary which is a free surface can be found because the pressure is constant and is known. Therefore the free boundary velocity is $\sqrt{2gz}$ and

$$\frac{1}{r}\frac{\partial\psi}{\partial\nu} = \sqrt{2gz} \qquad ..(4)$$

where ν denotes a direction normal to the free boundary.

For a flow with axial symmetry the continuity equation is,

$$\frac{\partial^2\psi}{\partial r^2} - \frac{1}{r}\frac{\partial\psi}{\partial r} + \frac{\partial^2\psi}{\partial z^2} = 0 \qquad ..(5)$$

Equations(4)and(5)can be replaced by finite difference equations derived from a square mesh net of side "a". In finite difference form, see Fig.41,

$$2a.\frac{\partial\psi}{\partial r} = \psi_1 - \psi_3$$

$$a^2\left(\frac{\partial^2\psi}{\partial r^2} + \frac{\partial^2\psi}{\partial z^2}\right) = \psi_1+\psi_2+\psi_3+\psi_4-4\psi_0$$

So that Eqn.(5) becomes

$$F_0 = \psi_1+\psi_2+\psi_3+\psi_4-4\psi_0-\frac{a}{2r_0}(\psi_1-\psi_3) \qquad ..(6)$$

and the relaxation pattern is as shown in Fig.41.

On a free surface there are usually unequal stars, but only either one or two of the limbs of a star are shortenad. The equation for one of these boundary points, such as that shown in Fig.42a is,

$$F_o=\psi_1\left[\frac{2(1-\frac{\xi a}{2r_o})}{1+\xi}\right]+\psi_4\left[\frac{2}{1+\eta}\right]+\psi_B\left[\frac{2(1+\frac{a}{2r_o})}{\xi(1+\xi)}\right]$$

$$+\psi_A\left[\frac{2}{\eta(1+\eta)}\right]-\psi_o\left[\frac{2}{\xi}+\frac{2}{\eta}+\frac{(1-\xi)\frac{a}{r_o}}{\xi}\right] \qquad ..(7)$$

Before starting the relaxation analysis a position for the free surface had to be assumed. The assumed boundary was that of the free cylindrical vortex,

$$z=\frac{c^2}{2gr^2} \qquad ..(8)$$

After the first relaxation has been carried out the position of the free surface can be checked from Eqn.(3), the value of (u^2+v^2) being calculated from the finite difference relationship, Fig.42b,

$$(u^2+v^2)^{\frac{1}{2}}.\ \sin\theta=\frac{1}{ar_A}\left[\frac{1+\xi}{\xi}\psi_B-\frac{\xi}{1+\xi}\psi_C\right] \qquad ..(9)$$

If the boundary condition, Eqn. (3), is not satisfied, the free surface has to be adjusted. Binnie and Davidson have suggested a method for determining the amount of shift required, although the direction of the required shift can be seen by inspection.

The argument is as follows:-

The surface has been chosen so that $w^2=2gz$ ..(10)

It is found that when q becomes significant

$$q^2+w^2\neq 2gz.$$

The value of w must therefore be changed by δw, so that

$$q^2 + (w + \delta w)^2 = 2gz = w^2$$

Therefore $\delta w \doteq \frac{q^2}{2w}$

Also $w = \frac{S}{r}$

Therefore $\frac{\delta w}{\delta r} = -\frac{S}{r^2}$

Hence $\frac{\delta r}{r} = \frac{q^2}{2w^2}$ ..(11)

It was found that the value of δr given by this expression was invariably too large so that successive corrections oscillated about the true value. By taking half its value each time the true value was approached more quickly. Once the boundary has been corrected the relaxation process is repeated, the effect of the corrections being restricted to only a portion of the network.

The region of the flow near the outlet was now divided into a finer mesh of $\frac{1}{2}$inch squares, values being interpolated from those found with the one inch squares. The relaxation process was then continued for this finer mesh until the residuals had been reduced to acceptable values. To check that the boundary values used for this finer meshwork were reasonably correct the mesh was then extended out to the next set of 1 inch squares and again relaxed and if the first boundary values remained unaltered, or almost so, then it was known that the fine mesh values for ψ were correct. Successively finer meshes can be obtained in this manner and the detailed behaviour in

the high velocity region of the outlet can be studied.

This method was used to calculate the surface profile for a given value of the swirl and depth of flow. Finer meshes were used in the vicinity of the outlet to obtain the value of the core size at outlet. These non-viscous results were compared with values measured for a similar strength of vortex and the results obtained are shown in Figs.44 and 45. Photographs of the experimental core profile are given in Fig.43. Fig.44 shows good agreement between the calculated surface profile and the measured surface profile, but Fig.45 reveals that, near the outlet, the measured and calculated profiles do not agree. Although the disagreement is not large, it is very important at the outlet section, for it can be seen that the measured outlet flow area is some 30% greater than calculated. This discrepancy is sufficient to account for the increased difference between the measured and the calculated outflows when the swirl is a maximum. It is presumed that the alteration in surface profile is caused by high viscous shearing in the region of the outlet, but this could not be calculated.

FIG. 41

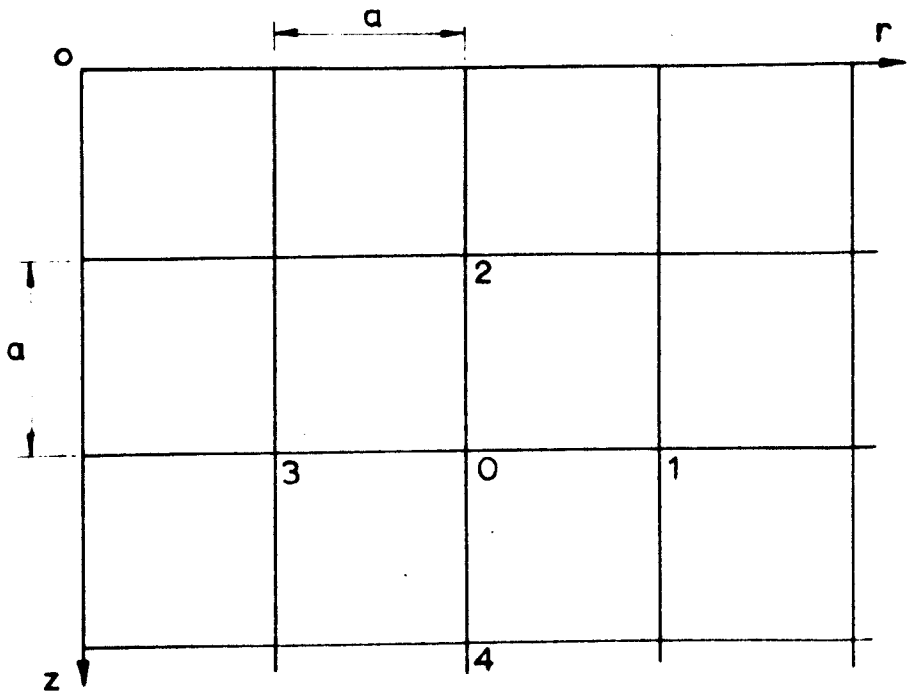

FINITE DIFFERENCE MESH

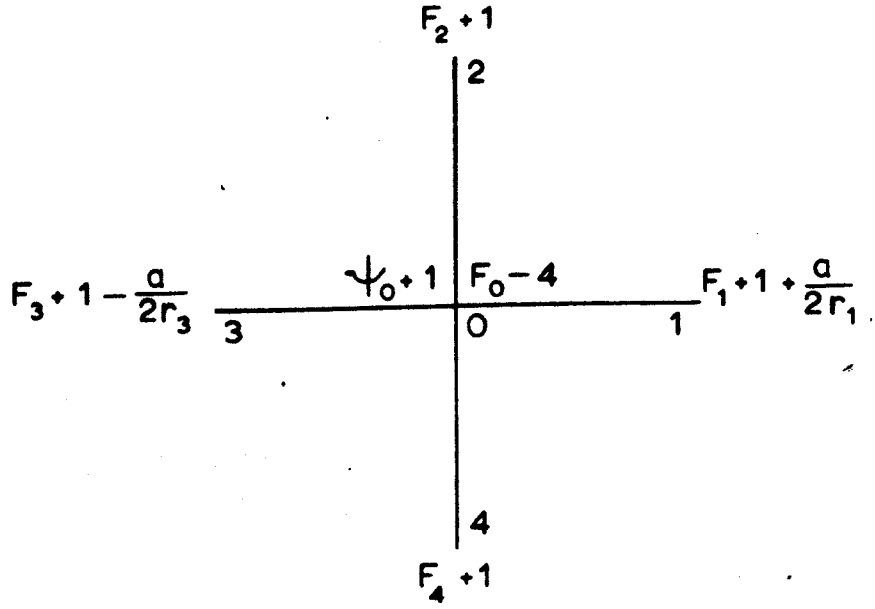

RELAXATION PATTERN :

STANDARD INTERNAL STAR.

FIG. 42

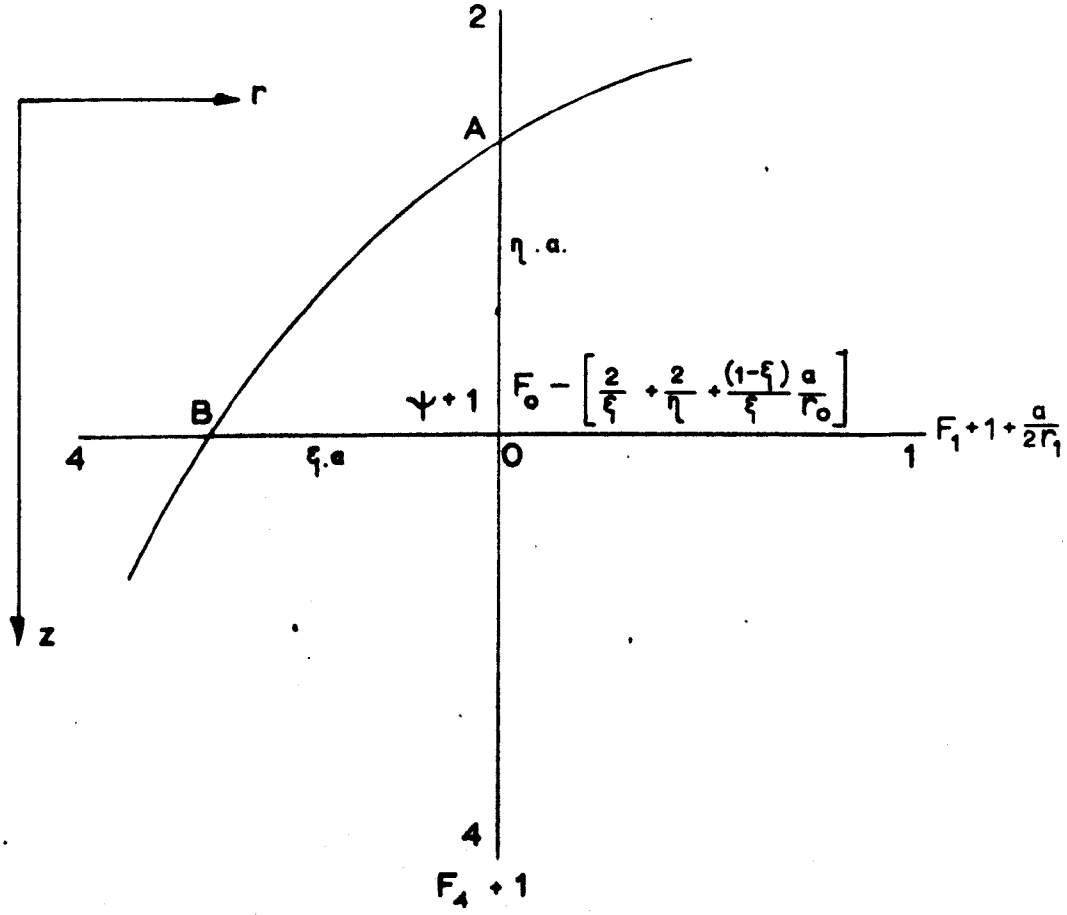

a) RELAXATION PATTERN FOR FREE BOUNDARY STAR.

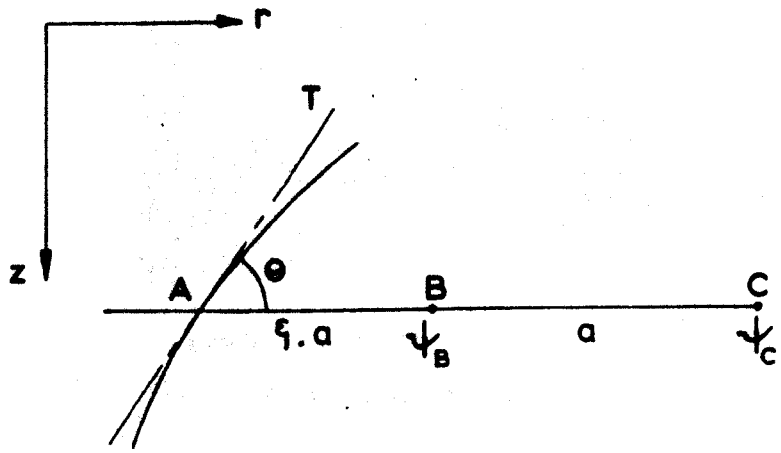

b). INFORMATION FOR CHECKING FREE SURFACE.

FIG 43

CORE PROFILE: C = 44INS.^{2}/SEC.
For comparison with relaxation analysis.

FIG. 44

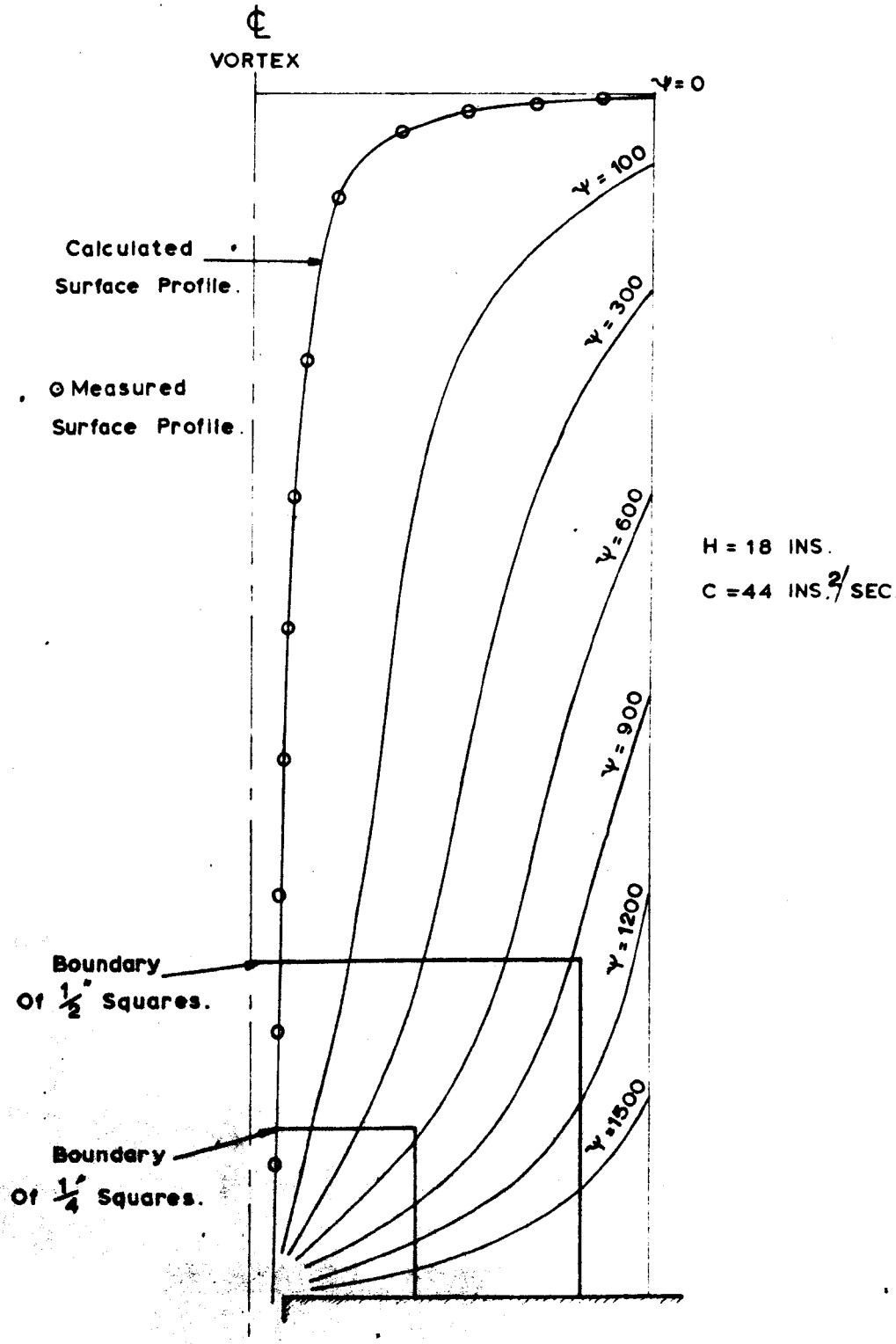

RELAXATION ANALYSIS.

Surface Profile And Streamlines.

FIG. 45

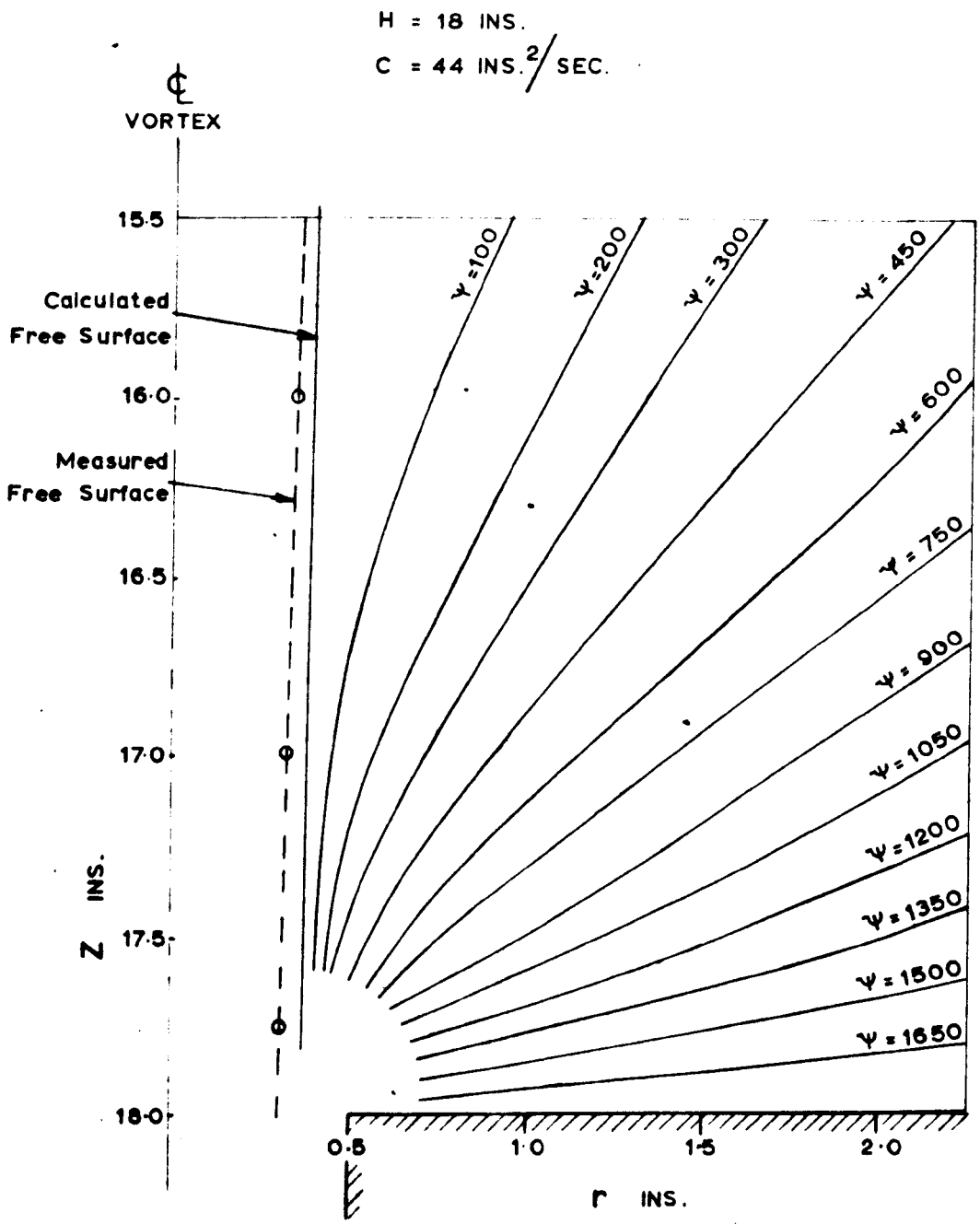

RELAXATION ANALYSIS.

Details Of Core Profile And Streamlines Near Tank Exit.

CHAPTER VI

AIR ENTRAINMENT WHEN WATER PASSES UPWARDS INTO A VERTICAL INTAKE PIPE.

1. Generation of Swirl.

A preliminary study was made using a model pump sump approximately square in plan with an asymmetrical inlet in one side, as shown in Fig.46a. A vertical suction tube was placed centrally in the sump with siphon action substituted for a pump. These excessively bad conditions produced swirl in the sump and a study was made of the velocity and submergence requirements at the intake necessary for vortices to form. It was found that there are two different types of behaviour: at low water depths the water in the sump formed a swirl which was concentric with the suction tube producing a steady draw down of the surface symmetrically around the outlet; at greater water depths this general circulation ceased and was replaced by intermittent air entraining vortices which formed near the suction tube. These conditions are shown diagrammatically in Fig.46 where sketch (a) represents the general swirl pattern and sketches (b) and (c) represent two patterns of intermittent vortices.

There are therefore two fundamentally different processes by which air entraining vortices are formed. The first of these conditions occurs when the inlet to the sump is asymmetrical, so that a general swirl is induced in the flow in the sump.

This condition is steady with time and can therefore give rise to a steady air entraining vortex. The second condition in which vortices are shed from discontinuities at the boundaries of the flow approaching the outlet can never be steady and the vortices formed will only be transient. A study of these two types of vortex formation was therefore made for the condition when the outlet leads vertically upwards from the flow.

2. The Swirl Concentric with the Suction Tube.

The necessary conditions for a steady free spiral vortex to occur are illustrated by the work already carried out in the small and large vortex tanks. A steady free spiral vortex depends on a constant and symmetrical supply of fluid with vorticity „c„, from its surroundings and also a constant removal of fluid from its centre. These findings are supported by the theorems of Boussinesq and St. Venant quoted in the previous chapter; St. Venant's statement implies that vorticity must arise from the boundaries while Boussinesq's extension indicates that this vorticity will decay and must therefore be removed at the centre. When a free spiral vortex forms in a fluid with a horizontal free surface there must be not only axial symmetry, but also the central axis must be vertical, perpendicular to the free surface. This is so because a rise in kinetic energy is accompanied by a corresponding fall in free surface level. Because the velocity distribution is symmetrical about the centre line, the fall in free surface level

must also be symmetrical about this centre line and it therefore follows that the axis of the vortex must be vertical.

Fluid is removed from the centre of a steady vortex so that the vertical axis of the vortex must coincide with the centre line of the outlet. When the outlet tube leads vertically upwards the position of the vortex core is occupied by the exit tube itself and the conditions for the formation of a steady vortex entraining air are now fundamentally different from the requirements when the exit tube is vertically downwards.
Fig.49 illustrates this condition and shows that if a steady vortex is going to be air entraining, the vorticity must be sufficiently strong to draw down the free surface until the width of the core at the intake level of the exit tube is equal to the outside diameter of the tube.

If the swirl reaches the very high value required by this condition there will be a sudden change from water flow to air entrainment, perhaps resulting in a loss of pump suction or at least considerable fluctuation in the water flow into the exit pipe. The approximate value of the swirl necessary to draw the surface down to this critical level can be calculated from the cylindrical vortex theory, which gives that

$$c = r.\sqrt{2.g.H}$$

This theory makes no allowance for other velocities apart from the swirl velocity w, the velocity components u and v may be small at points remote from the pipe exit but near the exit these velocities will generally become considerable. Therefore in the vicinity of the intake, when conditions are approaching the critical, the free surface profile will be modified by the intake velocities.

The only analysis that can be applied to this problem is a relaxation analysis and such a relaxation analysis using one set of experimental readings was undertaken. Fig.49 shows the free surface that can be calculated from cylindrical vortex theory and Fig.48 shows the modifications to this surface calculated by the relaxation analysis; the streamlines given by this analysis are also sketched in. The free surface is only modified very close to the outlet. The relaxation analysis was carried out for several strengths of vortex each of which gave free surface profiles ending at various distances down the suction tube. The analysis indicated the influence of the vertical and radial components of velocity near the outlet and showed how they modified the cylindrical free vortex profile.

The surface profile was modified only slightly unless the free cylindrical profile was within about half an inch of the bottom of the suction tube. For the critical value of the swirl found by this method the corresponding free cylindrical vortex

profile was within $\frac{1}{4}$ inch of the bottom of the tube; in this region the additional velocities near the outlet were sufficient to draw the surface profile down to the bottom of the tube.

For the critical condition when the free surface is drawn down to the bottom of the tube the pressure in the entrance to the outlet tube must be equal to atmospheric pressure. Therefore, for this critical condition Bernoulli's equation will give the value of the vertical velocity in the outlet tube if it is assumed that the vertical velocity is uniform across the outlet. Applying Bernoulli's equation at the outer tube radius at the outlet section and also at a large radius where the total energy is H,

$$H = \frac{v^2}{2g} + \frac{c^2}{2g r^2}$$

The quantity flowing is v. A where A is the internal area of the outlet tube.

$$\therefore \quad Q = A \sqrt{2gH - \frac{c^2}{r^2}}$$

Experiments were made to determine this critical value so that it could be compared with the relaxation analysis and the above theory.

3. Upward flow in a central outlet tube.

The small vortex tank was modified for this series of tests by blocking the bottom outlet and installing a vertical, perspex suction pipe connected to a rubber hose to act as a syphon. The perspex tube was 18 inches long, 0.75 inches internal bore and 1.0 inch external diameter. The perspex tube was mounted so that its submergence could be adjusted by sliding it in a vertical sleeve and its position relative to the vertical centre line of the tank could also be changed. The necessary intake velocity was obtained by changing the operating head of the syphon.

In the first series of tests the outlet axis was made coincident with the tank centre line and the total inflow was supplied through the tangential inlets so that maximum swirl was generated. The syphon was set to give a velocity greater than $\sqrt{2gh}$ and submergence and flow rate were adjusted until the required surface profile was obtained. After several tests near-critical conditions were obtained. Typical results of these tests are shown plotted in Fig.49 and comparison is made with the simple theory. Fig. 48 shows the results of the relaxation computation for a condition similar to Fig.49. Details of this analysis are given in Chapter V. For this test the measured quantity of outflow was 23.1 cu.ins/sec. while the calculated value for the theory given is 28.2 cu.ins/sec using the non-viscous value of the swirl and 26.0 cu.ins/sec. using the measured value of the swirl.

Both the measured surface profile and the measured swirl indicate that energy losses are not negligible, yet there is still approximate agreement between the practical results, the simple theory and the relaxation analysis.

Two interesting phenomena were observed during these experiments, firstly a small core was seen to form between the bottom of the tank and into the exit pipe. This core was concentric with the axis of the vortex and was nowhere connected to the free surface; it is visible in the photograph in Fig.47. Presumably the pressure of this core must be equal to the vapour pressure of the water or slightly higher if there is much dissolved air present in the water. This core therefore has no connection with air entrainment and results from the very high free vortex velocities near the pipe axis. The second phenomenon appeared after an experiment had been running for perhaps 10 or 15 minutes when the undisturbed water surface began to oscillate; it was not a wave motion oscillation, the surface remained flat and became tilted about an axis through the centre of the tank. The axis of tilt moved steadily around the tank giving the appearance of a surface oscillation. At the same time the vortex core became asymmetrical and a subsidiary core formed down one side of the exit tube. This subsidiary core rotated around the exit tube in phase with the surface oscillation, photographs of which are shown in Figs. 50 and 51. When this instability had built up, the subsidiary core entrained air into the outlet.

In the beginning of the exit pipe there were now two cores which rotated around each other as predicted by vortex theory for two vortices of similar sign. This intertwining of the two cores can be seen in the photograph in Fig.51. The core of this subsidiary vortex is not vertical but this does not contradict the theory, for the required pressure-velocity distribution is maintained by the tilting of the water surface.

Whether this instability can build up and a subsidiary core form in the less steady and less symmetrical conditions of a pump sump is doubtful, for even in the controlled conditions of the small vortex tank it was some 10 or 15 minutes before the subsidiary core was established.

4. Experiments with Outlet Tube Off-Centre.

The syphon setting and inlet quantity were now kept constant but the outlet tube was moved 1 inch off-centre. With this slight eccentricity, (the ratio of tank radius to eccentricity being 11 to 1), the main vortex remained approximately central and a strong intermittent vortex formed. After 2 minutes this vortex entrained sufficient air to break the syphon. The intermittent vortex formed is shown in Fig.52.

The eccentricity of the syphon was now increased to 2 inches and now only a slight main vortex formed. The operating head for the syphon was therefore greater and the water level was soon sucked down until syphon action ceased.

Eccentricities of 3 inches and greater were now used but for these higher eccentricities there was no trace of a vortex despite the very strong swirl present in the tank. The water level was drawn down to zero in each test without a vortex core forming. This evidence shows the need for almost complete symmetry if a steady vortex is to form. When the intake was in the outer part of the tank it was effectively in a strong uniform flow. The fact that no core, even of a transient nature, forms under this condition can be very useful. Several papers on prevention of air-entrainment have stated that velocities of approach to an outlet must be kept as low as possible, but the present result indicates that the opposite may well be true. The results show that it is advantageous to operate an intake in a strong, almost uniform flow; under this condition no core will form.

5.Transient Air-entraining Vortices.

The formation of a transient air entraining vortex was studied and some of the necessary conditions were determined. It has previously been shown that for a steady vortex to form the centre line of the vortex must be vertical and concentric with that of the outlet and in the previous section it has been shown that for such a vortex to be air-entraining the swirl must be very high. Suppose that a vortex is shed from part of the boundary enclosing the flow approaching the outlet. This vortex will be carried towards the outlet and will at the same time be decaying. The axis of this vortex must be vertical and it must begin and end on boundaries, the free surface and the tank bottom. If this vortex reaches the neighbourhood of the outlet before it decays, its lower end can now terminate in the outlet so that the decayed vorticity from its centre is removed. The removal of fluid from its centre creates a necessary condition for formation of a vortex-core in a viscous fluid, but the supply of vorticity is limited to the amount of the original vorticity that still remains. The core which forms will therefore only last while it still has residual vorticity.

The outlet tube itself attempts to draw water symmetrically from all sides; when water is supplied from one side of the sump there is necessarily a flow past the outlet to provide the necessary supply to the far side of the sump. One important observation was made, namely that the flow past the outlet

causes vortices to be shed from the outlet itself and these vortices being in the immediate vicinity of the outlet cause air-entrainment. This particular cause of air-entrainment can be prevented by placing the outlet near the back wall of the sump so that it draws water only from the direction of supply. It was also observed that when the outlet is situated in a strong uniform flow the vortices shed from it are removed before they can develop into air-entraining vortices. Therefore there are two methods by which transient air-entrainment may be prevented. The first method is by using very low approach velocities and smooth boundaries so that no strong vortices are formed, special care being taken to prevent shedding of vortices from the outside of the outlet pipe by siting it near a boundary. The second method is to site the intake in a strong uniform flow so that no vortex is near the outlet for sufficient time for an air-core to form.

FIG. 46

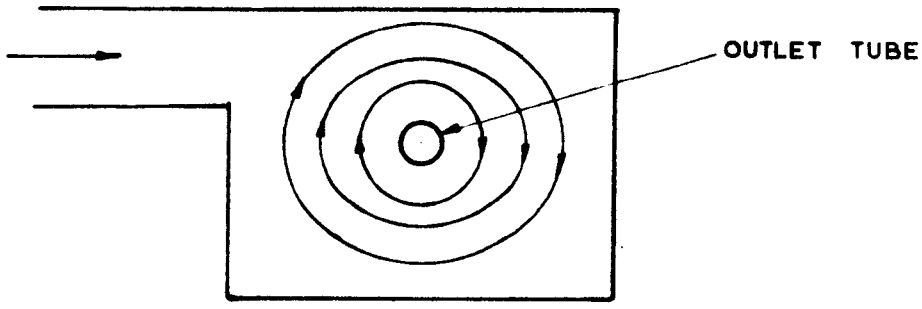

a) ASYMMETRICAL INLET INDUCING A GENERAL SWIRL CONCENTRIC WITH OUTLET.

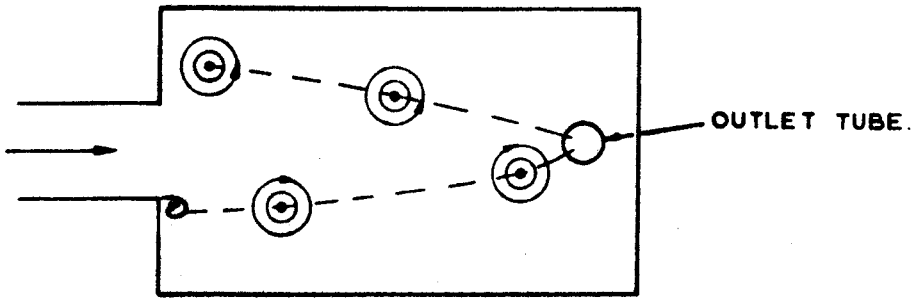

b) VORTICES BEING SHED FROM BOUNDARY AND CARRIED TOWARDS OUTLET.

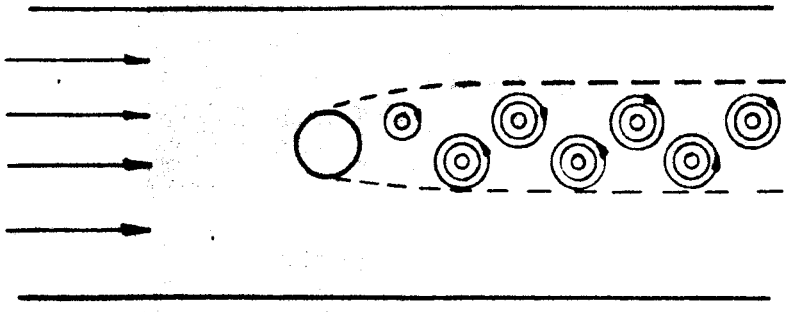

c) VORTICES SHED FROM OUTLET TUBE. THIS ONLY HAPPENS FOR UPWARDS OUTLET TUBE.

THREE METHODS BY WHICH AIR-ENTRAINING VORTICES CAN ARISE.

FIG 47

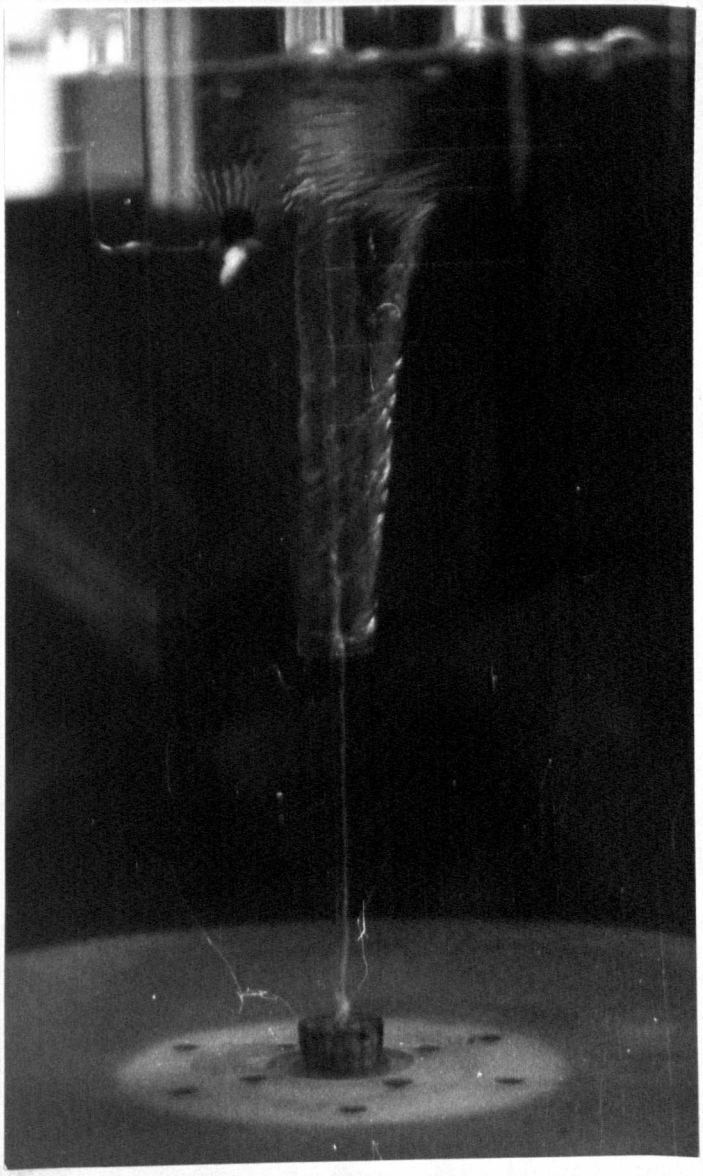

UPWARDS OUTLET

Critical steady vortex for comparison with the relaxation analysis.

FIG. 48

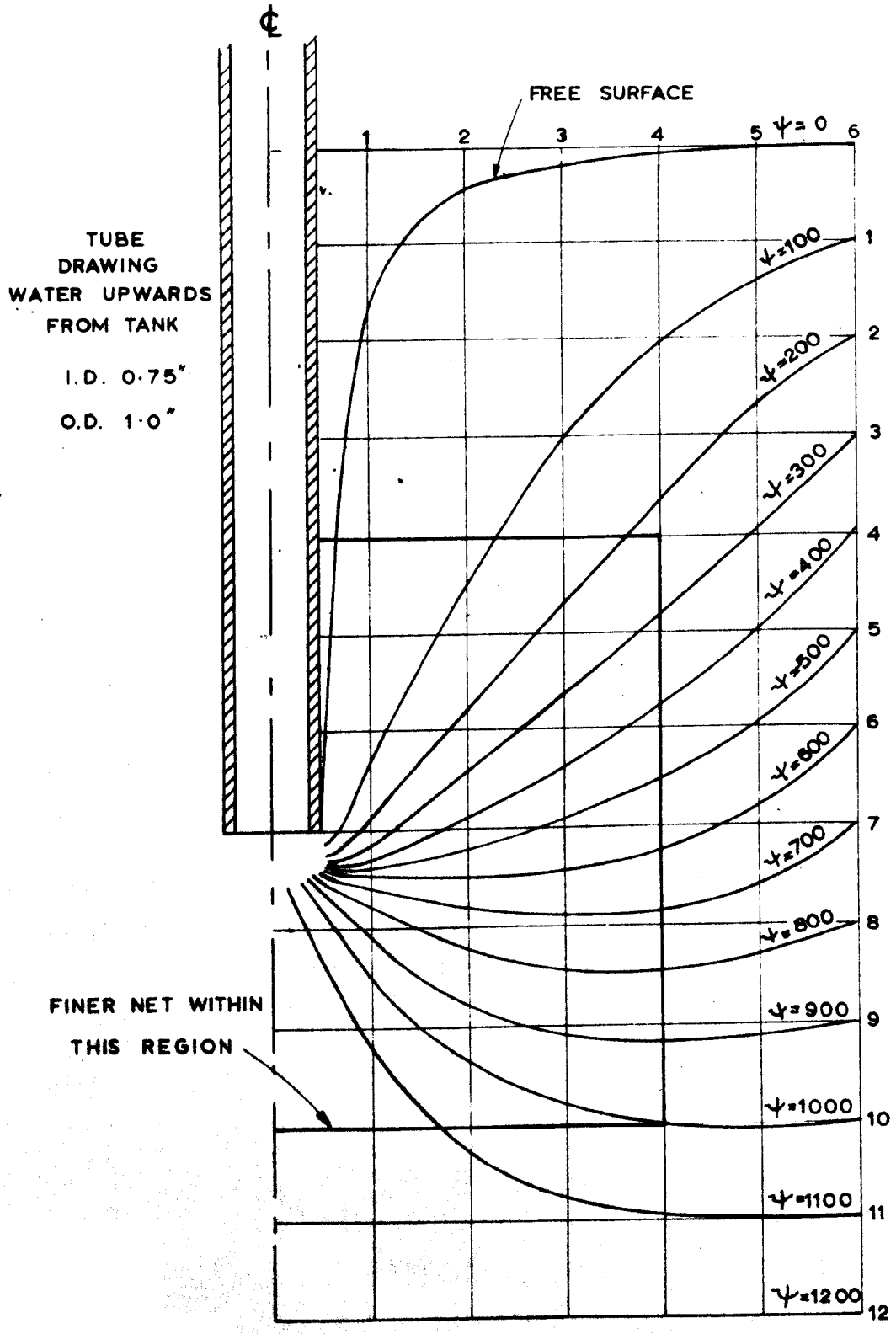

UPWARD FLOW — RELAXATION ANALYSIS

CRITICAL FREE SURFACE AND STREAMLINE PATTERN.

CRITICAL SWIRL C = 36·1 IN.^{2}/SEC.

FIG. 49

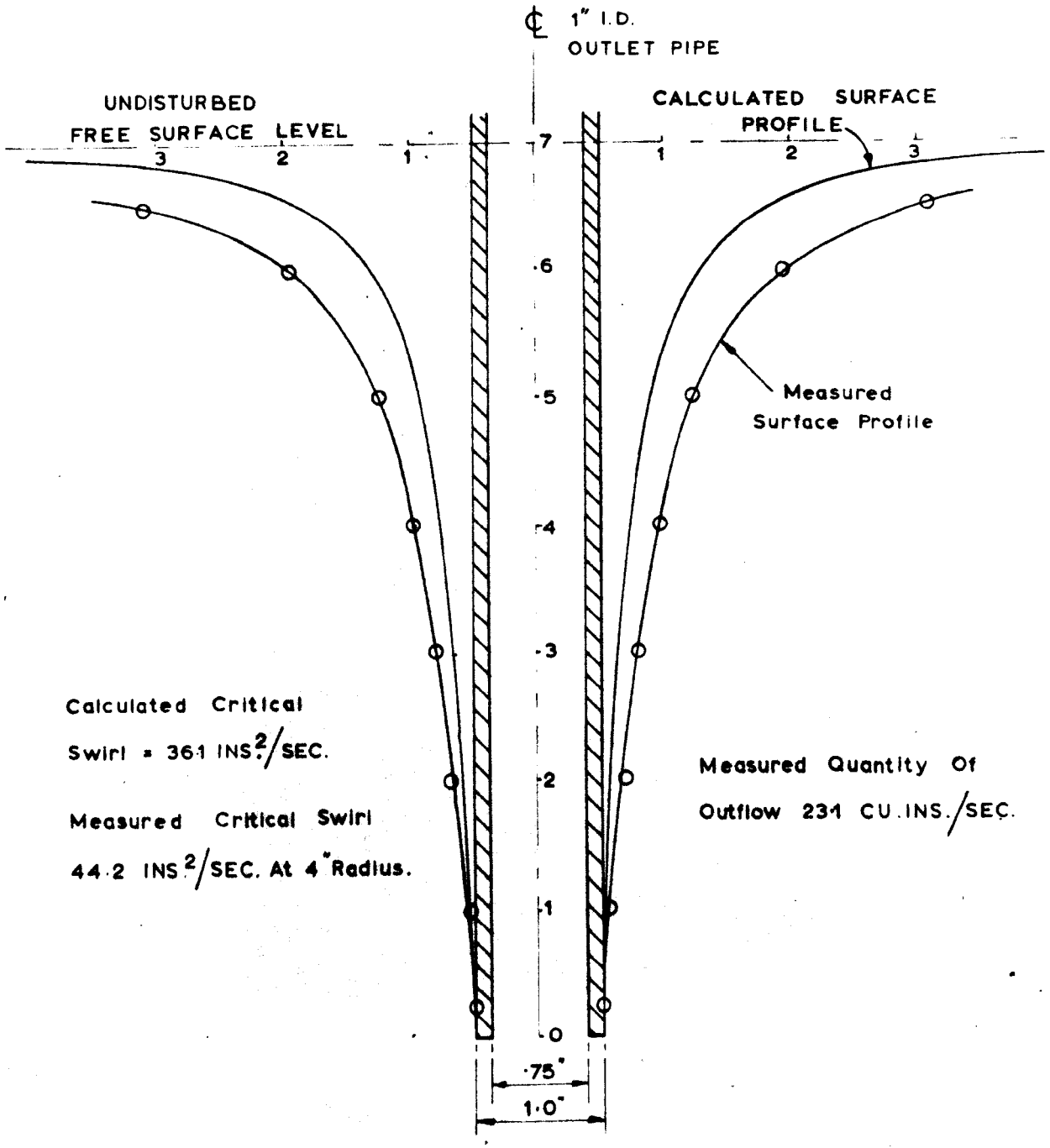

UPWARD FLOW.

Comparison Of Calculated And Measured Surface Profiles For Critical Drawdown.

FIG 50

UPWARDS OUTLET.

Formation of subsidiary core.

FIG 51

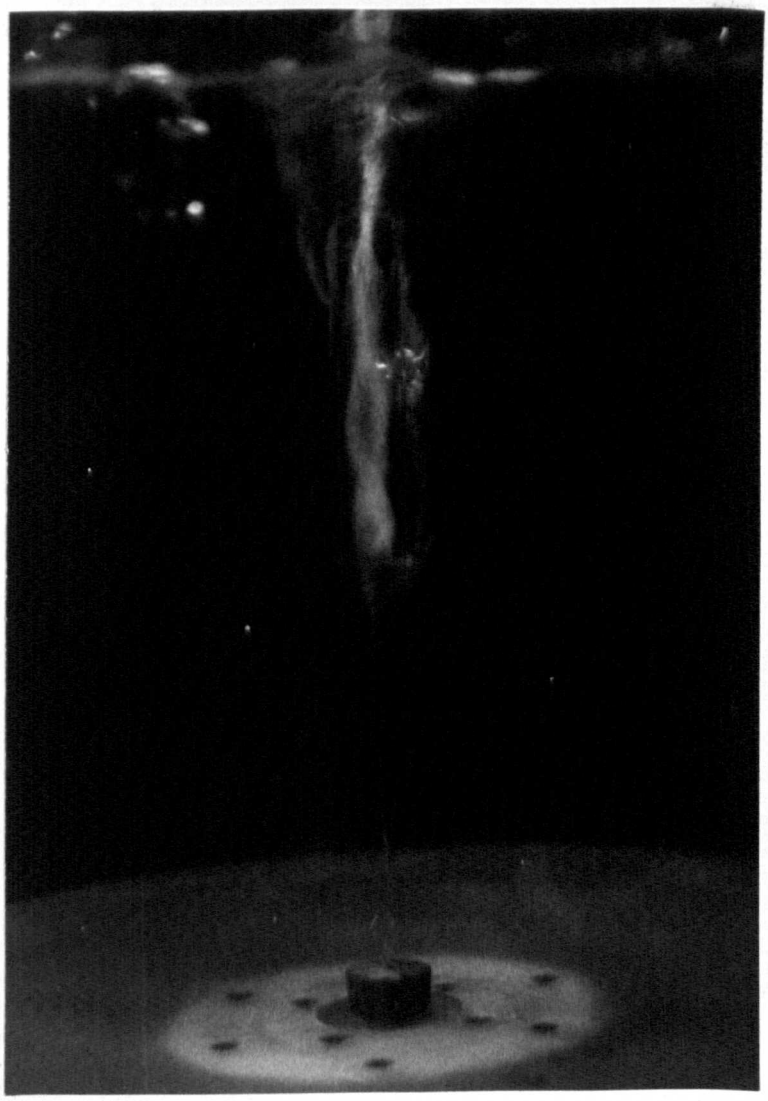

UPWARDS OUTLET.

Subsidiary core is rotating around outlet and the two cores form a spiral.

FIG 52

UPWARDS OUTLET.

The outlet tube has been moved 1" away from $\mathbb{C}_L$ of tank.

CHAPTER V11

CONDITIONS IN THE OUTLET TUBE

The investigation has so far been concerned with conditions in the vortex tank, prior to the water entering the outlet. Attention was now turned to the flow conditions in the outlet pipe. Two outlet pipe arrangements have been studied, an outlet vertically downwards from the base of the tank and an outlet vertically upwards, drawing water from the tank. It has been shown that the formation of air entraining vortices under these two conditions can be fundamentally different, and so the conditions in these two outlets will be considered separately.

Several questions arise concerning the history of the air-core and the swirling flow in the outlet tube. Does the air-core persist or does the air become dispersed in the form of air bubbles? How quickly does the swirl die away and what influence do bends in the pipeline have? To answer these questions the experiments described in this chapter were made.

1. Outlet tube vertically downwards.

The apparatus used for these tests is shown diagrammatically in Fig.54. A cylindrical tank with tangential inlets for inducing the required swirl

was supported about 6 feet above the laboratory floor. From the centre of this tank was a 4 foot long perspex tube of 1¼ inches bore which led vertically downwards and was in turn connected to a right angled bend and horizontal straight also of 1¼ inches bore. At the end of this horizontal tube was a control valve and a measuring tank.

In the first experiments the control valve at outlet was left fully open and a free spiral vortex was produced in the top tank. The flow at the outlet to the tank therefore had an air core of radius "b" and was travelling at the critical velocity for the amount of swirl present. In travelling down the vertical outlet tube the flow accelerated and stayed in contact with the tube wall so that the air core increased in size. The flow therefore consisted of an annular film of water with both swirl and vertical velocities. This flow persisted down the vertical tube but was completely altered on turning the bend and entering the horizontal tube, when the swirl was destroyed and the horizontal tube ran part full with the major portion filled by air. Readings of vertical and swirl velocities and film thicknesses were made in the vertical portion of the outlet to determine the effect of viscous retardation on the flow:

details of these readings are given later.

Partly closing the valve at outlet produced a hydraulic jump first in the horizontal tube and later in the vertical tube. In the horizontal tube the jump occurred according to the standard analysis[18] for such a jump: air was still carried through in the form of large bubbles at the top of the tube. No previous reference has been found to the type of hydraulic jump which occurred in the vertical tube; this jump has therefore been examined in detail and an analysis has been developed. Because the jump is a transition from a thin annular film of water around the periphery of the tube to the condition with the pipe running full, it will be referred to as the annular hydraulic jump.

It should be noted that the annular hydraulic jump can be produced without the presence of swirling flow. The essential upstream condition is that there should be an annulus of water moving vertically down a pipe and this condition can be produced when the entrance to the vertical pipe acts as a circular weir: a bellmouth entrance could produce this flow condition most efficiently.

A photograph of a typical annular hydraulic jump is given in Fig. 59 It will be seen that there is an almost instantaneous change from annular flow to pipe-full flow; it will also be seen that there is a tongue of very turbulent water standing on the transition and within the oncoming annular flow.

This highly turbulent tongue entrains a quantity of air which is then carried downstream in the form of bubbles. When the jump occurs there is a decrease in momentum which results in an increase in static pressure downstream of the jump; it is this increased downstream pressure which projects the tongue of fluid upwards from the jump.

2. Theoretical Analysis.

An analysis will now be developed based on momentum change. The symbols used have the following significance:-

a	radius of tube.
b	radius of air core.
g	gravitional acceleration.
h	tongue height.
k	downstream air blockage factor.
p	pressure (above atmospheric).
Q	volume flow per second.
r	non-specific radius.
S	vortex strength, w.r.
t	thickness of fluid film, a-b.
v	average vertical velocity.
w	swirl velocity
θ	flow angle measured clockwise from vertical.
Ω	angular velocity downstream of jump.
Suffix 1	above jump.
Suffix 2	below jump.

Fig.55 is a diagrammatic representation of the annular hydraulic jump, while Figs. 56 and 59 are photographs of the jump. Consider the vertical momentum and angular momentum separately.

Vertically, there is a pressure p_2 immediately below the jump. The pressure above the jump will be atmospheric at radius 'b' and p_1 at radius 'a' arising from the centripetal component. As a first approximation p_1 will be neglected in comparison with the downstream pressure p_2.

By continuity,

$$Q = \pi.(a^2 - b^2).v_1 \qquad ..(1)$$

where a and b are tube and air-core radii respectively and v_1 is the average upstream vertical velocity.

The air bubbles downstream cause a certain decrease in flow area, so that, if (1 - k) is the fraction of the tube blocked by air, we have,

$$Q = k.\pi.a^2.v_2 \qquad ..(2)$$

Hence
$$v_1 = \frac{k.a^2}{(a - b)(a + b)}.v_2 \qquad ..(3)$$

Considering change of vertical momentum and the downstream pressure produced

$$p_2.\pi.a^2 = \rho.Q.(v_1 - v_2) \qquad ..(4)$$

Substituting from equation 3 for v_1,

$$\frac{p_2}{\rho.g} = \frac{Q}{\pi.a^2.g}.v_2 \left[\frac{k.a^2}{(a - b)(a + b)} - 1\right] \qquad ..(5)$$

Eliminating v_2 from equation (2),

$$\frac{p_2}{\rho.g} = \frac{Q^2.(b^2 - a^2 + k.a^2)}{k.\pi^2.a^4.g.(a - b)(a + b)} \qquad ..(6)$$

If there is no air blockage k equals unity and equation (6) reduces to,

$$\frac{p_2}{\rho.g} = \frac{Q^2.b^2}{\pi^2.a^4.g.(a - b)(a + b)} \qquad ..(7)$$

Boundary layers and other viscous effects make it impossible to write down exact expressions for swirling velocities upstream and downstream of the jump. For ideal, non-viscous flow both the upstream and downstream distribution would be that of a potential vortex in which velocity is inversely proportional to radius. Measurements of velocities upstream and downstream of the jump are given in Figs. 57 and 58 and it will be seen that the assumption of potential vortex distribution upstream of the jump is not unreasonable.

Downstream a potential vortex would produce very high shears near the central region of the tube and it can be seen that the measured distribution approximates more nearly to that of a forced vortex in which velocity is proportional to radius.

Assuming a free vortex distribution upstream and a forced vortex distribution downstream, the conservation of angular momentum gives the following relationship between upstream and downstream swirl velocities.

$$\text{Angular momentum upstream} = \sum_{r=b}^{r=a} \delta I.\frac{d\theta}{dt} \qquad ..(8)$$

Now $\delta I = 2\pi.r.\delta r.v_i.\rho.r^2$

Also $\frac{d\theta}{dt} = \frac{w}{r} = \frac{S}{r^2}$ because w.r. = S, a constant, for free vortex flow.

Therefore angular momentum upstream = $2\pi.v_1.\rho.S.\int_b^a r.dr$ ..(9)

Therefore upstream momentum = $\pi.\rho.v_1.S.(a^2 - b^2)$ ..(10)

Downstream $\frac{d\theta}{dt} = \frac{w}{r} = \Omega$, a constant for a forced vortex distribution.

Therefore angular momentum downstream = $\int_b^a 2\pi.r.\delta r.v_2.\rho.r^2.\Omega$ ..(11)

= $\pi.\rho.v_2.\frac{a^4}{2}.\Omega$ ..(12)

Putting equations 10 and 12 equal,

$$v_1.S.(a^2 - b^2) = v_2.\Omega.\frac{a^4}{2} \quad ..(13)$$

Eliminating v_1 and v_2 from equation (3),

$$S = \frac{\Omega.a^2}{2k} \quad ..(14)$$

For a given upstream velocity distribution equation 14 allows the corresponding downstream velocity distribution to be calculated. The values obtained from equation 14 are plotted in Fig.58 with the measured downstream velocity distributions.

3. Pressure at the Base of the Tongue.

The first experiments soon made it clear that the pressure required to produce the necessary momentum change was greater than could be developed by a static column of water of the height of the tongue. The water circulation within the tongue was therefore studied.

Because of the considerable unsteadiness, turbulence and aeration within the tongue it was not found possible to make any velocity measurements, but the general circulation was studied by injecting dye into various parts of the tongue with a hypodermic syringe.

By injecting intermittently the path of the dye could be followed and the picture of the circulation built up by this method is shown in Fig.55. At the base of the tongue it was difficult to see how the water circulated because there appears to be a crossing of streamlines. It was then realised that the tongue could be considered as a separate circulation balanced on the jump, the water at the centre of the tongue being forced upwards by the pressure p_2 with a maximum velocity sufficient for it to reach the top of the tongue, namely $\sqrt{2g.h}$ where h is the height of the tongue. After reaching the top of the tongue the water then falls back freely down the outside of the tongue and again attains a velocity of $\sqrt{2g.h}$ when it reaches the bottom. It is then turned through 180° and travels up the centre of the tongue again. The state can be analysed as follows :

Let the area of base of tongue = A

Quantity travelling upwards must equal quantity returning downwards. Therefore at base, flow area = A/2 and velocity, $u = \sqrt{2gh}$. So that $Q = \frac{A}{2}\sqrt{2g.h}$.

The tongue is considered to be a jet with a free surface so that its internal pressure is everywhere zero. Therefore at the base the pressure p_2 produces the necessary momentum change from $Qp.\sqrt{2gh}$ downwards to the same value upwards, and this pressure acts over the area A.

Therefore $p_2 \cdot A = Qp(u_1 - u_2)$

Substituting for Q, u_1 and u_2,

$$p_2 = 2pgh.$$

The base pressure p_2, is therefore twice the pressure that would be developed by a static column of water of height h.

There are two factors which have not been allowed for in the above analysis. Firstly not all the water rises to height h and so not all the water has a velocity of $\sqrt{2gh}$ at the base of the tongue. Secondly as water moves up or down in the tongue viscous shearing and turbulence will destroy kinetic energy. Whichever of these effects is greater will determine whether p_2 is less than or greater than $2\rho gh$.

4. Experimental Observations.

For the present series of tests the strength of the vortex and the depth of water in the upper tank were kept constant. The flow at outlet from such a tank is in the critical flow condition and the entry to the perspex tube acts as a control section. Therefore, provided the annular hydraulic jump occurs below the pipe entry, the outflow from the vortex tank will be constant. In these tests the depth of water in the vortex tank at a radius of 4 inches was 18.5 inches, the swirl velocity at this radius was 11.9 inches per second and these conditions gave a flow quantity of 41.6 cubic inches per second.

In each test the throttling valve at outlet was adjusted until a jump occurred in the required positions. Four positions of the jump were chosen and photographs were taken using a square, water-filled perspex box to remove distortion. Tongue height and

bubble formation were determined from these photographs. The thickness of the water film upstream of the jump could not be measured with sufficient accuracy from these photographs because a change in thickness of 0.01" might represent a velocity change of 1 ft. per second or more, so that the tongue heights calculated from these film thicknesses were not reliable. It was therefore decided to measure the upstream velocity distribution and then to use this velocity distribution and the measured flow quantity to calculate the average upstream film thickness. Either the upstream velocities or the film thicknesses can be used to calculate the tongue heights.

Because the flow has both axial and tangential velocity components it is not possible to use a pitot tube unless flow direction is first determined. Velocity measurements were therefore made using a cylinder 0.125 inches in diameter with a small hole 0.040 inches diameter for measuring pressure in a given direction. By plotting pressures in different directions this cylinder could be used as a yaw meter, giving both direction and magnitude of the velocity. Calibration of this cylinder in a flow of known direction indicated it was accurate to about $\pm \frac{1}{2}^{\circ}$. Upstream of the jump static pressure was found to be equal to atmospheric pressure and therefore the dynamic pressure could be determined directly. Downstream of the jump the vortex structure caused static pressures in the flow to be lower than the wall-static pressure.

To overcome the difficulty of measuring the true static pressures within the flow the cylinder was used as a double pitot; pressure readings were taken both upstream and downstream in the direction of flow. The total difference in pressure determined in this way will give the velocity if the Reynolds Number of the flow is known approximately.

From the magnitudes and directions of the velocities measured, the distributions of upstream and downstream axial and tangential velocities were determined. Values of the upstream axial velocities were then used to calculate tongue heights for various air blockage factors and these values were compared with those obtained experimentally; they are shown plotted in Fig.60. Also the upstream tangential velocities were used to calculate the downstream velocity distribution and, again, comparison was made with the measured values, these being plotted in Fig.58.

The air blockage could not be determined from the velocity measurements because the distribution of air was not uniform, and therefore the air-water mixture had a varying apparent density which could not be determined. The quantity of air at outlet could be measured but this is not necessarily a true measure of the air blockage at the jump because some of the air bubbles have a rising velocity greater than the downward water velocities and so are not carried through.

The measurements of velocity and pressure immediately upstream and downstream of the jump give the values of total energy at these positions. From these values the energy lost in the jump can be found. The energy lost in the jump can also be calculated from the upstream conditions and the momentum equation for the jump. The values obtained are shown in Fig.61 where the energy lost is expressed as a percentage of the upstream energy and is plotted against upstream velocity. It will be seen that the energy loss rises considerably as the upstream velocity increases.

5. Position of the Annular Hydraulic Jump.

The momentum equation for the annular hydraulic jump can be satisfied for any value of the upstream velocity, so that, from consideration of momentum alone, the jump can occur at any position in the tube. Experiments show that, if the valve setting at outlet is altered so that the energy level immediately upstream of it is changed, the jump will move upstream or downstream until the new energy balance is satisfied. The position of the annular hydraulic jump is therefore determined by the energy losses throughout the system.

Measurements of total energy were made at a number of positions in the flow system for the different positions of the annular hydraulic jump. The values obtained are plotted in Fig.62. The energy line with no jump present, shown in bold inter-connected dashes, indicates the high rate of energy loss for the high speed annular flow.

If a jump occurs, there is an energy loss in the jump itself but the rate of loss of energy in the pipe-full flow below the jump is much less, so that the energy line soon rises above the line with no jump.

The value of the total energy immediately upstream of the control valve can, within limits, be controlled by the valve setting. It is apparent both from the above discussion and from consideration of Fig.62 that once the value of the energy upstream of the valve is determined the jump position is also determined. In these experiments a control valve has been used, but this valve might equally well be replaced by the throttling action of a more extensive pipework system or a rise in level of the outlet.

A calculation was made of the energy that would be lost for the same rate of flow through a smooth pipe with no swirl velocities and with the pipe running full. It was found that the losses with swirl present were some three times higher. This higher rate of energy loss can be explained qualitatively by the higher shears induced near the pipe wall by the swirling velocities. Quantitative measurements are made difficult because the swirling velocities are being constantly reduced by friction as the flow moves further down the pipe.

In the annular flow the pressure is zero, so that the energy is entirely kinetic. Fig.63 shows a plot of vertical and swirling velocities in the annular flow measured at four positions down the tube.

Also shown in Fig.63 are the idealised, non-viscous vertical and swirl velocities. It is apparent from this figure that the effect of viscosity is considerable on this high speed flow and particularly so for the swirling velocities which are rapidly approaching zero. At present there is no way of calculating these losses.

Therefore, although the position of the annular hydraulic jump is known to be determined by a balance of energy losses, it is not at present possible to calculate these losses either upstream or downstream of such a jump and thus predict its position.

It has been shown that successive throttling of the flow forces the jump further up the tube. At point will be reached where the jump forms at the exit to the vortex tank: this is the condition discussed in Chapter V when considering the minimum swirl necessary to produce a vortex core if the vertical outlet velocity is less than $\sqrt{2gH}$. At this critical condition the velocity above the jump is, theoretically, $\sqrt{2gH-\frac{c^2}{b^2}}$ which is the critical velocity for this outlet condition. A jump to the pipe full condition implies an increase in specific energy and therefore for the jump to occur at this critical section, the upstream conditions in the vortex tank must change to provide the necessary increase in energy. The critical section at the outlet to the tank is therefore the limiting position of the annular hydraulic jump because above this position the flow is below critical.

6. Behaviour of Air Bubbles Downstream of Jump.

Downstream of the annular hydraulic jump it has been shown that the swirl velocity distribution is approximately that of a forced vortex. The central regions of the tube are therefore at a lower pressure than the outer regions at any given cross-section so that air bubbles will tend to move into the central regions of the tube. This formation of a core of bubbles can be seen in Fig.56 which shows photographs of the hydraulic jump occurring in the vertical tube. It will be seen that the bubbles do not form a central core, but the core is in the form of a helix. A study was made to determine the cause of this helix. At first it was thought that there was some lack of symmetry in the upstream flow but observation did not confirm this. The next line of enquiry was an attempt to study the stability of the flow. It was thought that there might be an analogy with a mass rotating about its centroid and free to slide on a rod which also rotated, this being an unstable system. If springs were introduced to represent some partial constraint of the mass it can be shown that there is a position of equilibrium at some point off-centre; Fig.64a illustrates this analogy and also shows a sketch of the streamlines when the centre of the swirl is off-centre. It was not found possible to establish this analogy.

Once the core has moved off-centre the streamline pattern must be as shown in Fig.64b even though the distribution of velocity is not that of a free vortex. This flow pattern is similar to that obtained as part of a vortex pair, and it can be shown that a vortex pair rotates about a common centre. Lamb[19] has extended this theory to show that the centre of a single vortex within a cylinder will describe a circle concentric with the cylinder. When vertical flow is added to the vortex flow it is seen that a helix is produced, but still no explanation is obtained of why the centre of the vortex should move off-centre in the first place.

7. Outlet pipe vertically upwards.

It has been previously shown that the formation of a vortex core into an outlet pipe leading upwards from a tank requires a strong local swirl and the core will probably only be transitory. Consideration will now be given to the history of an air core when entering such an outlet and the result will be compared with the observations of transitory cores.

Fig. 52 shows a vortex core leading into the outlet. At entry to the outlet Bernoulli's equation gives, as previously,

$$H = \frac{w^2}{2.g} + \frac{c^2}{2.g.b^2}$$

because the pressure at the surface of the core must be zero.

Water can only flow upwards either by changing kinetic or pressure energy into potential energy. With a free air surface present it is not possible for the pressure energy level to change and therefore the water can only move upwards by exchanging its kinetic energy for the potential energy gained. From the continuity equation, as v decreases so the flow area must increase and therefore the air core will steadily close. Once the air core has closed the pressure can drop in exchange for the increased potential. Despite the closing of the air-core air entrainment can still continue because of the formation of small air bubbles from the thin tail of the core.

Observations made during the formation of air-entraining vortices confirmed the previous argument even though the vortices were only transitory. Therefore with an upwards outlet there is no possibility of an air-core persisting as was possible with the downwards outlet, but it is still possible for there to be a continuous stream of air bubbles passing up the outlet whenever a transitory vortex core forms.

FIG 53

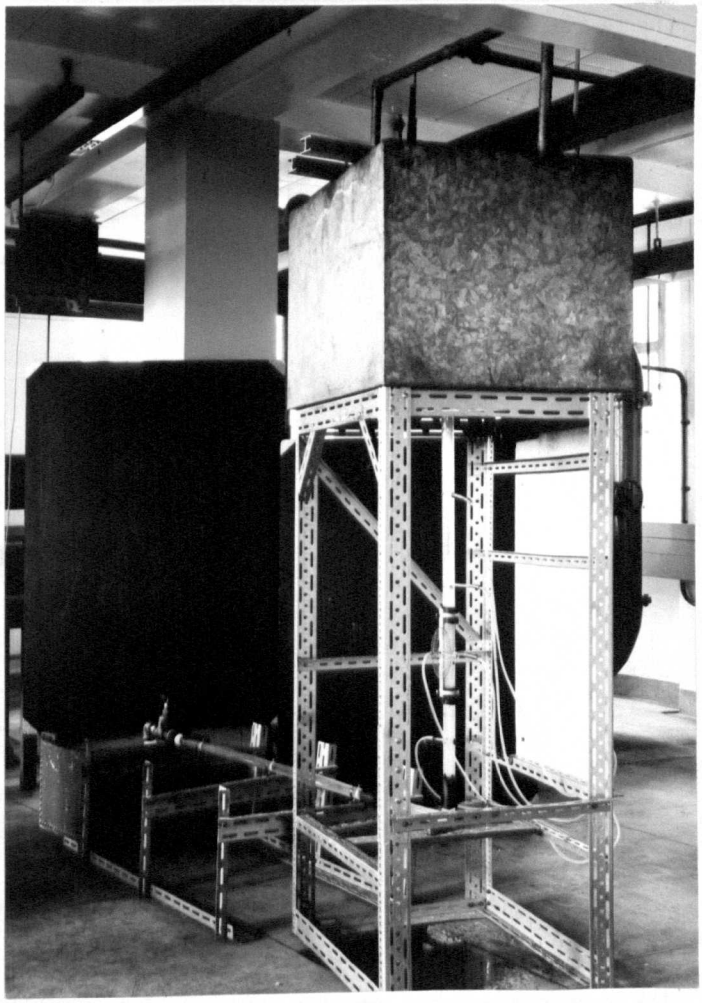

Apparatus to study conditions in downwards outlet tube.

FIG. 54

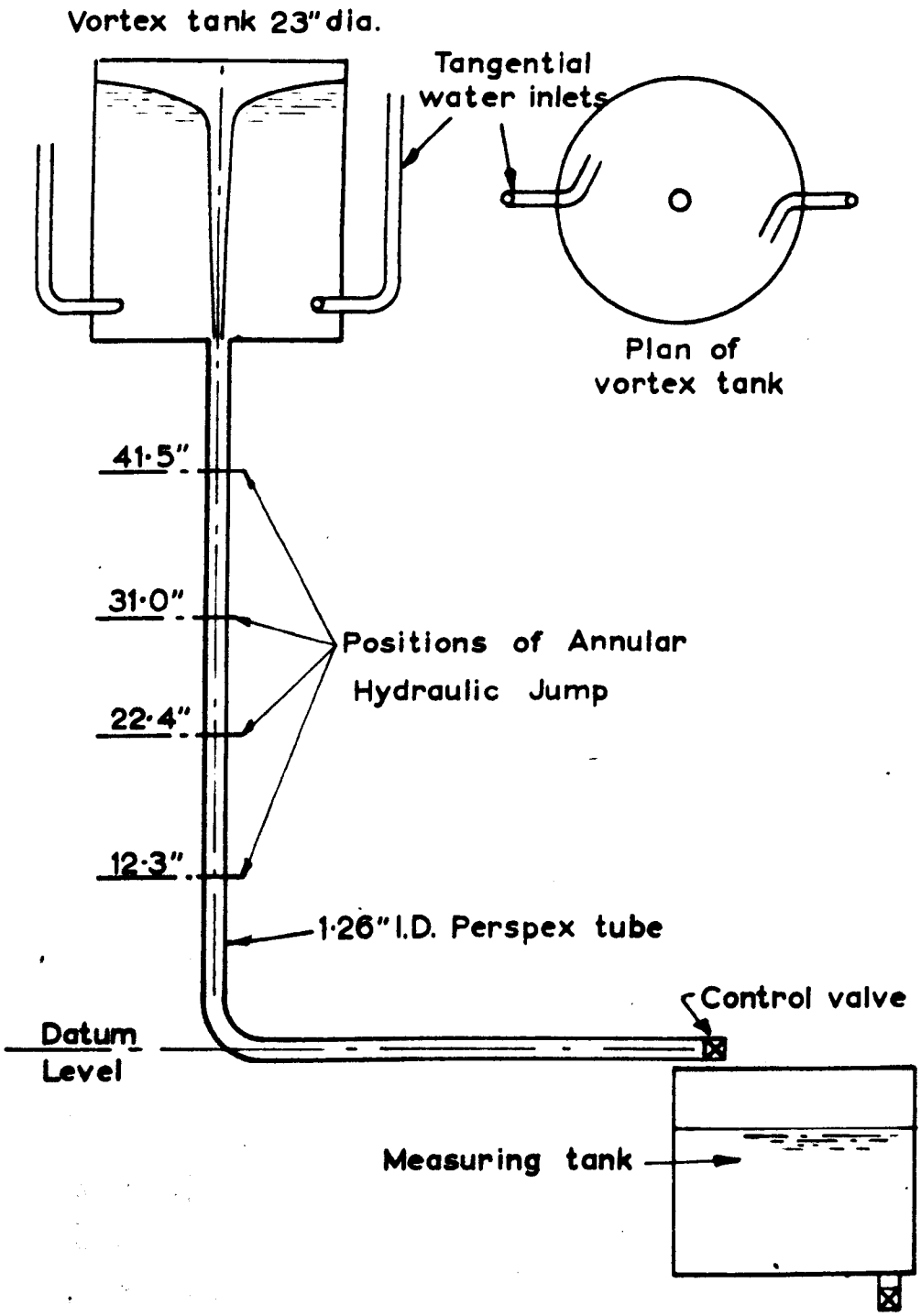

LAYOUT OF APPARATUS

FIG. 55

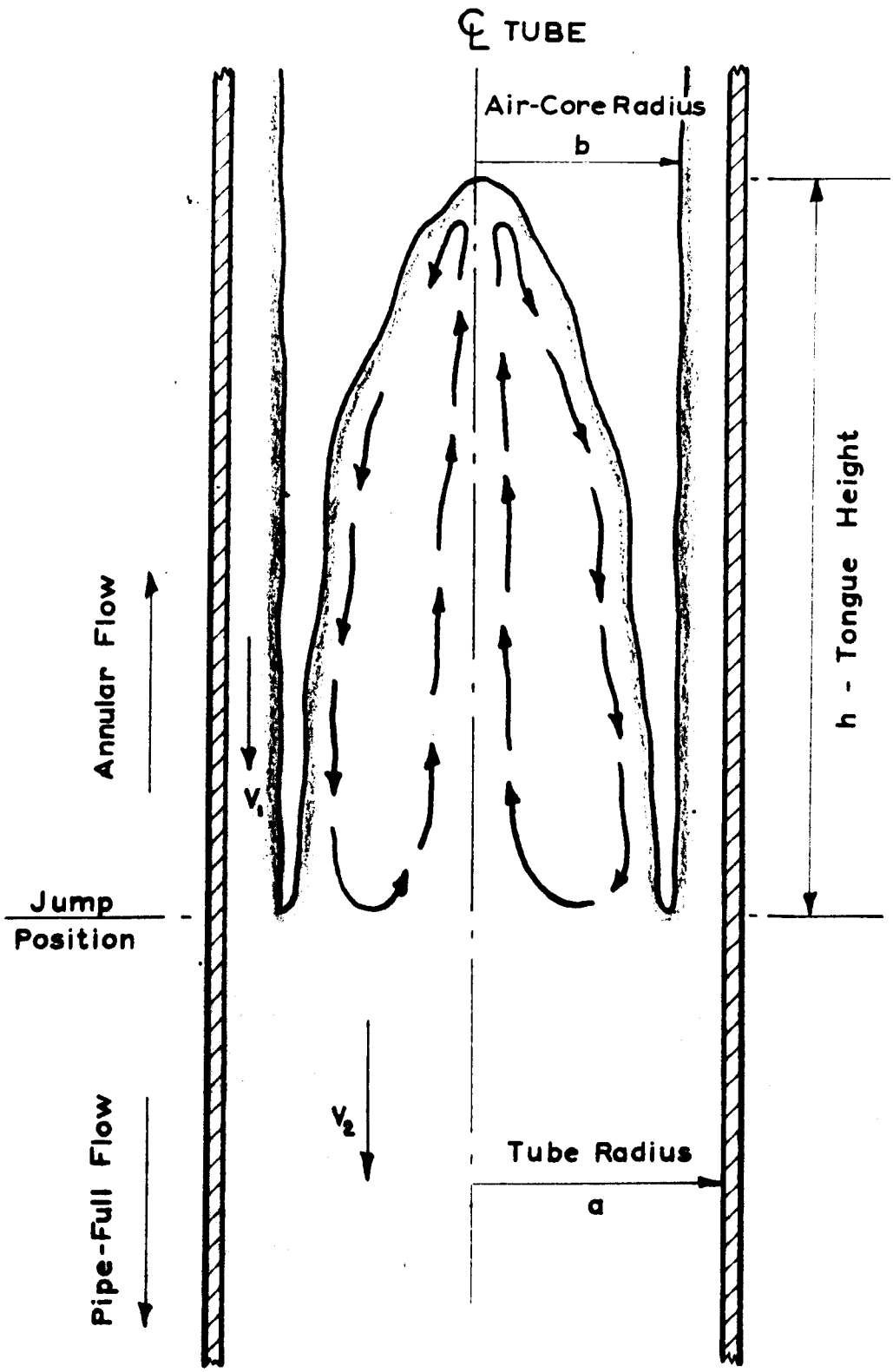

DIAGRAM OF ANNULAR HYDRAULIC JUMP
SHOWING CIRCULATION IN TONGUE

FIG 56

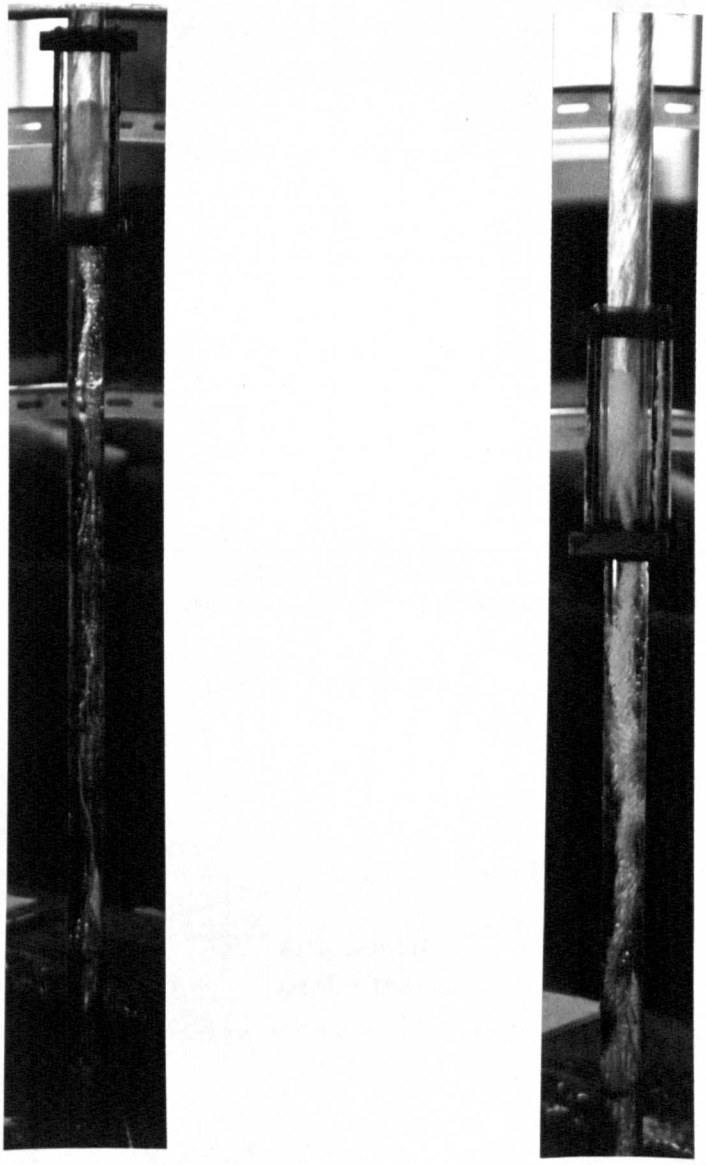

VIEWS OF VERTICAL OUTLET TUBE

The Annular Hydraulic Jump is occuring in each; note the spiraling of air bubbles below the jump.

FIG. 57

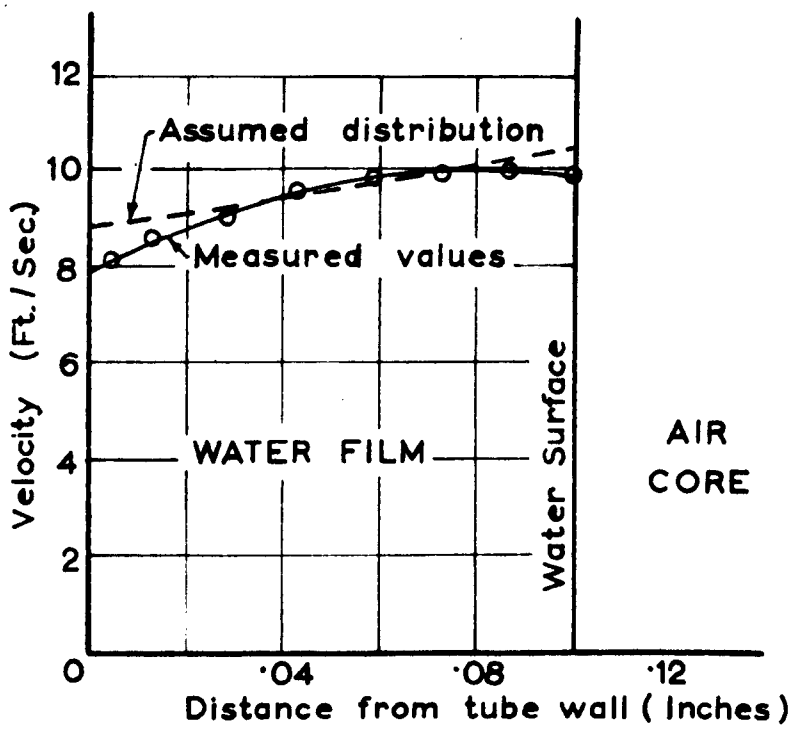

JUMP AT +22·4

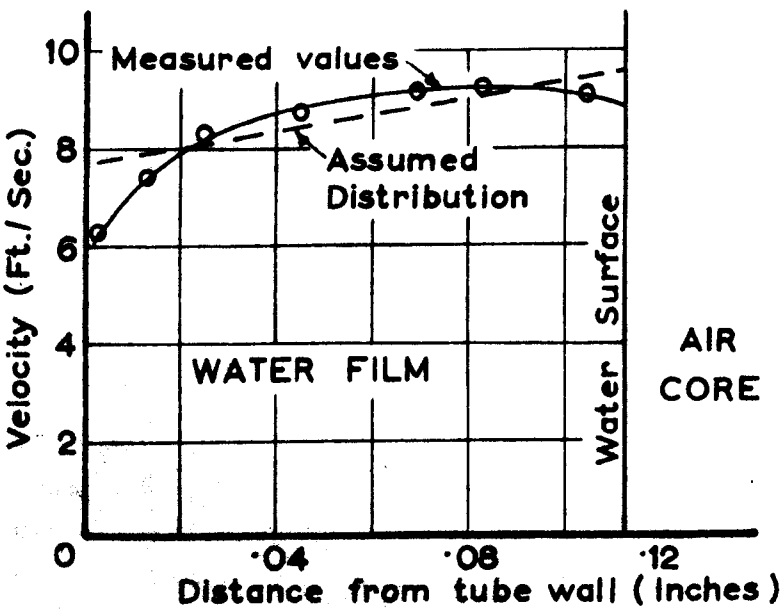

JUMP AT +31·0

UPSTREAM VELOCITY DISTRIBUTIONS

FIG. 58

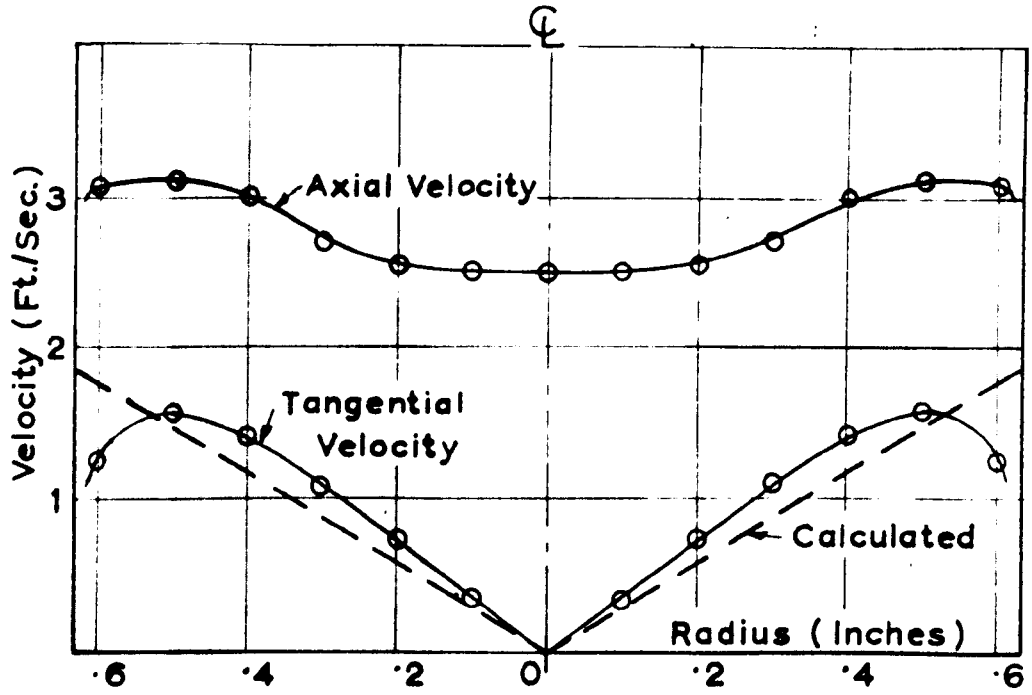

DOWNSTREAM VELOCITY DISTRIBUTION AT + 19·6"
WITH JUMP AT + 22·4

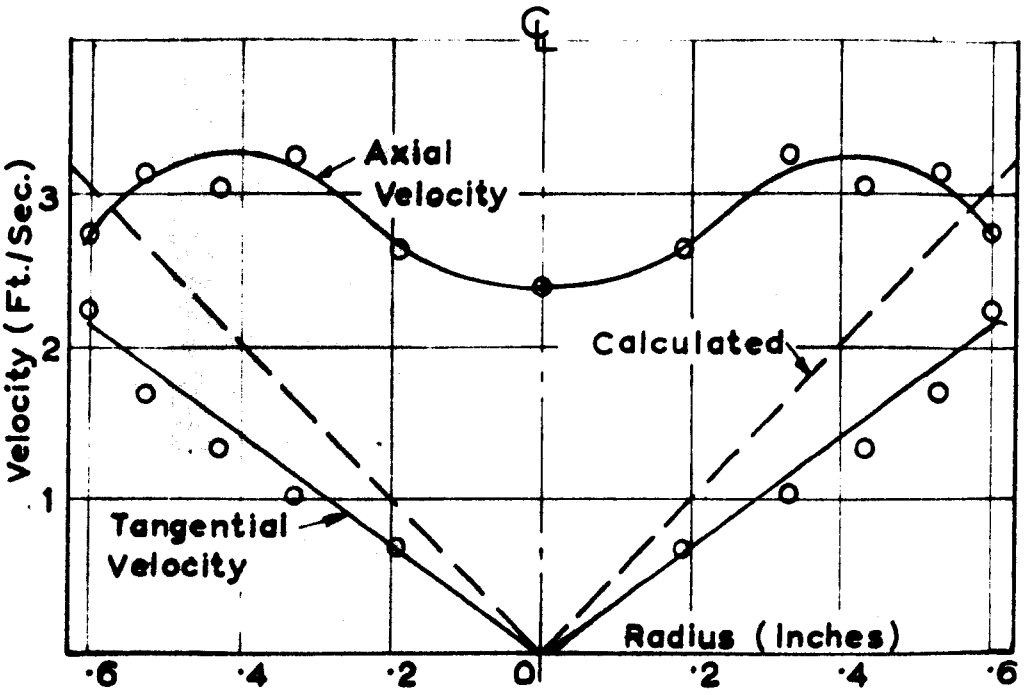

DOWNSTREAM VELOCITY DISTRIBUTION AT +27·8"
WITH JUMP AT +31·0

FIG 59

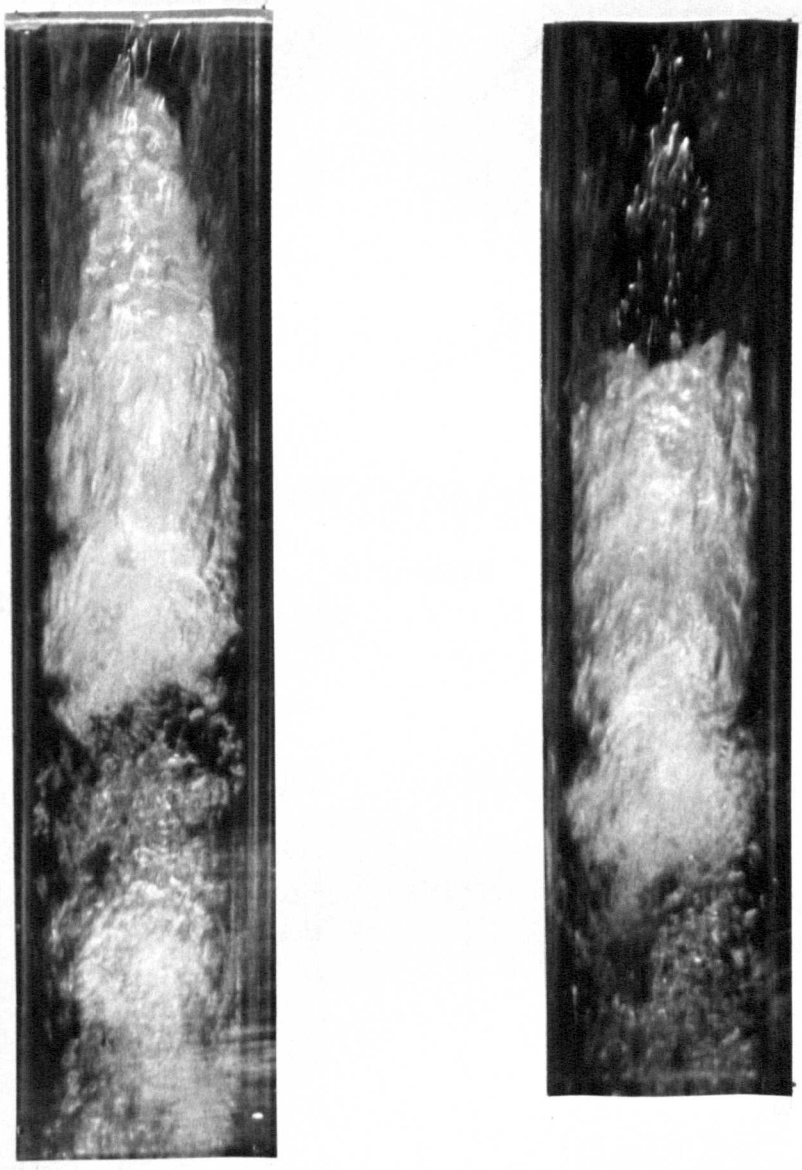

TYPICAL ANNULAR HYDRAULIC JUMPS:

COMPARE WITH FIG 55.

FIG.60

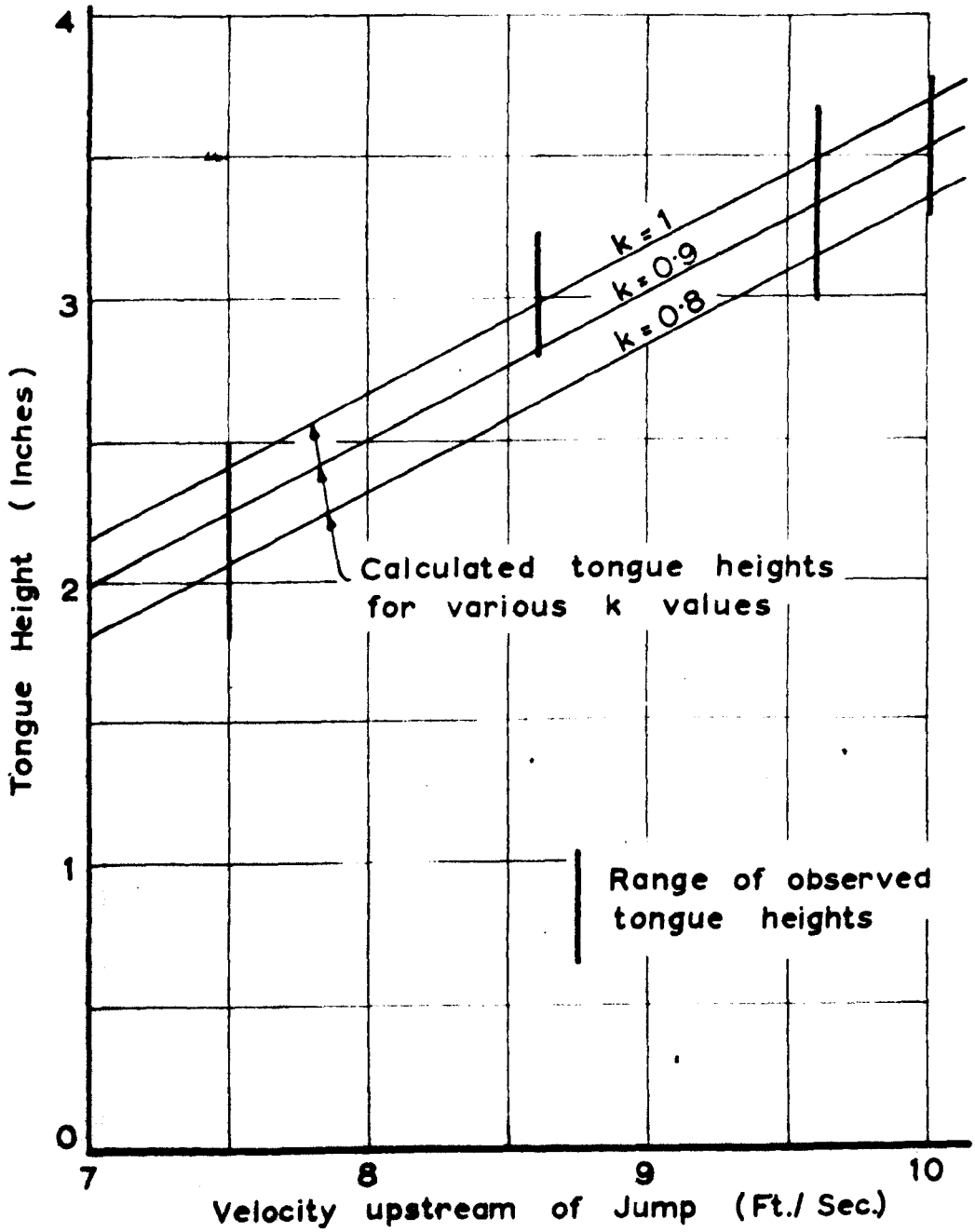

TONGUE HEIGHTS
FOR GIVEN UPSTREAM VELOCITY

FIG. 61

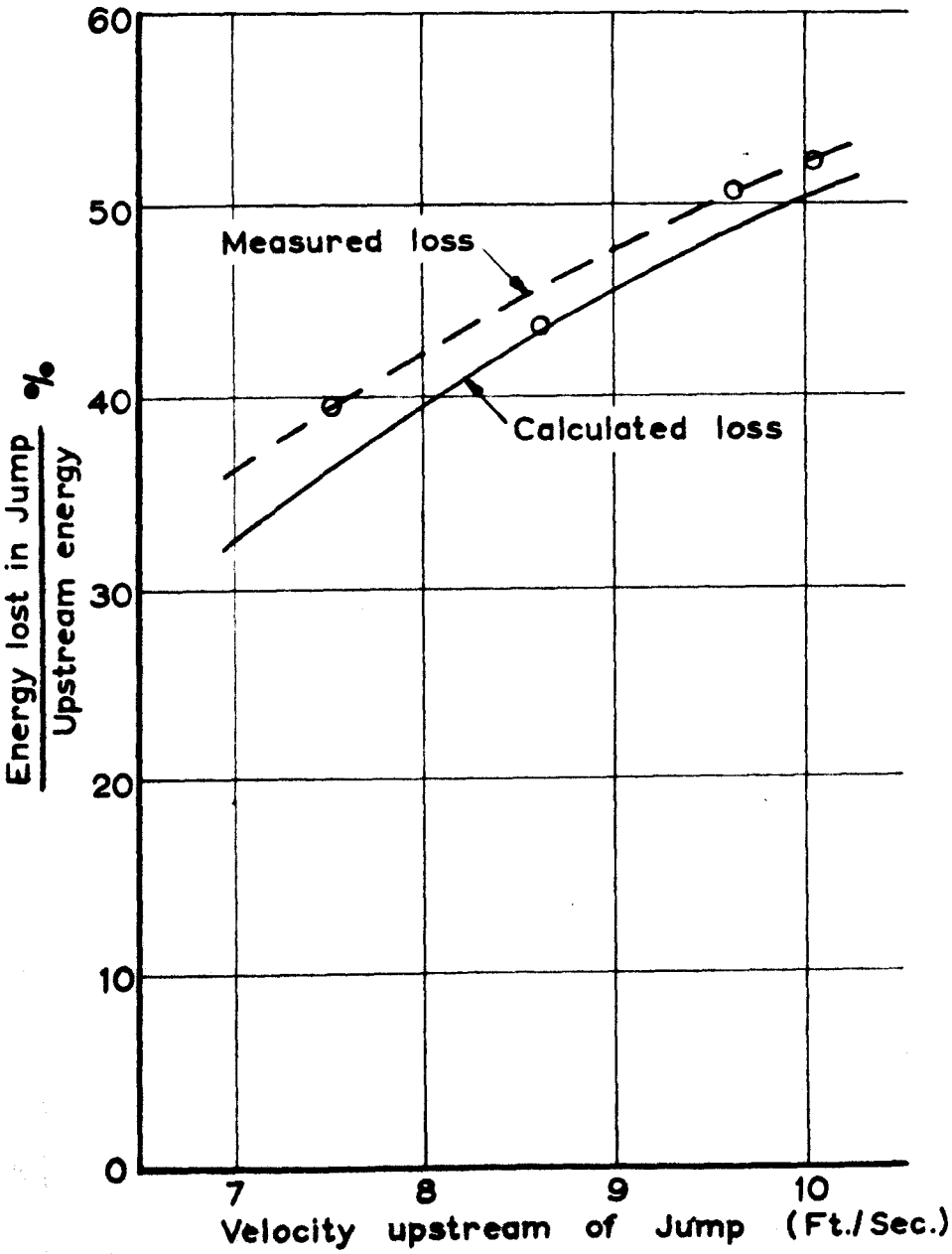

PERCENTAGE ENERGY LOSS IN
ANNULAR HYDRAULIC JUMP

FIG. 62

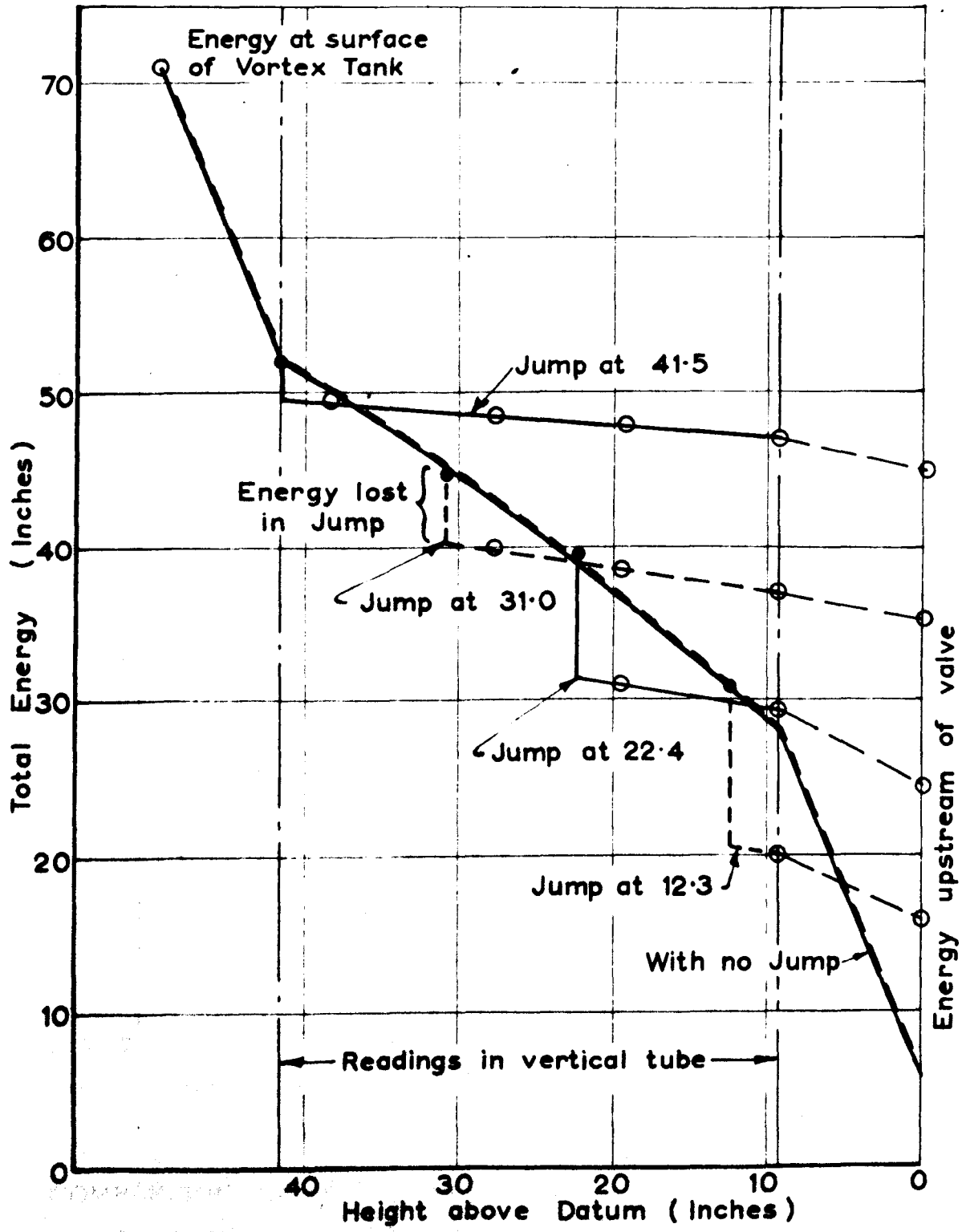

ENERGY GRADIENTS

FIG.63

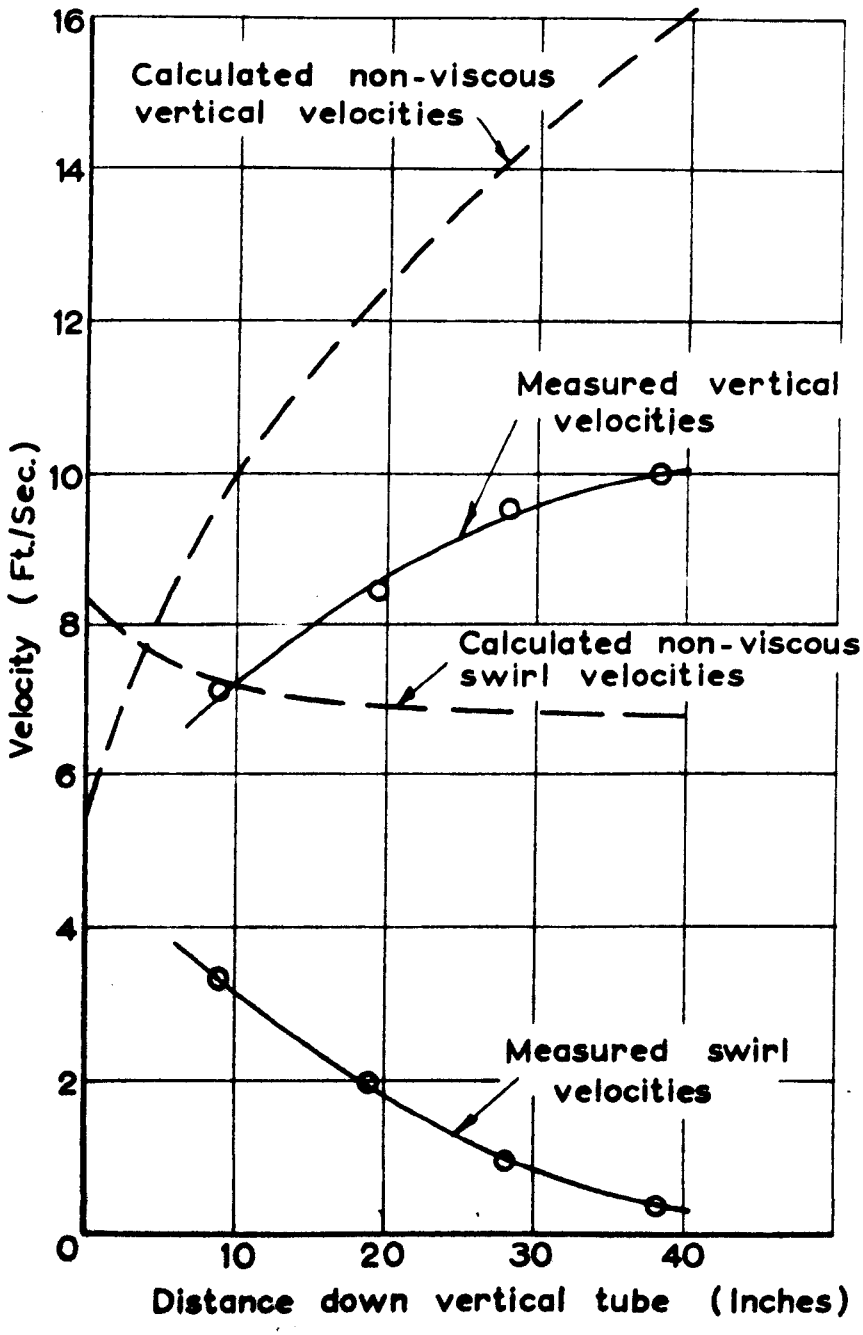

COMPARISON OF IDEAL AND MEASURED VELOCITIES OF ANNULAR FLOW DOWN VERTICAL TUBE

FIG. 64

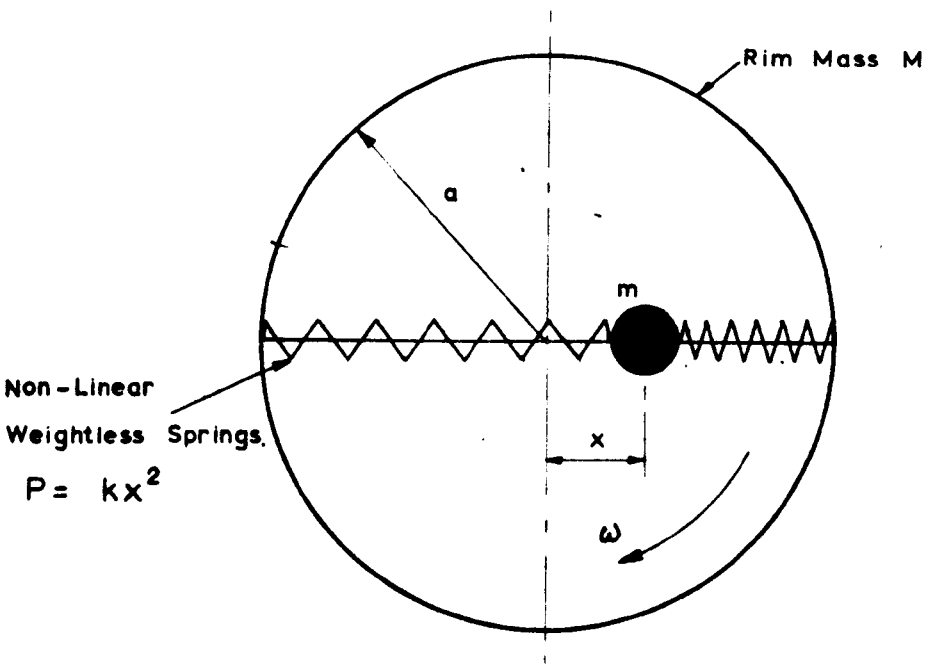

a). Mechanical Analogy Of Spiralling Of Air Core.

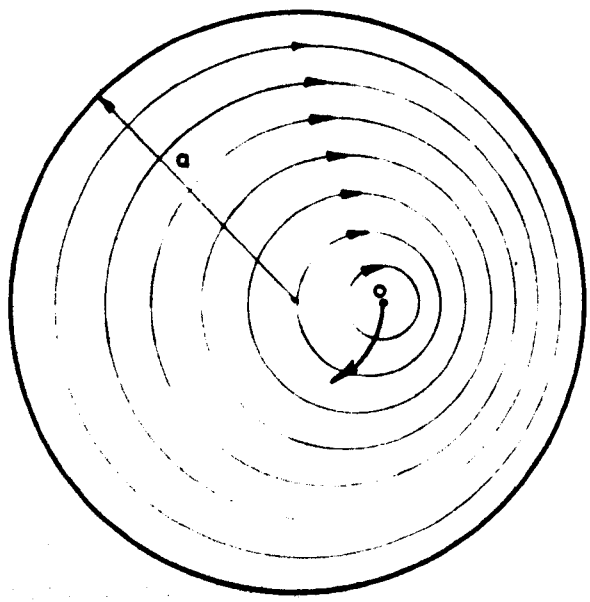

b). Streamline Pattern For Swirl Velocities.

CHAPTER VIII

CONCLUSIONS

1. Velocity distributions and Surface Profiles

The measurements of velocities within the structure of the free spiral vortices showed the measured tangential velocity distribution to be in close agreement with that of the ideal, free cylindrical vortex. It was therefore possible to assign a value of the vorticity, c, to any particular vortex and make a comparison of measured quantity of discharge, with that calculated from a non-viscous theory, for the same values of vorticity and water depth. Qualitative agreement with the non-viscous analysis was obtained, but quantitative agreement could only be reached by introducing a coefficient of discharge which was itself a function of the vorticity. The modification of the non-viscous theory caused by the viscous shear stresses cannot therefore be allowed for by using a constant coefficient of discharge, although experiment has shown that the coefficient of discharge only varies slightly until high values of vorticity are reached, when the alteration becomes large.

The radial velocity component was generally too small to be measured because of the presence of higher vertical and tangential components, but it was established that radial

flow is confined to a small region near the free surface and another region at the bottom of the tank, near the outlet. This radial flow at the surface then became a strong vertical outflow on the surface of the vortex core. The apparent lack of radial flow throughout the remainder of the vortex structure is in agreement with the vorticity theorem that there is no flow across a vortex tube and is supported by a particular integral of the Navier-Stokes equations, which shows that the tangential velocity distribution would be considerably changed by anything but a very small radial component.

The study of the vertical velocity components has revealed an interesting flow pattern in which the flow is alternately upwards and downwards. These vertical velocities appear to be related to the tangential velocity gradient, because they only occur where this gradient is large. It is thought that these vertical velocities are supplied from the radial flow at the top and bottom of the tank and that they supply fresh fluid to a region of the flow where radial velocities cannot or do not occur. The vertical flow pattern is therefore a form of secondary flow set up by the vortex shear gradient.

Despite the measured tangential velocity distribution being very nearly in agreement with the non-viscous distribution, the measured quantity and that calculated from

the non-viscous theory are only approximately in agreement, particularly when the swirl is large. Measurement of the free surface profile showed that this, too, was in good agreement with that calculated from the free cylindrical theory, though this theory cannot give the free surface near the exit from the tank where vertical and radial velocities are significant. A relaxation analysis was used to obtain the non-viscous surface profile near the outlet for a particular high value of swirl and comparison with the measured profile showed that the measured flow area at outlet was about 30% greater than that calculated. This increase in flow area produces the rise in coefficient of discharge at high values of swirl and is probably caused by the high viscous shear stresses near the outlet, which reduce the vortex velocities in this region.

2. Similarity of vortices and vortex formation.

Using two sizes of apparatus it has been shown that two geometrically similar vortices are obtained when the velocities are scaled by the Froude Number. Slight discrepancies were found, amounting to a maximum difference in velocity of about 12%, from the scaled values, but even this maximum error is slight when it is considered that Reynolds Numbers differ by eight times in the two sizes of apparatus. Therefore, once a vortex has been generated, similar behaviour will be obtained in a model only if the

Froude Number is identical with that of its prototype.

There are two mechanisms by which swirl is generated in the flow approaching an outlet. Firstly the water entering a vessel may have a tangential velocity component relative to the outlet so that a rotation of the water around the outlet is induced. Swirl generated in this way will be steady and will vary linearly with inlet velocity; this type of swirl generation is used in the vortex tanks in this investigation. For this first type of swirl generation complete similarity between a model and its prototype will be obtained by operating at equal Froude Number. Secondly, swirl is generated when vortices are shed from the boundaries of the flow and these vortices are carried towards the outlet where they may produce transient air-entrainment. Because the shedding of vortices is not independent of the Reynolds Number of the flow, complete similarity may no longer exist when using the Froude Number as a similarity criterion. The vortices formed in the lee of a bluff body at low Reynolds Number are standing eddies which remain in the same position and do not move away downstream. When the Reynolds Number is increased, there is a critical value above which the vortices are shed and move away downstream to form the well known Karman vortex street. If vortices formed by some separation of the flow from a boundary are to produce air-entrainment, either they must be formed very near

the outlet, or else they must be shed at a discontinuity and carried towards the outlet. The strength of vortices formed in this way is linearly related to the flow velocity, so that Reynolds Number will only influence the problem if the air-entrainment depends on vortices being shed. If this is true, similarity can only be obtained if the model is sufficiently large so that, when operating at similar Froude Number, the Reynold's Number is not decreased below the threshold value for vortex shedding. It must also be remembered that the shed vortices are decaying as they are carried towards the outlet and this is also influenced by Reynolds Number.

In a small model operated with Froude Number equal to that of the prototype, the Reynolds Number of the flow is probably reduced below the critical vortex shedding value. Some work was carried out to investigate the possibility of distorting the model geometrically by exaggerating the outlet diameter. In this way the approach velocities could be increased while maintaining equal Froude Number at exit, so that the Reynolds Number of the approaching flow was more nearly equal to that of the prototype. At first the only factors affecting the formation of vortices were thought to be the velocity of outflow, the submergence, the swirl and the outlet diameter. If this were so, it would be possible to make the required exaggeration of outlet size without

destroying similarity, but experiment has shown that outlet size is not the only significant dimension; the results obtained with different sizes of outlet not being in agreement when plotted non-dimensionally. However, these results did agree when quantity divided by outlet diameter was plotted against depth,and swirl was plotted non-dimensionally, Fig.35. This agreement indicates that a distortion may be feasible, but to establish this result experiments are required with both a model sump and its prototype and various exaggerations tried.

Previously, the velocity scale distortion suggested by Denny has been mentioned. In a 1/16 size model Denny showed that similarity was obtained when velocities in a geometrically similar model were equal to that of the prototype. The model velocities were therefore four times greater than demanded by Froude Number similarity, but still sixteen times less than given by Reynolds Number. On the present hypothesis, it is suggested that this velocity increase was necessary for vortex shedding to occur.

3. Restricted Outlet.

When the water was permitted to discharge freely through the outlet, even a low value of swirl produced a vortex core. Limiting the velocity of outflow also determines a certain critical value of the swirl below which no vortex core can form.

Limiting the outflow velocity to three quarters of the free discharge value will demand a higher swirl than would normally be present, while restricting the velocity to half of the free discharge value will make it impossible for a vortex core to form,because such a strong swirl cannot be generated. The velocity to be restricted is the velocity at the critical outlet section and an increase in velocity after this section would not be detrimental. A bellmouth outlet could therefore be beneficial in limiting the outlet velocity at this critical section. In this way air-entrainment can be prevented, but swirl can still be present in the outlet and may cause a loss of efficiency of a pump, particularly of the axial flow type. Flow straighteners could be used to remove the swirl.

4. Upwards Outlet.

Steady vortices are unlikely to be air-entraining when the outlet is vertically upwards because the outlet tube occupies the position of the air core, but swirl in the outlet tube can reduce the flow and can lower the efficiency of a pump connected to it. Care must therefore be taken to prevent any general swirl. Transient vortices shed from the flow boundary are the principal cause of air entrainment and they can be prevented by careful design of the inlet to the sump and by reducing the velocities in the flow approaching the outlet so that vortices are not shed.

Attention has been drawn to the shedding of vortices from the outside of the outlet pipe and the resulting air-entrainment. These vortices are prevented if the outlet is sited near a boundary so that there is no flow past it.

In contrast to lowering the velocities approaching the outlet, placing the outlet in a strong almost uniform stream prevents air-entrainment completely, even when the outlet velocity is high and the submergence low. This result, opposite to the usual idea that velocities near the outlet must be kept low, is possible because no vortex remains near the outlet for long enough for a core to form.

When studying the formation of steady vortices at the upwards outlet an interesting instability was seen to develop. When a steady vortex had been established for a few minutes, an oscillation of the free water surface slowly developed and at the same time a subsidiary vortex core was formed which rotated around the outlet in phase with the surface oscillation. This subsidiary core took, perhaps, ten minutes to form and it sometimes became strong enough to entrain air. No explanation for the formation of this subsidiary core can be offered; the flow quantity increased after its formation so that, presumably, it satisfies a minimum energy requirement.

5. Conditions in the Outlet Tube and the Annular Hydraulic Jump.

The direction of the outlet tube, whether vertically upwards or downwards, influences the behaviour of an air-core. For the upwards outlet the pressure must fall as the flow rises further up the tube so that the air-core cannot persist, while for the downwards outlet the flow accelerates under gravity and the air-core can become larger. Therefore a very strong vortex may cause the breakdown of upward flow, while for less strong vortices the air core enters the outlet and then breaks up into air bubbles which are carried through with the flow. For all directions of outlet tube the formation of a vortex has two detrimental effects, firstly, it restricts the quantity of flow to the value corresponding to the particular outlet submergence, diameter and swirl and, secondly, it may also entrain air into the outlet. The transient formation of vortices at an intake will therefore cause sudden restriction of the flow with consequent surging of the flow as these vortices form and break .

For vortex flow in a downwards outlet tube, the transition referred to as the annular hydraulic jump has been described and analysed. An interesting feature of the analysis is the separate treatment of the vertical and swirl velocities, which is shown to be justified by the experimental results. The position of the jump has been

discussed qualitatively by considering energy losses through the system, but it was not possible to calculate these energy losses, even for the pipe-full flow, because of the changing swirl velocities which gradually decay as the flow passes down the tube. When the upstream velocity is high, a large proportion, perhaps 60%, of the upstream energy is dissipated in the jump. For some applications, this means of destroying energy may prove as useful as the well known hydraulic jump of open channel flow.

APPENDIX 1

DETAILS OF THE PHOTOGRAPHIC METHODS

Two main problems were encountered when photographing the pellets, firstly, the light was scattered by the water between the pellets and the camera and secondly it was difficult to obtain sufficient intensity of light to give the required streaks on the photographs. The solution of these problems was slightly different for each size of apparatus.

In the small tank any general lighting was scattered by the water and had an intensity as great as that of the illuminated beads. The photographs were therefore taken at night with no general lighting and the beads were illuminated by a narrow, parallel beam of light directed downwards through the free water surface. Some results were obtained with the beam of light centrally placed, but the free surface near the core acted as a lens and scattered the light away from the core. Photographs of beads near the core were obtained by shining the beam of light through the flat outer portion of the free surface and angling it so that it shone on the vortex core. This beam of light had to be made as bright as possible and it had to be made parallel. High intensity spot lamps with as much as 1000 watt bulbs were

tried but the absorption of the lens system was considerable. The best lighting was obtained from a 12 volt car headlamp bulb in an 8 inch spotlight reflector, but the bulb was overrun at 14 volts and this gave a light with a very high colour temperature. The bulbs lasted for about 2 or 3 hours. The beam of light obtained was masked to give a parallel beam of from 1 to 2½ inches in diameter according to the region being photographed.

Various films and developers were tried to obtain the maximum sensitivity so that the feint streaks of the faster moving pellets could be recorded. Very fast films such as Ilford HPS gave too much grain and were unsatisfactory even when very fine grain developers were used. After much trial the best results were obtained with Ilford HP3 developed in Microphen for 15 minutes at 68°F. HP3 is rated at 34° Scheiner.

In the large apparatus, the velocity measurements depended on the instantaneous stroboscope images which had to be joined by a streak given by a small amount of constant illumination. It was found impossible to photograph the very small wax pellets used in the small tank and some larger plastic pellets of 7 m.m.diameter were used. When readings were to be taken in the large tank the water in the general laboratory supply was renewed and it remained photographically

clear for about 10 days. The stroboscopes were placed alongside each camera while the constant illumination was provided by one 500 watt masked spotlamp shining through the outer flat portion of thefree water surface. A careful balance had to be maintained between the constant illumination and that of the stroboscopes. The type of film and developer used for the small tank was again used for the large tank.

REFERENCES

1. Binnie G.M. Experiments on Bellmouth and Syphon Spillways. J.I.C.E. V.10 p.65, 1938.

2. Binnie A.M. and Wright. Laboratory Experiments on Bellmouth Spillways. J.I.C.E. V.15 p.197, 1941.

3. Denny D.F. and Young G.A.J. The Prevention of Vortices in Pump Sumps. B.H.R.A. Paper S.P.583.

4. Binnie A.M. and Hookings G.A. Experiments on Whirlpools. Proc.Roy.Soc.A. 194, p.398, 1948.

5. Binnie A.M. and Davidson J.F. The Flow under Gravity of a Swirling Fluid. Proc.Roy.Soc.A. 199, p.443,1949.

6. Denny D.F. Experimental Study of Air Entraining Vortices. P.I.M.E. 1956, p.106.

7. Markland and Pope. Vortex Formation in Sumps. P.I.M.E. 1956, p.95.

8. Dornaus W.L. Stop pump problems before they begin. Power Eng. 64 p.89, Feb.1960.

9. Fraser W.H. Hydraulic Problems at Intakes. Trans.A.S.M.E. V.75 No.4 p.643.

10. Iverson H.W. Pump Submergence for High Specific Speed Pumps. Trans.A.S.M.E. V.75 No.4 p.635.

11. Folsom R.G. Performance of Deep Well Pumps. Uni.of California. Pump Test Labs. Tech.Memo.No.6.HP-14.

12. Brewer D. Vortices in Sumps. Allen Eng.Review, March 1957.

13. Annis R.K. Power V.83 No.5 p.69, 1939.
Power V.83 No.7 p.84, 1939.

14. Uppal, Gulati and Sharma. Vortex occuring in a River Model.
J.I. of Eng. (India) V.39 No.6 p.1, Feb.1959.

15. Allen N.D.De.G. Relaxation Methods.

16. Rayleigh, Lord. On the Dynamics of Revolving Fluids.
Proc.Roy.Soc.A. 93 P.148, 1916.

17. Truesdell. Kinematics of Vorticity.

18. Elevatorski. Hydraulic Energy Dissipators. p.46 et.seq.

19. Lamb. Hydrodynamics. 5th Ed. p.246.

20. Calvert and Williams. Flow of Air-water Mixtures in Tubes.
A.I.Ch.E.Journal, March 1955, p.75.

21. Slotboom J.G. Gaslift Pumps. IX International Congress of
Applied Mechanics V.II. p.371, 1957.

22. Akers and Crump. The Vortex Drop. P.I.C.E. Aug.1960,p.443.

23. Kolf and Zeilinski. A Vortex Chamber as an Automatic Flow-
Control Device. P.A.S.C.E. V.85. No.HY12. Dec.1959.

24. Hamilton Smith. Hydraulics.